Reconstructing Scotland's Pine Forests

Thomas P. Adams

A thesis submitted in fulfilment of the requirements
for the degree of Doctor of Philosophy
to the
University of Edinburgh
July 2010

Abstract

The Caledonian pinewoods are a habitat of crucial environmental and cultural importance, and the sole home of many rare species. However, they have seen steady decline in recent centuries, through the establishment of hunting estates and forestry plantations. A recent trend in management is the attempted transformation of existing plantations (dense communities with a regular spatial structure and low variance in size and age) towards a state mimicking the perceived natural condition, which has a lower density, irregular spatial pattern, high variance in size and age. This presents a problem for traditional forestry practices, which were conceived primarily with "even-aged" plantation populations in mind. The shift towards management of an uneven-aged structure requires a more in-depth consideration of individual trees' life-cycles and their effect upon long-term population dynamics.

In recent years, great advances in computational and mathematical models for spatially interacting populations have been made. However, certain complications have prevented them from being utilised to their full potential for the purposes of forest management. Forest communities are not only spatially structured; the size of each tree plays a role in its ability to acquire resources for growth and survival. Existing models of population dynamics are discussed, and their extension to incorporate both size- and spatially- structured interactions is presented. The key aspects of populations' structural development are studied. Data from both plantation and semi-natural Scots Pine stands in Scotland allow parameterisation of a stochastic individual-based model, which in turn provides insights into the behaviour of real populations, and the importance of spatial effects and heterogeneity in individuals. A partial differential equation (moment) approximation to the stochastic model is presented. While this is analytically intractable, numerical integration and heuristic analysis of the equations enable clearer identification of the drivers of population structure. Many results are concordant with existing models of both qualitative forest stand development and theoretical dynamics of spatially-structured populations, while others are specific to joint size-space structure.

This deeper understanding of the population dynamics allows robust recommen-

dations for diverse uneven-aged stand management objectives to be made. Approaches to accelerating the transformation of plantation stands towards a "natural" state (using two key operations: thinning – removal of trees, and planting) are investigated. Finally, approaches to so-called "continuous cover forestry" – the practice of maintaining a quasi-natural state while also obtaining economic value from a forest – are also considered. In both cases, the model's simplicity enables clearer conclusions than would be possible using other approaches.

Declaration

Except where otherwise stated, the research undertaken in this thesis was the unaided work of the author. Where the work was done in collaboration with others, a significant contribution was made by the author.

T.P. Adams
July 2010

Acknowledgements

I would like to record my thanks to all those who have helped me in the course of this work. In particular, the following:

- My supervisors Graeme Ackland, Glenn Marion and Colin Edwards for guiding me through the last three and a half years and providing assistance and inspiration.
- E.P.S.R.C., BioSS and Forest Research for financial support.
- My parents for their unfailing encouragement and support throughout.
- Katie for letting me live in her flat for two years, even though I only planned to stay for a few months.
- Members past and present of the we-rock climbing email list – and my brother Robert in particular – for keeping me sane, and to whom this thesis is dedicated.

Contents

Publications

- Thomas Adams, Graeme Ackland, Glenn Marion and Colin Edwards. Effects of spatial correlations and dispersal in size-structured model populations. *In review*.
- Thomas Adams, Graeme Ackland, Glenn Marion and Colin Edwards. Understanding plantation transformation using a size-structured spatial population model. *In review*.

Chapter 1

A new application for population ecology

1.1 Introduction

Forest management is in a period of transition. Traditionally, its motivations centred on the maximisation of forest output for timber production, but a general rise in awareness during the late 20th century of the impact that man has on his surrounding environment has also led to an explosion of interest in the ecological benefits that carefully managed forest stands are able to provide (Franklin et al., 2002; McIntosh, 2006). In Scotland, this has manifested itself in measures to conserve and increase the range of the main native forest community: the Caledonian Pinewoods (Steven and Carlisle, 1959). This habitat has come under threat from the development of plantations and hunting estates, but is also home to many species found nowhere else in the United Kingdom. A significant piece work by the UK Forestry Commission has been dedicated to better understanding these communities, part of which has considered the conversion of existing plantation forests to a state closer to that formed by nature in the long-term.

The difficulties involved in such an enterprise are many. Remnant unmanaged populations are relatively small, and there is a certain lack of knowledge of the true natural state (Bennett, 1995, and Colin Edwards, personal communication). It is also difficult, if not impossible, to set up short term experiments in real populations that can accurately predict the long term response of forest populations to management regimes (especially those intended to fundamentally alter population structure). Such obstacles have lead to an interest in the application of theoretical and computational models.

Population-level stochastic birth-death processes (Bailey, 1964) are a key tool in

the field of population ecology, in part due to their ease of application to a variety of systems, and also because they are amenable to mathematical analysis (although this is far from straightforward).

However, in real populations, individuals grow and age, exhibiting different behaviour or characteristics as they do so (DeRoos et al., 2003). Any such structure is completely ignored by the basic birth-death model, which assumes total birth and death rates are related directly to the number of individuals in the population. Secondly, individuals in biological populations experience varied interactions with one another, depending on their relative size, age and location. The inhomogeneity of these interactions (Law et al., 2003) is also ignored by basic non-spatial birth-death models, which assume that the population is "well-mixed".

The implication is that it is not only the number of individuals that should be tracked, but rather that the state of each and every one (for example, its size, and the conditions applying to it) must be taken into account as the population develops. As a result, and at the opposite end of the spectrum, ecology has a rich history of the development of *individual-based models* (IBMs), applied with varying levels of rigour and specificity to every imaginable type of population (see e.g. Grimm, 1999; Busing and Mailly, 2004). This alternative approach is also not without its difficulties. Incorporating dependence of individual behaviour on a range of characteristics quickly leads to intractability, and results are not always generalisable (Grimm and Railsback, 2005).

For those searching for generic models, there have however been some very useful developments. Dynamical size-structured population models were developed some time ago, the most well known being those of von Foerster (1959) and Sinko and Streifer (1967). These models consider the temporal evolution of a density of individuals (as a function of size/age) which grow, reproduce and die, but still use the mean-field assumption. Another body of work, *spatial point-processes*, deals with pattern generation in populations as a result of interactions between individuals (Cressie, 1993; Diggle, 2002; Illian et al., 2008). Temporal evolution of such point processes, allowing a generalisation of birth-death processes onto a spatial arena, was only considered more recently (Renshaw, 2002; Sarrka and Renshaw, 2006). However, these models do not directly allow an understanding of the feedback between spatial structure and temporal population dynamics.

This latter topic was studied with great success by Bolker and Pacala (1997) and Dieckmann and Law (2000), who considered the basic properties and temporal evolution of the stochastic spatial birth-death process, and its dynamical system approximation (*spatial moment models*). By accounting for spatial correlations in individual location, this work provided a logical next step from mean-field models

of temporal population dynamics, allowing insight into how spatial dependence of individual level processes influences population-scale dynamics (Bolker et al., 2003; Law et al., 2003; Murrell et al., 2004).

One case in which spatial and size structure are particularly important is the population dynamics of plants. From birth, the location of a plant is fixed; its life experience is thus entirely determined by local population structure (Murrell and Law, 2003). Point-process methods have now been applied with some success to plant and forest data (Stoyan and Penttinen, 2000; Renshaw et al., 2009), and the dynamical insights of Bolker, Law et al. have found application in topics such as the maintenance of rainforest diversity (Law, 2007), community dynamics of grasslands (Turnbull et al., 2007), predator-prey models (Murrell, 2005) and disease dynamics (Filipe and Maule, 2003). It is also hoped that they can inform forest management (Gratzer et al., 2004). However, up to now these models have generally not included size structure.

By comparison, traditional forest management for timber production is a fairly simple procedure. Trees are planted, in a regular spatial pattern, at a higher density than would occur naturally. As a result, trees in these *stands* (small populations of a few hectares in area) tend to be fairly homogeneous in size, and do not express the full extent of their potential lateral growth (Figure 1.1a). They are generally felled in one or a very few thinnings, at a time determined using *yield tables* (charts predicting stand scale growth and return at different ages). The land is then replanted, or left for the soil to regenerate.

Over the years there has been a general trend away from the practice of *clearcutting* (the removal of all trees at once), to so called *selection management* (Nyland, 2002, pg. 213), which removes individual trees from a stand based upon their characteristics, such as size. The same yield tables (which were developed for even- (single-) aged stands), and the forester's intuition, often form the basis of this approach. However, uneven- (multi-) aged stands are necessarily inhomogeneous, meaning there is wide variation in the experience of different individuals. This has meant that, in common with ecology, forestry has seen a profusion of arguably even more complicated and specific IBMs (even including physiological processes) for different scenarios (O'Hara, 2001; Porté and Bartelink, 2002), which are correspondingly intractable. Conservation oriented forest management takes a further step away from traditional forestry. It focuses on the structural characteristics of forest stands, their sustainability, and the ecological value that is obtained from them, often aiming to create stands with a highly irregular structure (see, for example, Figure 1.1b).

Contemporary management and conservation of Caledonian pinewood communities in Scotland encapsulates many of the issues described above. The importance of the pinewoods has come to be recognised over the last century (Edwards and Mason,

Figure 1.1: (a) 78 year old plantation stand at Glenmore, Highland. (b) Semi-natural (unmanaged) stand at Glenmore, Highland.

2006; McIntosh, 2006). This can largely be credited to the highly influential book of Steven and Carlisle (1959) which describes in detail the ecology of the primary species (Scots pine, *Pinus sylvestris L.*), the history of the habitat, and 12 main remaining fragments of pinewood in Scotland. The previous extent of this habitat type was over 100 times the current area, its steady decline over recent centuries a result of the introduction of grazing animals and the establishment of hunting estates and forestry plantations (Bennett, 1995; Holl and Smith, 2007).

Forestry practices, both in Scotland and abroad, have seen great increases in intensity, with active planting occurring over the last several centuries (Steven and Carlisle, 1959). This often favours non-native, fast growing species (in Scotland, Sitka Spruce, for example), though Scots pine does form a significant component of the current plantation inventory. In an era that favours the regeneration of the native habitat type, and when timber has relatively low value (Colin Edwards, personal communication), *transformation* of existing plantations is a very appealing option (Malcolm et al., 2001). The most effective route from a plantation to a quasi-natural state is sought (Schutz, 2002).

As with all ecological populations, there are many factors that complicate our understanding of the behaviour observed in the field. Although Scots pine is found most frequently as a canopy monoculture, it is sometimes mixed with Birch (*L. Betula Pubescens*). In lower density stands (that is, those with plenty of open space) Rowan (*L. Sorbus aucuparia*) and Juniper (*L. Juniperus communis*) are often found, though these do not compete for canopy space. Ground vegetation, topology and soil type in pinewood stands vary widely (on both local and non-local scales, (Arkle, 1996)), which affects regeneration success and potential for growth. Finally, there is the omnipresent Red deer (*L. Cervus elaphus*), which presents significant problems for regeneration and mortality of young trees. In this work, we ignore complicating factors and consider models for the development of single species populations, implementing only essential structural components. This provides a baseline for subsequent comparison and extension, as we begin to unravel the behaviour of pinewood populations.

This problem lends itself to analyses using spatial birth-death-growth processes, and such analysis is the essence of the thesis. We investigate the generic aspects and driving forces of pinewood population dynamics, and will also seek applications of the models developed to conservation oriented management problems, such as transformation and *continuous-cover forestry* (an uneven aged management regime that promotes the development of ecologically and economically beneficial forests).

1.2 Thesis outline

Chapter 2 introduces a generic stochastic individual-based model of a population inhabiting a spatial arena, and discusses general aspects of its behaviour. Individuals are able to grow, reproduce and die. Functional forms and parameters are configured to ease comparison with material presented in later chapters.

In Chapter 3, a comprehensive analysis of growth data from semi-natural Scots pine stands is carried out. This seeks to identify the key explanatory variables and the most appropriate functional form for individual tree growth, and begins to consider the influence of additional factors for which data is unavailable.

Various aspects of forest stand behaviour, such as regeneration, are very difficult to determine from data analysis. Chapter 4 takes a different approach, confronting the simulation model with data from various stages of stand development, allowing insights into how birth, growth and mortality processes in real stands may differ from the simplistic formulation presented in Chapter 2.

Chapter 5 provides a brief review of mathematical models for population dynamics, including those derived by Bolker and Pacala (1997); Dieckmann and Law (2000), to approximate the behaviour of spatial birth-death processes. It discusses the extension to approximating a spatial birth-growth-death process, and presents the results of numerically integrating these equations.

In Chapter 6, the application of the individual-based simulation model to uneven-aged management objectives is studied. Approaches to plantation transformation are compared. This chapter also considers factors that must be taken into account in a continuous-cover forestry regime, and how this should be applied.

Chapter 7 discusses the main results of the thesis, their robustness and applicability to real pinewood (and indeed other more general spatial) populations, and suggests areas that would benefit from further study.

Chapter 2

An individual-based simulation model of a population structured in size and space

2.1 Introduction

The primary goal of this chapter is the development of a minimal model of a forest population, incorporating essential processes, but omitting complicating factors. Simplicity assists in understanding the behaviour of the model, but it also allows straightforward comparison with stand-level data. This should help to allow generic insights into population dynamics, and provide a good base for extension to other applications.

A spatial, size-structured model of a single species population is introduced and applied to development from a high density plantation towards an old-growth state. An alternative model incorporating only "mean-field" interactions (that is, including no spatial dependence) is also described. The behaviour of the mean-field and spatial models is compared in Section 2.6.

For each aspect of the model definition, the most obvious extensions are identified, with a view to further analysis. Those applying to the growth function are investigated through data analysis in Chapter 3, and the effects of the most important changes overall are investigated directly in Chapter 4.

2.2 Model construction

2.2.1 State space and basic principles

The development and fate of individuals is to be tracked in both size and space. A generic approach is to extend a Markovian birth-death process (for a well-mixed population) to a spatial arena (Bolker and Pacala, 1997; Law and Dieckmann, 2000), also incorporating growth. Individuals (and also rates and events pertaining to them) are denoted by an index i, each having size defined by a single measure s_i, and location $\vec{x}_i$ in two-dimensional (continuous) space. The process of events is integrated through (continuous) time t. The manner in which events occur, and the impact of other individuals ("interaction") is defined below.

2.2.2 Growth

Background

Trees vary greatly in their morphological characteristics. They may have different branch architecture, different trunk diameter/height ratio and so on. These variations are most apparent between species, but life-history and environmental factors can also lead to dramatic differences between conspecific individuals (for example, note the difference in appearance between a plantation individual and an open-grown tree of the same age).

Implementing individuals with a vast array of structural characteristics would produce a very complicated model and disguise any clear indicators of stand development and dynamics. Thus, a single size measure "dbh" (diameter at breast height (1.3m)) is considered. This is the single most widely used metric in forestry, mainly due to its ease of measurement in the field, which will be useful in confronting the model with data.

Dbh also has the benefit of correlating with other important size measures (which are less frequently or easily collected). Total tree height is usefully viewed as being related to dbh by a power law $h = \theta_1(\mathrm{dbh})^{\theta_2}$ (Drew Purves, personal communication) or an exponential function $h = \theta_1(1 - \exp(-\theta_1 \mathrm{dbh}/\theta_2))$ (Strigul et al., 2008), where θ_1 and θ_2 are species-specific parameters. Data from geographically separated Scots pine stands, shown in Figure 2.1a, provides support for either function – the latter providing a slightly better fit, and (more realistically than the power law) an asymptotic height.

Biomass is also often computed from dbh using a power law, height having minimal influence as an additional predictor (Ter-Mikaelian and Korzukhin, 1997).

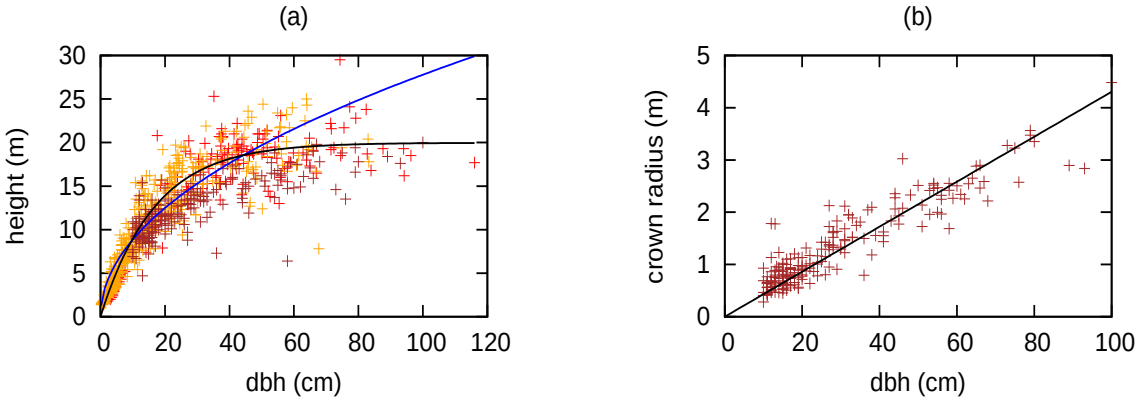

Figure 2.1: (a) Tree height against dbh for two unmanaged stands in the Black wood of Rannoch and one in Glen Affric, plotted together. The pattern is the same for all stands despite their geographical separation. Fitted curves: power law (blue), exponential (black). (b) Crown radius against dbh for trees in the Glen Affric stand (the only stand for which these data were available). This follows a linear relationship.

Another useful relationship is that between dbh and total crown (exposed foliage) radius, which is generally observed to follow a linear relationship with roughly the same coefficient across species (Drew Purves, unpublished data, and see Larocque, 2002). This is again supported by relevant data for a Scots pine stand at Glen Affric, shown in Figure 2.1b.

Zeide (1993) points out two underlying principles of biological growth:

- growth is multiplicative – that which grows is itself capable of growing
- relative growth rate ($= (ds/dt)/s$) is always decreasing, and there is a limit imposed by finite space

The implication is that individuals should approach an asymptotic maximum size. It is apparent when studying real communities that individuals do not increase in size forever, or infinitely. Further, there appears to be good empirical evidence to suggest that a tree's growth is determined by size related factors, rather than its age (Martinez-Vilalta et al., 2006; Mencuccini et al., 2005, and see Chapter 3).

To simplify construction, and to assist with later parameterisation, the growth rate should have a minimum of parameters. For the same reason, it must also display behavioural stability under parameter variation. Finally, it would be useful if its form were amenable to mathematical analysis.

Implementation

For its agreeable mathematical properties, and following Purves and Law (2002); Schneider et al. (2006), we initially use the Gompertz model for individual growth, reduced by a term incorporating the effect of neighbourhood interactions (Wensel et al., 1987). This satisfies the requirement that each tree has an asymptotic maximum size. Additionally, quantities related by power laws to other quantities that display Gompertz growth (for example, biomass to dbh), also display Gompertz growth (Seber and Wild, 1989). The Gompertz model is described by the equation

$$\frac{ds}{dt} = s\,(\alpha - \beta \ln(s)) \tag{2.1}$$

and is a special case of the Richards (1959) model, which is discussed later (Section 3.4). For this model, a definition for discrete "individual growth events" is required. The definition of a growth event is here a fixed size increment of size ds (in the same way that a birth or a death is a fixed increment in the number of individuals). The rate of occurence of such growth events, assuming Gompertz growth, is

$$G_i(t) = \frac{1}{ds} s_i(t)\,(\alpha - \beta \ln(s_i(t))) \tag{2.2}$$

As $ds \to 0$, $G_i(t) \to \infty$, as the total growth per unit time must remain constant ($G_i(t)ds = ds/dt$). For presented simulations $ds = 0.1$cm, which provides smooth growth over the timescales simulated. Taking ds much too large means that growth events occur too infrequently relative to mortality and birth (not shown).

Neighbourhood interaction $\Phi_i(t)$, a measure of the combined effect of neighbouring individuals on a focal individual's experience (and defined more precisely in Section 2.2.5), may be incorporated into the growth function as:

$$G_i(t) = \frac{1}{ds} s_i(t)\,(\alpha - \beta \ln(s_i(t)) - \gamma \Phi_i(t)) \tag{2.3}$$

In the absence of interaction ($\Phi_i(t) = 0$), the asymptotic size of an individual is $s^* = \exp(\alpha/\beta)$. Under intense competition, the right hand side of Equation 2.3 may be negative. In this case, we fix $G_i(t) = 0$ (similarly to e.g. Weiner et al., 2001). To facilitate comparison with data, the initial size of an individual in the model simulation is taken to be 1cm.

Possible extensions

Different growth forms, age dependence as an alternative to size.

2.2.3 Mortality

Background

Do trees have a tendency to die at a certain age, or do they experience some constant risk of death throughout their lives? Taylor and MacLean (2007) mention key factors contributing to individual tree mortality:

- size
- vigour/growth rate
- competition
- stand density

In the framework described all of these are connected. In reality, it is likely that the probability of mortality is highest in very small individuals (due to grazing and competition for light) and then plateaus above a size of 10-20cm dbh (trees having acquired enough resources by this time to be less affected by shading) (Taylor and MacLean, 2007). Harcombe (1987) found little evidence for increase in mortality at larger sizes (corresponding to great age) for a variety of species, but pointed out that this could be due to a sample of very few old trees.

This lack of clear evidence to the contrary suggests adoption of a simple rule for mortality: a baseline rate that remains constant for the duration of a tree's lifespan, and a competition-dependent component. This formulation has been used previously by many authors for both theoretical and empirically oriented studies (see e.g. Bolker and Pacala, 1997; Law and Dieckmann, 2000; Strigul et al., 2008; Wunder et al., 2006).

Implementation

Mortality of an established individual then occurs at a rate

$$M_i(t) = \mu_1 + \mu_2 \Phi_i(t). \tag{2.4}$$

μ_1 is the fixed baseline mortality rate, and μ_2 scales the effect of interaction with neighbours (again, defined in Section 2.2.5). In the absence of clear evidence to the contrary, the same inteeraction function is here applied to both growth and mortality.

Possible extensions

Age/size dependence of mortality.

2.2.4 Reproduction

Background

Estimation and modelling of reproductive processes of plants, and specifically trees, has long been a stumbling block in model development (Clark et al., 2004; Gratzer et al., 2004). This is due to the multiple processes involved in reproduction:

- seed production
- seed dispersal
- establishment/early growth pressures,

and to the difficulty in analysing each of these – postulates are easy to make, but appropriate data collection is problematic.

Seed production of trees is generally regarded to be proportional to exposed foliage area (Clark et al., 2004; Ribbens et al., 1994), and hence also to individual basal area. In the case of Scots pine, seed production begins at around 20-30 years of age, and is also periodic in magnitude (3-4 years, synchronised between trees: "masting"). Climatic conditions during the year of seed production complicate matters further (Malcolm et al., 2001).

With regard to dispersal, commonly implemented spatial seedling distributions ("dispersal kernels") include negative exponential ($\exp(-kx)$: Malcolm et al., 2001; Bolker and Pacala, 1997) and Gaussian (Law and Dieckmann, 2000). It is also thought that around 80% of a pine's seed lands within 2.5 tree heights of the producer's base (Colin Edwards, personal communication) However, Kot et al. (1996) suggests that the majority of dispersal data are probably also leptokurtic (heavy-tailed), rather than normally or negative exponentially distributed, and subject to very large variability. In a reasonably populated stand, we might thus expect a large degree of overlap in parent dispersal range.

Seedling establishment is subject to browsing (deer, rabbit, sheep), competition from other vegetation, microtopography (Arkle, 1996; Edwards and Rhodes, 2006) and light environment (Bollandsas et al., 2008). These pressures continue during the early years of a tree's life, affecting possibilities for growth and survival.

Implementation

Based upon the ideas described above, and in view of the limited definitive information available, a fairly simple basic reproduction model can be constructed. Ignoring the relatively short term cyclical nature of (and the non-contribution of juveniles to)

seed production, reproduction is assumed proportional to individual basal area, that is

$$B_i(t) = f\pi\left(\frac{s_i(t)}{2}\right)^2 \tag{2.5}$$

with a constant rate f to be determined. On the assumption of reasonable dispersal overlap, offspring's locations are selected at random – there is no spatial effect of dispersal. The influence of including local dispersal will be investigated in Chapter 4.

The estimated time to reach the 1cm "initial size" from establishment is around 20 years (Sarah Taylor, unpublished data, and see Table 4.2). Explicit environmental heterogeneity is not incorporated in to the basic model, but competition is. An *establishment probability* may thus be defined

$$\mathbb{P}_e = \left(1 - (\mu_1 + C\mu_2\Phi_{\mathtt{offspring}}(t))\right)^{20}, \tag{2.6}$$

where $\Phi_{\mathtt{offspring}}(t)$ is the interaction experienced by an individual of size 1 at the proposed location. In order to remove the time lag, this makes the assumption that the population is at a constant state during the establishment process. C allows enhanced mortality of seedlings (Mason et al., 2004) (though the presence of a canopy is not always detrimental to seedlings; see Barbeito et al., 2008, and Chapter 4). In this chapter we use $C = 1$.

Possible Extensions

Dispersal rules, altering C in establishment probability. Time lagged rate of reproduction.

2.2.5 Interaction

Background

Each of the processes detailed above depends on an as yet undefined "interaction". This dependence is typically achieved by means of a predefined "kernel", a mathematical function that assesses the structure of an individual's neighbourhood according to predefined criteria. In a size and space structured model, the kernel takes a value dependent upon separation distance between an individual and its neighbour(s), and their sizes – which are assumed to be its sole determinants.

Assumptions are that interactions are additive, and that the effect of location and size difference are independent (they can be computed separately and multiplied

together). Furthermore, we shall use the same interaction Φ_i for computation of all applicable (birth/death/growth) rates.

Implementation

Using the above assumptions, the interaction experienced by a *focal individual* i due to its *neighbours* j can be defined generally as

$$\Phi_i(t) = \sum_{j \in \omega_i} F_1(s_i, s_j) F_2(\vec{x}_i, \vec{x}_j) \tag{2.7}$$

where ω_i is the entire population, excluding individual i. One fairly generic form for a size and location dependent interaction kernel (Raghib-Moreno, 2006; Schneider et al., 2006) is a Gaussian decay in competitive inhibition with separation, multiplied by a tanh function to incorporate asymmetry due to size difference. That is

$$F_1(s_i, s_j) = s_j(\tanh(k_s(\ln(s_j) - \ln(s_i))) + 1) \tag{2.8}$$

$$F_2(\vec{x}_i, \vec{x}_j) = \frac{k_d^2}{\pi} \exp(-k_d^2 |\vec{x}_i - \vec{x}_j|^2) \tag{2.9}$$

where $k_d, k_s \in [0, \infty)$ (Figure 2.2). The normalisation factor in $F_2()$ ensures that the integral over the kernel (in polar coordinates, since it takes a value dependent upon separation distance only) is equal to 1. The use of a tanh function for size dependence allows the spectrum from completely symmetric ($k_s = 0$) to completely asymmetric competition ($k_s \to \infty$) (Schneider et al., 2006). It is also worth noting that, in the limit $\lim_{d \to \infty} \exp(-|\vec{x}_i - \vec{x}_j|^d)$, a sharp edged "top-hat" kernel could be obtained (subject to normalisation).

The use of log-size in the kernel means that the asymmetry depends on size ratio, as opposed to absolute size. Multiplying interaction by the size of the neighbour considered reflects increased interaction with larger individuals, independent of the size difference (consider characterising the interaction between two tiny individuals with given separation/size-difference, compared to that between two large ones with the same separation/difference).

Possible Extensions

Altering the interaction form, non-independence of size and location kernel components.

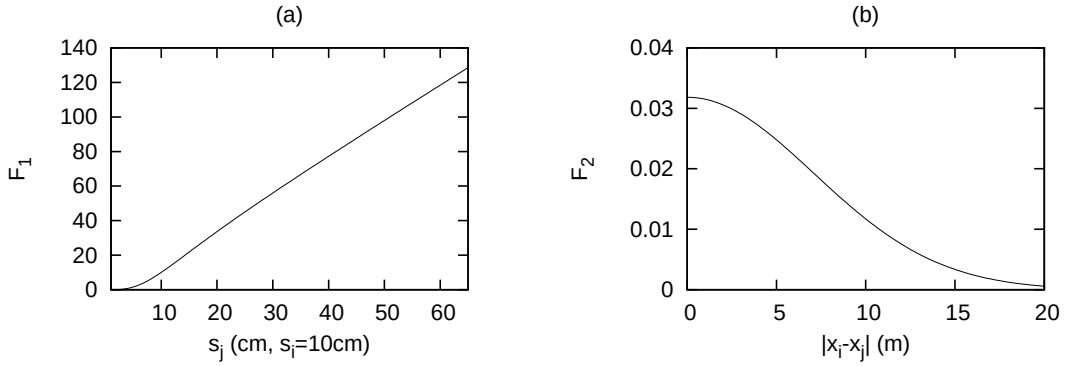

Figure 2.2: *The interaction kernel.* (a) The effect of altering neighbour size (with $k_s = 1.2$), assuming that s_i is fixed at 10cm. The inclusion of the s_j multiplier in the term means that the effect of smaller neighbours (that is, smaller than the focal individual i) is non-linear, and larger neighbours approximately linear. In the absence of the multiplier, F_1 would be an increasing nonlinear function of the ratio s_j/s_i. (b) The effect of altering neighbour separation distance (with $k_d = 0.1$), which becomes negligible above around 15m in the parameterisation used in this chapter.

2.2.6 Total event rate and Gillespie algorithm

As defined, the model is a discrete state space Markov process. At a given point in time, the total event rate for the system is

$$R_{tot}(t) = \sum_{i \in \omega} (G_i(t) + M_i(t) + B_i(t)) \tag{2.10}$$

where i are individuals in the population ω (individual rates are summarised in Table 2.1). A rigorous way of simulating a stochastic process of this nature is a so-called "Gillespie" algorithm (Gillespie, 1977). Based on the current state of the system, the Gillespie algorithm determines the amount of time until the next event (the *inter-event time*), and the precise event that will take place at that time. As such, it is a "continuous-time" algorithm; there is no fixed timestep (the time between events is determined solely by the rates of the events themselves).

The waiting time for an event to occur (t_{event}) is an exponential random variable. Draws from an exponential distribution with rate R_{tot} may be made with a transformation of a uniform random variable $z \sim U[0, 1]$:

$$t_{event} = \frac{-\ln(z)}{R_{tot}}. \tag{2.11}$$

The event that will take place is determined by ordering all possible events; picking a random value between zero and R_{tot} allows selection of a particular event with a

Table 2.1: Equations governing rates and interactions in the stochastic simulation model outlined in Section 2.2. Definitions and values for particular parameters are given in Table 2.2.

Description	Model term	Definition
Rates		
Growth	$G_i(t)$	$\frac{1}{ds} s_i(t) \left(\alpha - \beta \ln(s_i(t)) - \gamma \Phi_i(t)\right)$
Death	$M_i(t)$	$\mu_1 + \mu_2 \Phi_i(t)$
Birth	$B_i(t)$	$fBA_i(t) = f\pi \left(\frac{s_i(t)}{2}\right)^2$
Interaction		
Individual interaction	$\Phi_i(t)$	$\sum_{j \in \omega_i} F_1(s_i(t), s_j(t)) F_2(\vec{x}_i, \vec{x}_j)$
Size dependent	$F_1(s_i(t), s_j(t))$	$s_j(t) \tanh\left(k_s \left(\ln\left(\frac{s_j(t)}{s_i(t)}\right)\right) + 1\right)$
Spatial kernel	$F_2(\vec{x}_i, \vec{x}_j)$	$\frac{k_d^2}{\pi} \exp(-k_d^2 \lvert\vec{x}_i - \vec{x}_j\rvert^2)$
Establishment probability		
	$\mathbb{P}_e$	$\left(1 - (\mu_1 + C\mu_2 \Phi_{offspring}(t))\right)^g$

probability proportional to its rate. Single events occur in the interval $[t, t + dt)$ with probability $dt \times r_{event}/R_{tot}$; the probability of two or more events occurring in the same interval is thus of order $O(dt^2)$ and can be neglected. Following an event, each individual's rates must be updated to reflect the change in state of the population.

2.3 Model data output

The chosen output metrics reflect the formulation and desired application of the model. We here draw on both spatial point process theory, and commonly accepted quantifications in forestry (though recent years have already seen some transfer of techniques between the two disciplines (Illian et al., 2008; Pommerening, 2002; Stoyan and Penttinen, 2000)).

2.3.1 Individual density

This is the number of individuals per m^2 of the simulation area A.

$$\rho = \sum_{i \in \omega} \frac{1}{A} \tag{2.12}$$

2.3.2 Basal area

This is the sum of cross sectional areas (at breast height) of trees in the population. It is a commonly used metric in forestry as a summary of wood volume (generally quoted

per hectare).

$$BA = \sum_{i \in \omega} \pi \left(\frac{s_i}{2}\right)^2 \tag{2.13}$$

2.3.3 Size density distribution

The size density distribution gives the proportion of individuals at different sizes (the size range divided into bins of a fixed width, here 2.5cm). This allows identification of, for example, the mean size of canopy trees, whether the canopy is "well-defined", the level of regeneration, and so on.

$$n(s) = \sum_{i \in \omega} \frac{I(s - 2.5 \leqslant s_i < s)}{N} \tag{2.14}$$

2.3.4 Pair correlation function

Functions describing spatial correlations are referred to as second-order statistics, as their calculation is based upon pairs of individuals.

The pair-correlation function (henceforth PCF) is a measure of the density of pairs of individuals with a given separation, relative to the population mean. It is a function of separation distance:

$$PCF(r) = \frac{1}{N^2} \sum_{i \neq j} \frac{I(r - dr < |x_i - x_j| < r)}{2\pi r dr} \tag{2.15}$$

where $r = dr, 2dr, 3dr, ...$ (dr is the "bandwidth"), N is the total number of individuals in the population, and $I()$ is the indicator function. It is discussed by various authors in application to spatial ecology (Penttinen et al., 1992; Pommerening, 2002; Law et al., 2009). $PCF(r) < 1$ indicates below average exclusion at separation r (e.g. competition induced mortality), whilst $PCF(r) > 1$ indicates clustering (as could be caused by local dispersal), or some characteristic separation (for example a wavelike pattern).

2.3.5 Mark correlation function

This function measures the relative size of individuals at a particular separation. Law et al. (2009) defines several types. Throughout, unless specifically stated otherwise, the mark correlation function (MCF) used is defined

$$MCF(r) = \frac{1}{\bar{s}^2} \sum_{i \neq j} s_i s_j \frac{I(r - dr < |x_i - x_j| < r)}{PCF(r) 2\pi r dr} \tag{2.16}$$

where $\bar{s}$ is the mean size of all individuals in the population. Dividing through by the PCF removes the effect of density from the function, such that $MCF(r) < 1$ means that there is size limitation (e.g. growth inhibition) at radius r, whilst $MCF(r) > 1$ means that there is size enhancement. Note that different combinations of s_i and s_j can lead to the same computed value.

2.4 Model behaviour

2.4.1 Model parameterisation

The parameter values used for simulations presented throughout Section 2.4 are shown in Table 2.2. Estimates for growth parameters (α, β and γ) were obtained from diameter increment data from "semi-natural" Scots pine stands, using a nonlinear mixed effects (NLME) approach (Lindstrom and Bates, 1990), described in more detail in Chapter 3. Other parameters are tuned to produce similar behaviour to real Scots pine populations, which also allows straightforward comparison of the results presented here with data in later Chapters. However, sensitivity to parameter variation over broad intervals is also assessed, in Section 2.5.

Table 2.2: Model parameters, description and values.

Parameter	Description	Value	Units
population rates			
f	immigration per m^2 basal area	0.15	individuals yr^{-1}
μ_1	baseline mortality	0.004	individuals yr^{-1}
μ_2	mortality interaction	0.00628	individuals yr^{-1}
α	Gompertz parameter a	0.1308	yr^{-1}
β	Gompertz parameter b	0.03158	yr^{-1}
γ	growth interaction	0.0157	yr^{-1}
c	seedling mortality enhancement	1	—
kernels			
k_d	interaction distance decay	0.1	m^{-1}
k_s	interaction size asymmetry	1.2	—

2.4.2 Additional configuration

All simulations presented in this thesis are made in a 1ha ($100 \times 100m$) square arena. Periodic (toroidal) boundary conditions are used, as we assume the model population represents a small component of a much larger population (edge effects are of interest in some applications, but not here).

An initial condition must also be chosen. A standard planting regime implemented in Scots pine plantations is a 2m square lattice, typically on previously planted ground (Colin Edwards, personal communication). Old stumps and furrows prevent a perfectly regular structure being created, so we start by assuming 0.01m dbh trees located with small random deviations from the exact lattice sites. The location $\vec{x}_i = (x_{1i}, x_{2i})$ of tree i is given by

$$\begin{aligned} x_{1i} &= x_{1i0} + (U[0,1) - 0.5) \\ x_{2i} &= x_{2i0} + (U[0,1) - 0.5) \end{aligned} \tag{2.17}$$

(all quantities in metres) where (x_{1i0}, x_{2i0}) are corresponding lattice sites and $U[0,1)$ are uniform random numbers.

2.4.3 Generic Behaviour

Various qualitative models of forest stand development are discussed by Franklin et al. (2002), and the general patterns described by these are observed in our model. Starting from the plantation configuration, the model population passes through several transient stages: (i) an initial growth dominated period, during which the plantation structure largely remains, and the canopy closes; (ii) a period of high density-dependent mortality as the impact of interactions begin to be felt; (iii) gap creation together with an increase in regeneration; (iv) the long-run meta-stable state, during which stand structure is more irregular and determined by the levels of mortality and birth.

Plantation

The plantation structure initiated by forest management has a higher density than a natural self-regenerating forest. Initially, reproduction is low, due to individuals' small size. Rapid growth of the immature trees means that basal area increases rapidly (see Figure 2.4a). Individual density falls equally quickly due to high levels of density-dependent mortality. Stochastic variation in growth and asymmetric competition lead to a gradual spread of sizes of individuals (the initial size distribution is a delta peak at s = 1cm). Size asymmetry is often cited as a key driving force in plant community dynamics (Adams et al., 2007; Perry et al., 2003; Weiner et al., 2001). In our model, competitive size asymmetry is the primary factor affecting the variance (spread) of the size distribution during the early stages of stand development: it is almost independent of any other parameter, or even starting spatial configuration (see Table 2.3, Section 2.5). In the spatial model, low reproduction means that spatial structure

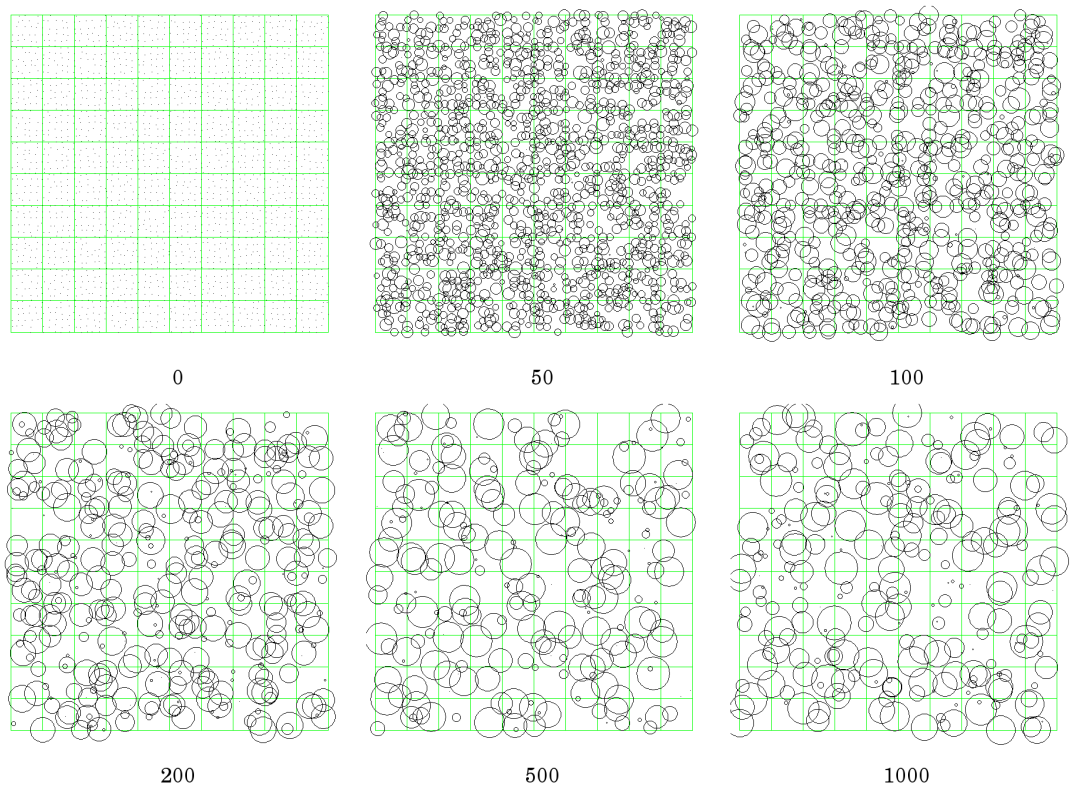

Figure 2.3: Maps of a simulated forest at 0, 50, 100, 200, 500 and 1000 years from planting. The diameter of each circle is proportional to the size (dbh) of the tree.

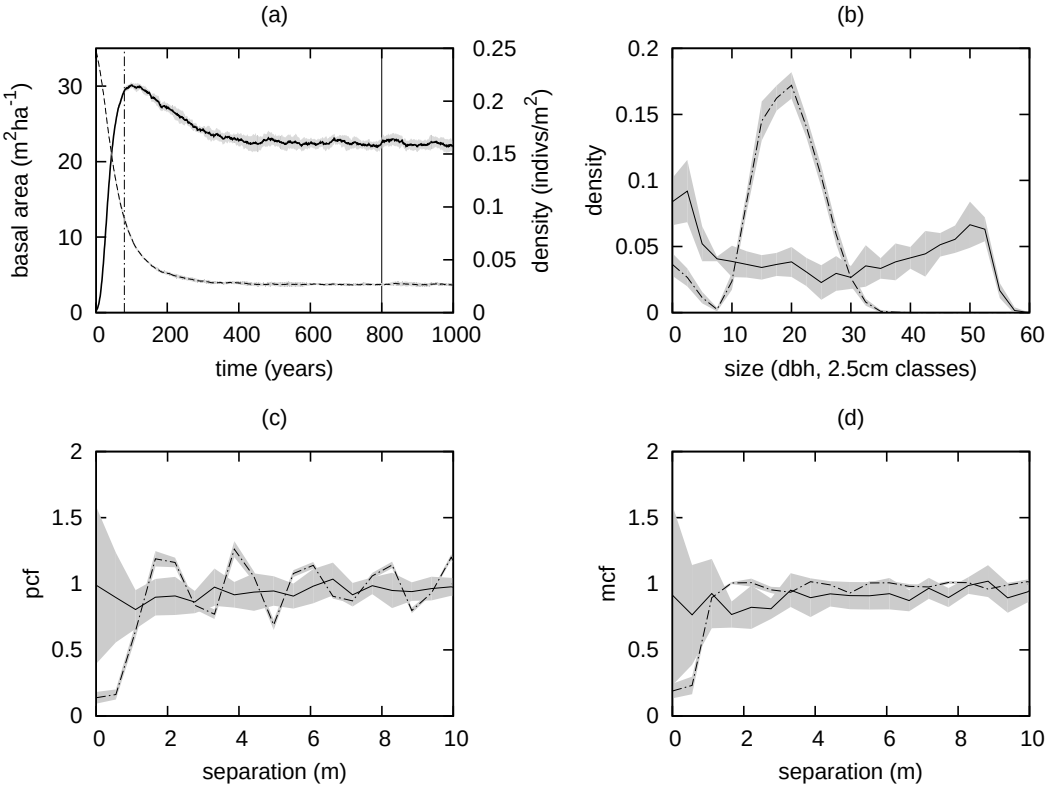

Figure 2.4: The transition from plantation to steady state: development of key metrics through time, based on parameters in Table 2.2. Mean simulation results (of 50 runs) are represented by lines within a grey envelope (standard deviation). (a) Evolution of density (dashed) and stand basal area (solid line). (b) Size distribution at 80 (dash-dot) and 800 (solid) years. (c) Pair correlation function – time/line style as (b). (d) Mark correlation function – time/line style as (b).

is governed by the starting configuration. The PCF clearly shows the signature of the lattice during this stage (Figure 2.4c, 80 years - peaks are at multiples of the lattice spacing). The MCF does not provide a great deal of useful information at this stage due to the regular pattern of trees. The period described above contains the cohort establishment, canopy closure and biomass accumulation stages of Franklin et al. (2002).

Transitional stage

The high basal area (and high competition) state generated during the "plantation" stage means that individual growth becomes stunted, and mortality rates are elevated. Basal area thus reaches a peak. Density-dependent mortality remains high, but is overtaken by density-independent (intrinsic) mortality, which opens gaps in the canopy. Consequently, more substantial regeneration begins to occur (gaps heighten $\mathbb{P}_e$ for many of the potential offspring, while high basal area ensures a large seed source) and a much broader age/size structure begins to develop. The initial regular spatial structure is erased during this period, through mortality, regeneration and differential growth. This change is apparent in both spatial correlation functions (not shown), and in maps of the stand at 300 years (Figure 2.3). During this period, a real stand would also see the accumulation of woody debris. This is the maturation stage of Franklin et al. (2002).

Long-run metastable state ("old-growth")

In the long run, the model reaches a steady state where fecundity, mortality and growth are in balance. Figure 2.4b (solid line) shows the typical size structure present in the long run. Only a small proportion of juveniles attain canopy size, but individuals of all sizes are present, and the asymptotic nature of growth means that individuals accumulate in the higher size classes as the system approaches equilibrium, until the size distribution stabilises. This is a consequence of the ability of trees to survive during periods when they are not growing. Caledonian Scots pine does not readily establish in low light conditions, and consequently produces a fairly low density, open forest. However, it can survive in the shade for long periods, and so local reductions in canopy density temporarily allow trees that have stunted growth to increase in size, refilling gaps. In the parameterisation used, local interaction does not have a great effect on the PCF, which is fairly close to homogeneous (Figure 2.4c). Mortality "due to" interaction occurs at only a slightly higher rate than baseline mortality (at equilibrium, $\mathbb{E}(\Phi_i) \approx 0.925$ in simulated populations, giving an interaction-induced mortality rate of $0.00628 \times 0.925 = 0.00581$).

In many real populations the generic properties of the observed state are actually determined by external disturbances (and the relationship between their extent and frequency), as opposed to demographic properties alone (Turner et al., 1993), bringing into question the utility of the terms "old-growth" or "equilibrium" in respect of real systems. Indeed, Oliver and Larson (1996) point out that due to external catastrophic disturbances, true old growth is rarely reached, taking up to 1000 years to attain.

2.5 Parameter sensitivity

Prior to further analysis of specific aspects of the model, and closer consideration of its behaviour in the context of available data for the populations of interest, it is important to identify the sensitivity of model behaviour to changes in the basic model parameters. The effect upon various representative stand statistics of changing each parameter by up to one order of magnitude about the baseline values used in Section 2.4.3 is considered here – a range which should encompass all realistic values for forest populations. We analyse model sensitivity in the plantation and long-run states separately.

2.5.1 Plantation development

Table 2.3: The effect on plantation development (as summarised by various statistics, detailed in the main text of Section 2.5.1) of increasing any parameter of the model in isolation. Subscripts "80" in the first four columns denotes the value of a statistic at 80 years. The right two columns relate to the point at which stand basal area is a maximum. Increasing "mortality" refers to increasing μ_1 and μ_2 whilst fixing their ratio, and increasing "growth" means increasing both α and β, whilst fixing their ratio.

	Statistic					
Parameter	ρ_{80}	BA_{80}	$\mathbb{E}(s_{80})$	$\mathbb{E}(s_{80})$	BA_{peak}	t_{BApeak}
rates						
f	$+$	$+$	0	$+$	0	$+$
mortality	$-$	$-$	$+$	$+$	$-$	$-$
growth	$-$	$+$	$+$	$+$	$+$	$-$
interaction						
μ_2	$-$	$-$	$+$	0	$-$	$-$
γ	$+$	$-$	$-$	$-$	$-$	$+$
kernels						
k_d	$+$	0	$+$	$+$	$+$	0
k_s	0	0	0	$+$	0	0

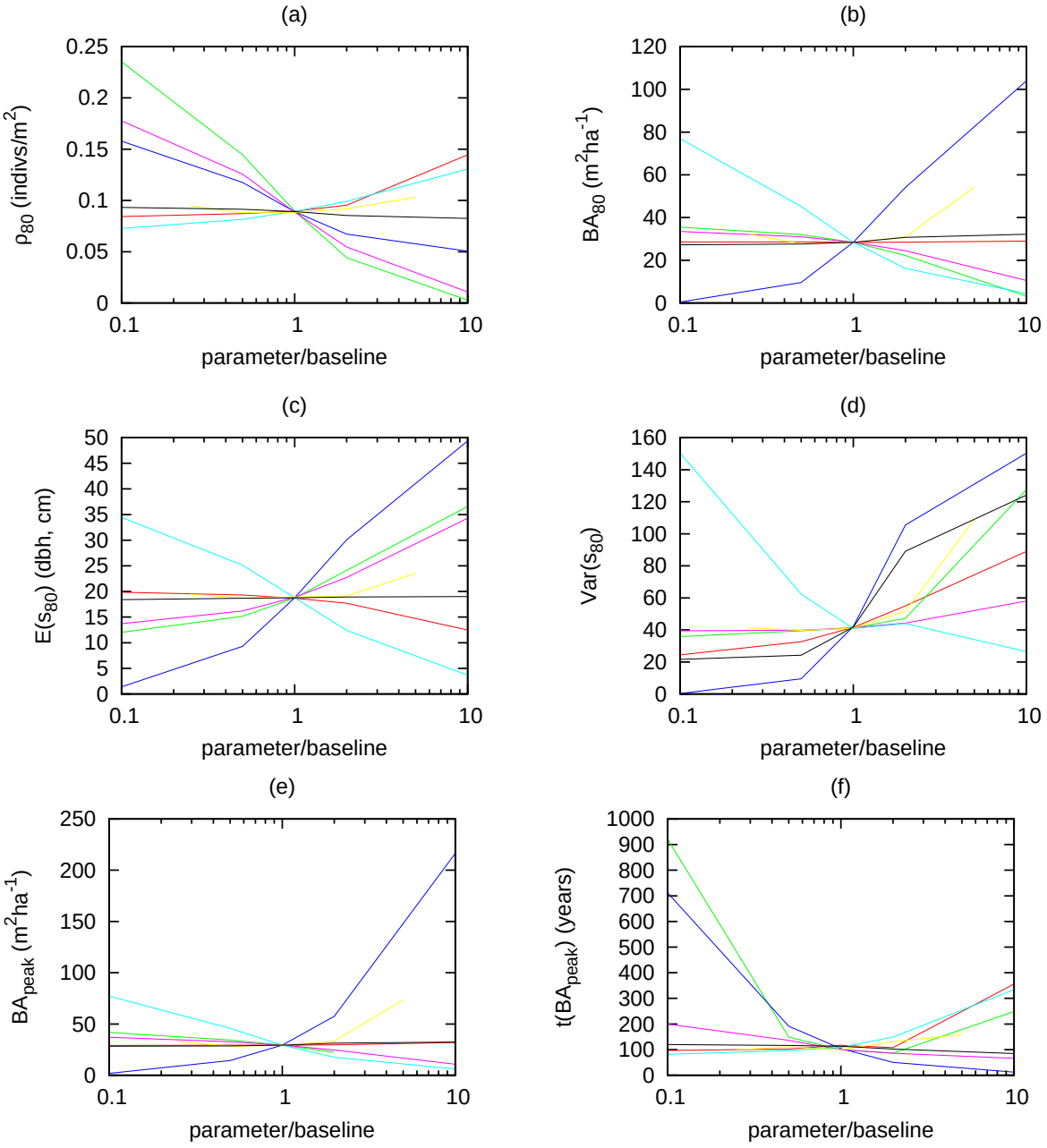

Figure 2.5: *Sensitivity of plantation development* to altering individual parameters (proportional variation from baseline parameters in Table 2.2 on horizontal axis). Statistics are described in the main text (Section 2.5.1). f (red), mortality (green), growth (dark blue), μ_2 (magenta), γ (cyan), k_d (yellow), k_s (black).

Statistics

The effect of parameter variation on the early development is considered by various summaries of the statistics detailed in Section 2.3. In turn, the statistics presented in Table 2.3 and Figure 2.5 are: ρ_{80}; the individual density at 80 years; BA_{80}, the stand basal area at 80 years; $\mathbb{E}(s_{80})$, the mean size at 80 years; $Var(s_{80})$, the variance of the size distribution at 80 years; BA_{peak}, the peak basal area; t_{BApeak}, the time of the peak in basal area (the duration of plantation development).

Results

The gradient of basal area increase (Figure 2.5b), and the magnitude of its peak (2.5e), is positively related to the speed of growth. The magnitude and time of the peak (2.5e) also decreases with increasing mortality rate. Fecundity has little or no effect on the transient to, or position of, the peak. See Figure 2.5(b,c,d).

Plantation size distribution is affected by a number of factors. The maximum size present is largely determined by the growth rate in the absence of competition. The shape and location of the main body of the distribution is then governed by the effect of competition on growth, and to a lesser extent, the mortality parameters. As growth interaction (γ) is increased, the mean size decreases, while increasing mortality leads to an increase in the mean size (since competition is lower as a result: Figure 2.5c). The variance of the distribution is affected to some extent by all parameters (Figure 2.5d), but observation of the actual distributions generated (not shown) indicates that the only parameter affecting the shape of the distribution of "canopy" trees is the asymmetry of competition (k_s – an increase widens the spread of canopy sizes).

The spatial structure of the plantation is defined by the initial condition; any structure present at stand initiation remains evident until a very large proportion of the original trees have been removed through mortality, and juveniles have begun to replace them. Random dispersal means that there is no distinct spatial structure in the regeneration.

2.5.2 Steady state

Statistics

The effect of parameter variation on steady state behaviour is considered by the statistics presented in Table 2.4 and Figure 2.6 are (values at 800 years): ρ, the individual density; BA, the stand basal area; ρ_{canopy}, the proportion of individuals with size greater than half the maximum; s_{max}, the maximum individual size,

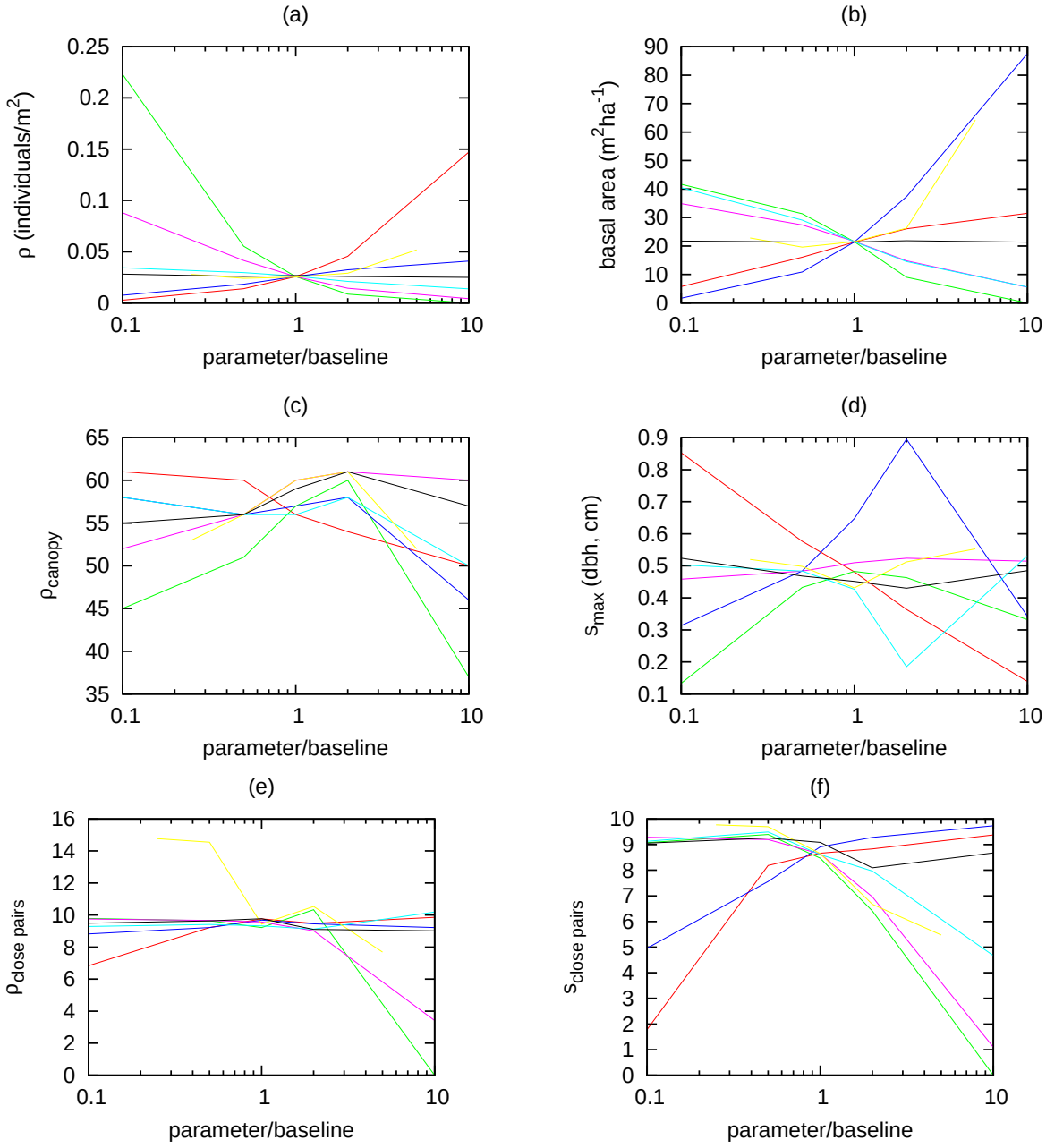

Figure 2.6: *Sensitivity of steady-state statistics* to altering individual parameters (proportional variation from baseline parameters in Table 2.2 on horizontal axis). The statistics are described in the main text (Section 2.5.2). f (red), mortality (green), growth (dark blue), μ_2 (magenta), γ (cyan), k_d (yellow), k_s (black).

$\rho_{closepairs}$; the integral of the PCF from 0–5m separation, $s_{closepairs}$; the integral of the MCF from 0–5m separation.

Table 2.4: The effect on steady state behaviour (as summarised by various statistics described in the main text of Section 2.5.2) of increasing any parameter of the model in isolation. Increasing "mortality" refers to increasing μ_1 and μ_2 whilst fixing their ratio, and increasing "growth" means increasing both α and β, whilst fixing their ratio. A star indicates variation across the observed parameter range, but no clear trend (see Figure 2.6).

	Statistic (steady state)					
Parameter	ρ	BA	ρ_{canopy}	s_{canopy}	$\rho_{closepairs}$	$s_{closepairs}$
rates						
f	+	+	−	−	+	+
mortality	−	−	+	+	0	−
growth	+	+	−	0*	0	+
interaction						
μ_2	−	−	+	+	−	−
γ	−	−	−	0*	0	−
kernels						
k_d	+	+	0	0	−	−
k_s	0	0	0*	0	0	0*

Results

In the parameter space considered, steady state density and basal area are increased by increasing fecundity or growth speed, or decreasing mortality (Figure 2.6a,b). Decreasing mortality further leads to a decrease in steady state basal area. This somewhat surprising result occurs due to the onset of density-limited, rather than mortality-limited, individual growth (due to the resulting higher competition). This result is most likely not relevant to most temperate tree species, however, which continue growing for the duration of their lifespan. In temperate forests, multiple resource limitation, too, means that density is relatively low (overall growth is too slow for very highly competitive situations to arise).

The PCF at short ranges (Figure 2.6e) is insensitive to variation in most parameters, except fecundity, interaction mortality (μ_2) and locality of interaction k_d. Increasing fecundity or growth (or reducing growth interaction) increases the average size of nearby pairs (higher MCF, Figure 2.6f), but has little or no effect on the pair density itself, while increasing k_d reduces the size of close pairs.

ρ_{canopy} (Figure 2.6c) shows large variation with all parameters, and it may be more instructive to consider the distribution visually, as in Section 2.5.3. The

maximum size of trees (s_{max}: Figure 2.6d) is affected most dramatically by fecundity (negative relationship) and growth parameters (increasing growth increases maximum size to a point, after which it decreases). The reason for this unexpected behaviour is likely to be that (in the case of simply increasing growth speed) more trees become larger, leading to an increase in the overall competition experienced by an individual, and a reduction in the effective asymptotic size in the steady state. Growth interaction has precisely the opposite effect.

2.5.3 Visualising parameter sensitivity

The model uses 8 parameters. However, the dynamics of the community depend solely on the three processes operating in the community: growth, reproduction and mortality. The relative speed of these affects the dynamics of the community in a generic way.

A simple way to visualise the behaviour of the model under variation of the basic process rates is given in Figure 2.7. This shows maps of simulated forests at (a) 100 years and (b) 800 years, across a wide parameter space. The x-axis is individual growth rate (changing both α and β, while fixing their ratio – changing the rate at which a common asymptotic size is approached), and the y-axis is the order of f/μ_1 – how quickly a tree reproduces, per unit size, compared to how quickly it dies (fixing ratio μ_1/μ_2). As f/μ_1 increases, the average stand density increases, and the population is less likely to become extinct. As a direct result of this increased density, competition increases, reducing the average size of trees. As growth rate increases, stand density increases, and the size distribution becomes more strongly bimodal (that is, the size of "canopy" trees is larger, and there are relatively more of them).

(a) 100 years

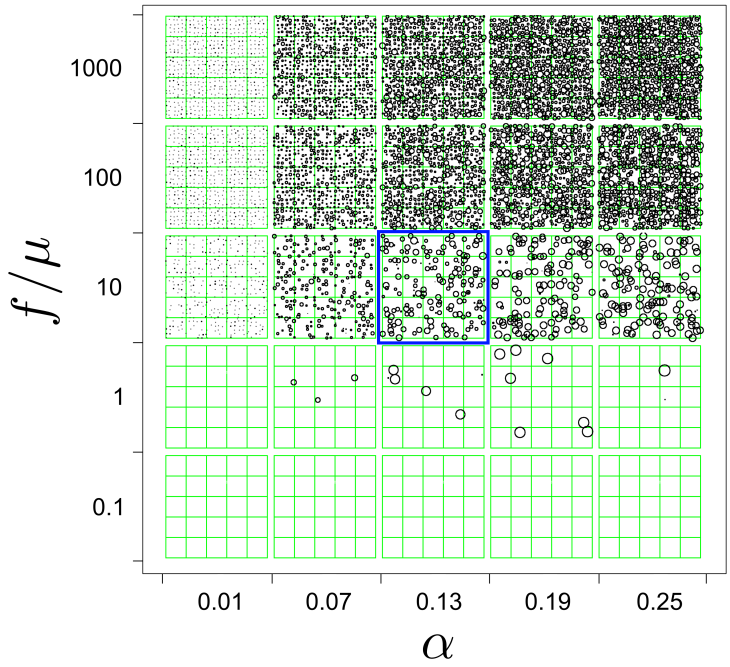

(b) 800 years

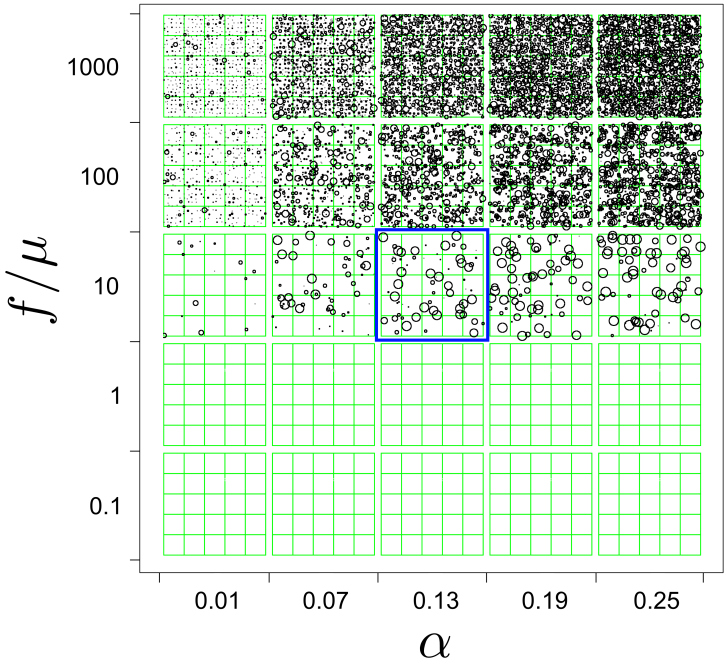

Figure 2.7: *Visualising simulated forests across a wide range of parameter space*, at (a) 100 years and (b) 800 years, each sub-grid showing a single simulation realisation. The horizontal axis shows variation in growth "speed" from approximately 0.5 to 10 times the baseline rate (time to a particular size), while the vertical axis displays variation in the ratio of birth to mortality (f/μ_1, 0.267× actual value), two orders of magnitude either side of the baseline (results using the parameters in Table 2.2 are marked with a blue box).

2.6 Equivalent mean-field interaction ("density dependent") model

2.6.1 Outline and definition

The model described above incorporates explicit size and spatial dependence. However, it is instructive to compare the results of the complete model with those obtained using a *mean-field* model, which is simpler to simulate and comprehend.

In this case we remain interested in the development of size-structure, but would like to remove spatial dependence of all events. The process may still be simulated in a spatial arena, but any spatial pattern is incidental to the dynamics. In a mean-field model, each individual has an identically "average" experience of life in the population. Essentially, this amounts to interaction being defined solely in terms of size, and the average population density distribution.

First, the count of individuals over size and space is approximated as $N(\vec{x}, s) = N(s)\mathbb{P}(\vec{x})$ where $\mathbb{P}(\vec{x})$ is the probability of being located at $\vec{x}$; the spatial distribution of trees is independent of the size distribution. This allows the decomposition of the interaction computation into distance and size components:

$$\Phi_i(t) = \sum_{x_j} F_2(\vec{x}_i - \vec{x}_j)\mathbb{P}(\vec{x}_j) \sum_{s_j} F_1(s_i, s_j)N(s_j). \tag{2.18}$$

In the limit $d\vec{x}_j \to 0$, the integral $\mathbb{P}(\vec{x}_j)$ over the simulated spatial arena of area A must yield 1.That is:

$$\int_A \mathbb{P}(\vec{x}_j)d\vec{x}_j = 1. \tag{2.19}$$

An assumption of constant density over space (that is, $\mathbb{P}(\vec{x}_j) = \text{constant}$) thus gives $\mathbb{P}(\vec{x}_j) = 1/A$. Letting $F_2() = 1$ everywhere, the first sum in Equation 2.18 takes the value $1/A$. Interaction in the mean-field version of the model is defined thus:

$$\Phi(s_i, t) = \frac{1}{A} \sum_{j \in \omega_i} f(s_i, s_j) \tag{2.20}$$

$$f(s_i, s_j) = s_j \tanh\left(k_s \ln\left(\frac{s_j}{s_i}\right) + 1\right) \tag{2.21}$$

2.6.2 Mean-field/spatial model comparison under "Scots pine" parameterisation

Figure 2.8 compares the basic behaviour of the mean-field model with that of the spatial model, under identical parameterisation (see Table 2.2). The evolution of basal

area is shown in Figure 2.8a; while the two trajectories are initially the same, in the long run the basal area of the mean-field model is lower, but not dramatically so (around 10%). Differences in the evolution of density are not discernible between the models, under this parameterisation.

Figure 2.8b shows size distributions of the mean-field model (red), and the spatial model (black/grey). At early times (80 years), the size distribution of the two models is almost identical; the homogeneous initial condition meaning that even in the spatial model, interaction is fairly similar for all individuals. The equilibrium states are somewhat different. Both models produce a bimodal distribution, with peaks at the smallest size (juveniles) and just below $s^* = \exp \alpha/\beta$ ("canopy" individuals). However, since each individual in the mean-field model experiences competition based solely upon its size, a sharply peaked canopy density in the size distribution is generated, as each individual has identical asymptotic size. Under the spatial model, the variation in competition over space leads to a blurring in size of the canopy, represented by a lower density, higher variance peak. Space appears to be essential in recreating the size variability in canopy trees that is observed in real forest communities.

A final point is that spatial correlation functions computed from data stands and the spatial model (compared in Figure 4.4a,b) display inhomogeneous (spatially non-random) patterns of individual location and size, which are impossible to recreate under a mean-field model (with random dispersal, and no neighbourhood effect, intrinsic spatial structure cannot occur).

The mean-field model, with its lack of spatial dependence, lends itself to a simple differential equation representation, while the spatial model is less simple to describe in this way. Such approximations are discussed in Chapter 5.

2.6.3 The mean-field model and parameter variation

The limited impact of explicit spatial interactions upon first order properties is a common observation in temperate forest ecology (Deutschman et al., 1999; Busing and Mailly, 2004). Under what circumstances would spatial effects become more important?

It might be expected that in dense spatially interacting populations, local variation in neighbourhood would allow increased growth in comparison with mean-field interactions. However, this is not seen in our model (under either low mortality or high fecundity, Figure 3a,b). Rather, in low density populations, the difference between the two models increases (density/basal area in the mean-field model being comparatively higher, Figure 2.9a,b) - an effect of finite area. Spatial interactions only

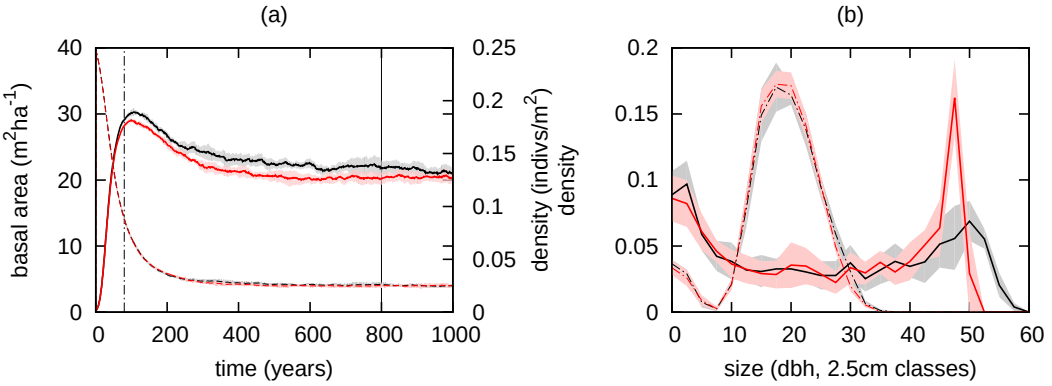

Figure 2.8: *Mean-field vs spatial simulations*. Comparing the basic behaviour using parameters from Table 2.2. Mean/standard deviation for spatial simulations is shown by black lines/grey regions, and for mean-field in red. (a) Total stand basal area (solid lines), which is consistently lower for the mean-field model than the spatial model (line) (despite individual density being almost identical – dashed lines). (b) Size density distribution at early time (80 years, dash-dot line) and equilibrium (800 years, solid line). The mean-field model produces a sharp "canopy" peak, whilst the spatial model has a higher variance in this region. This is much more in keeping with patterns observed in real data for forest trees (spatial model comparison with natural stands is shown in Figure 4.4).

directly affect the realised density when the overall effect of interaction is relatively strong in relation to basic population rates. That is to say, increasing γ (the effect of interaction upon growth) or μ_2 (the effect of interaction upon mortality) both widen the gap between simulated spatial and mean-field populations (mean-field populations having the lower density/basal area - Figure 2.9d,e). Increasing k_d (localisation of interaction in the spatial model) reduces the effective neighbourhood size, and as a consequence increases density and basal area (Figure 2.6).

2.7 Summary

A simulation model of individual birth, growth and death was introduced, which incorporates interactions between individuals. In order to illustrate basic properties, such that they are comparable with other forest data, the model was parameterised using data from Caledonian Scots pine stands (detailed more comprehensively in Chapters 3 and 4). However, it was found that behaviour is robust to fairly substantial parameter variation about the values used – no fundamental changes are observed.

The behaviour of the model replicates the qualitative models of forest stand development discussed by authors such as Oliver and Larson (1996) and Franklin et al. (2002), which were developed by observation of forest stands in nature, as opposed

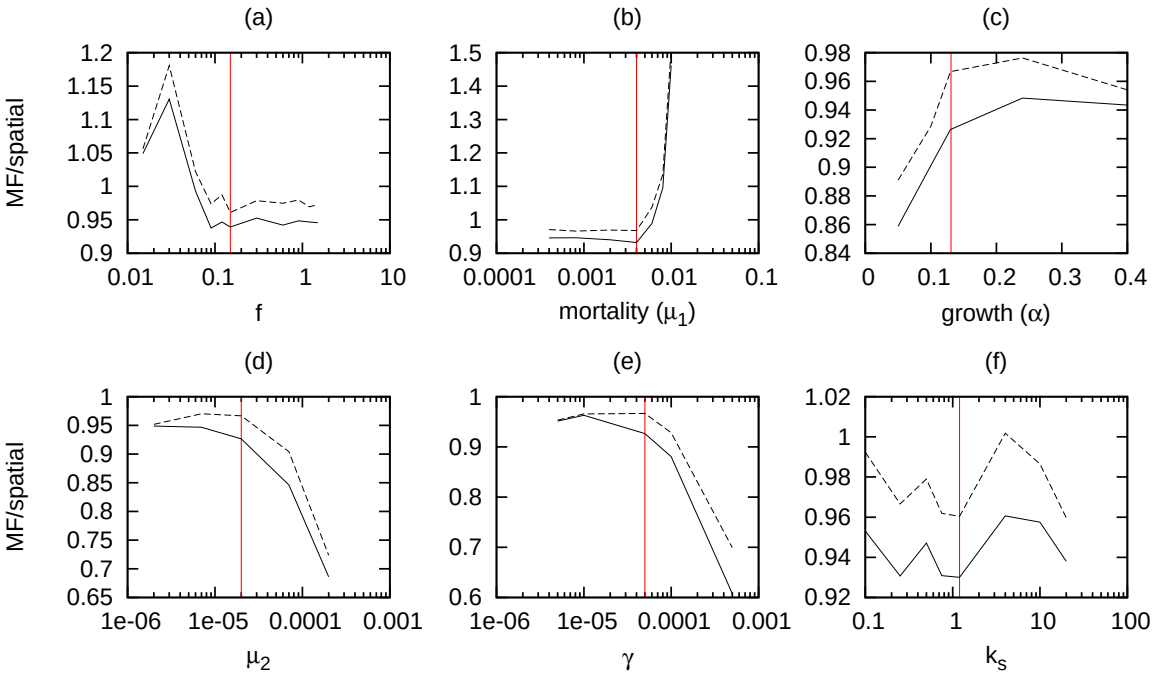

Figure 2.9: *Mean-field vs spatial simulations – changing parameters.* The effect of space Sensitivity of the discrepancy between mean-field and spatial model density (dashed line) and basal area (solid line) to model parameters (keeping all others fixed at values in Table 2.2). Altering growth entails altering both α and β, fixing their ratio (the value of α is shown). A mortality change entails altering both μ_1 and μ_2 fixing their ratio (the value of μ_1 is shown). Size distributions do not display any more distinct difference than that seen in Figure 2.8.

to theoretically. This comparison is useful both in affirming the dynamics of the simulation model, and in understanding different stages of stand maturity, identifying the most important processes as the population develops.

A comparison between mean-field and fully spatial models was made. The output of the models is fairly similar, the main difference under the "Scots pine parameterisation" being the level of variation in canopy individual size. This is because of the relatively weak influence of interaction on individuals' growth. Differences become more apparent by altering the parameters – but only those directly applying to interaction.

Chapter 3

Analysis of Scots Pine growth data

3.1 Introduction

The growth of trees in plantation stands is generally observed to be fairly homogeneous. In natural stands (and indeed non-natural stands which have developed unhindered for a long time), variation is evident; individuals of the same age having allocated biomass differently (to trunk, branches, foliage, and so on), or simply growing at different rates overall.

The simulation model described in Chapter 2 implements a growth function for a single size measure, dbh – "diameter at breast height" (1.3m above the ground). It assumes that the sole determinants of dbh growth rate are dbh itself, and a measure of local interaction, Φ. There is no memory of previous states, and factors such as height, age, and morphology are subsumed into dbh and Φ. This reflects both the data that is generally available for forest stands, and the desire to retain as simple a simulation model as possible.

In order to determine whether the data justify additional model complexity, this chapter has several key goals relating to the growth of Scots pine stands:

- identify the main determinants of individual growth (Section 3.3)
- identify the generic form of individual growth (Section 3.4)
- understand observed variation between individual growth trajectories (Section 3.5)

The overall goal of the chapter is to identify the most appropriate mechanistic model of individual tree growth for Scots pine, both in terms of adequately explaining the available data, and being appropriate to the goals of the simulation model described in Chapter 2.

Figure 3.1: *Example radial increment cores* (not from trees at the Black Wood of Rannoch). From increment cores such as these, it is possible to determine a tree's (radial) growth rate at all points through its life. However (in common with some trees at Rannoch), these cores exhibit clear asymmetry, which means that radial increment is not necessarily an accurate predictor of total growth. `http://www.tree-ring.co.uk/images/TreeSpecies_files/CoreCHHF5_6.jpg`.

3.2 Data

The main dataset used for analysis in this chapter was collected at the Black Wood of Rannoch by Forest Research, UK Forestry Commission. Several study plots were established in 1948, but the area has not been subject to management within the last 90 years, hopefully allowing insight into the natural growth of uneven-aged stands. The location of the (few) dead trees in 1948 is also known, and it is thought that no other trees were present in the plot after WW1.

There are four 0.8ha (80×100m) plots ($j = 4, 5, 6, 7$), which were surveyed in 1983, 1994 and 2005, with diameter $s_i(t)$ and location $\vec{x}_i$ of all trees ($i = 1, .., N_j$) recorded at each survey. Additionally, at the 1994 survey, radial increment cores (giving historical annual radial growth increments $g_i(t)$, Figure 3.1) were taken from all sufficiently large trees at a height of 1.5m above the ground. This allows age $a_i(t)$ to be determined, and estimation of individual diameter at previous times ($s_i(t) = s_i(1994) - 2\sum_t^{1994} g_i(t')$). Increment core data is not typically available for forest stands, especially at this level of detail (for every tree in the stand, with spatial locations known). The data thus provide a unique opportunity to study the effects of neighbourhood upon individual growth.

Chapter 2 defined a measure of local interaction for an individual, $\Phi_i(t)$. For the data plots this is computed at the current time using the location and size measured by the surveys, and is estimated for previous times using $s_i(t)$ for all trees "present" in the data at t. The true value of $s_i(t)$ (and consequently $\Phi_i(t)$) becomes less certain the further back in time the estimate; furthermore, $\Phi_i(t)$ must be considered unknown prior to 1918 as other unknown trees were present.

There are several other complicating factors with the data. Firstly, increment data is only available for a small subset of the trees in Plot 5, and it is therefore not considered here. Secondly, Plot 6 has a region at one corner for which a survey was not made, due to the establishment of a survey by another organisation. Finally, a

pylon line was laid through Plot 7 in 1972; the locations, but not the sizes, of the trees that were removed are known.

In summary, and with the caveats noted above, the data may be treated as quintuples consisting of:

- location $\vec{x}_i$
- age $a_i(t)$
- size (diameter at breast height) $s_i(t)$
- growth rate (radial increment) $g_i(t)$
- interaction $\Phi_i(t)$

for $t(years) \in [1918, 1994]$, for each individual $i = 1, .., N_j$, for each plot $j = 4, 6, 7$.

3.3 What are the determinants of growth in Scots pine stands?

This section aims to identify the principal determinants of individual growth rate $g_i(t)$. In preliminary investigations, a variety of approaches were investigated. These investigations used one of two simplifications of the data: (i) the entire data set, treating all quintuples as independent (ignoring the fact that they consist of repeat measures from a group of individuals), and (ii) considering quintuples from a single year (only one from each individual). Various regression techniques (linear models/analysis of variance, nonlinear least squares, generalised additive models) were applied using both simplifications. In general, fits were very poor, with limited explanation of the data. Statistically, there are clear issues with approach (i) above, such as non-independence of measurements from the same individual, and fewer measurements at earlier times (not all individuals were present in 1918). The fact that each growth/size measurement actually sits on an "individual" curve leads to a strong skew in the residuals of fits using the entire dataset in this way. Neither does using data from only a single year allow useful analysis; it is found that growth increments exhibit large scatter with respect to all other variables considered in isolation.

Figures 3.2 and A.1 (Appendix A.1) show *regression trees* (Breiman et al., 1984; Ripley, 1996 – outline of algorithm in Appendix A.1) computed for growth in each of plots 4, 6 and 7. These aim to determine the most important descriptors in variation of the dependent variable, and how they affect one another. This variation is represented by binary splits, enabling identification of regions in the data values where certain variables interact and become important.

Figure 3.2 includes only age, size and competition (interaction) as explanatory variables. To understand the information presented in the figure, lets us consider first plot 4 (Figure 3.2a). The top node informs us that age is the most important explanatory variable for growth. The vertical length of the branches indicates the relative amount of variation explained. For trees that are younger than 72.5 years, the next most important variable is (instantaneous) interaction. For the trees that are younger than 72.5 years, and experience interaction of less than 194.988, growth is most greatly dependent upon a further subdivision of age; those that are younger than 15.5 years experiencing a mean growth rate of 0.7241cm yr^{-1}, whilst those that are above this threshold experience a mean of 0.4419cm yr^{-1}. The other branches may be interpreted in a similar way.

The effect of interaction is less prominent in the regression tree computed for plot 6 (Figure 3.2b). The second most important variable after age for this plot is size. For young, small individuals, competition is a factor in the growth rate, though much less important than age or size.

In plot 7 (Figure 3.2c), age is also the most important variable, followed by interaction. This is the only plot in which current interaction is determined to be an important factor for mature trees. It is also the stand containing fewest old trees.

Figure A.1 (Appendix A.1) present similar information to Figure 3.2, but also includes location. This is an important factor in determining growth (particularly in plot 6), but in general the patterns are not *trends* at the scale of the plot, which might be suggestive of small-scale environmental heterogeneity. Furthermore, location does not explain a great deal of additional variance in stands 4 and 7.

These results point primarily to the importance of age in determining individual growth rate. Intuitively this is sensible, as all individual growth curves level out over time, but to different sizes (Figure 3.3). This conclusion is however based upon consideration of all data points individually, and the data are not evenly represented across age/size/competition, as mentioned above. Furthermore, the fact that variation exists between individual curves is indicative that growth *cannot* be described deterministically by age or size: competition or another source of variation must also have an effect (Section 3.5).

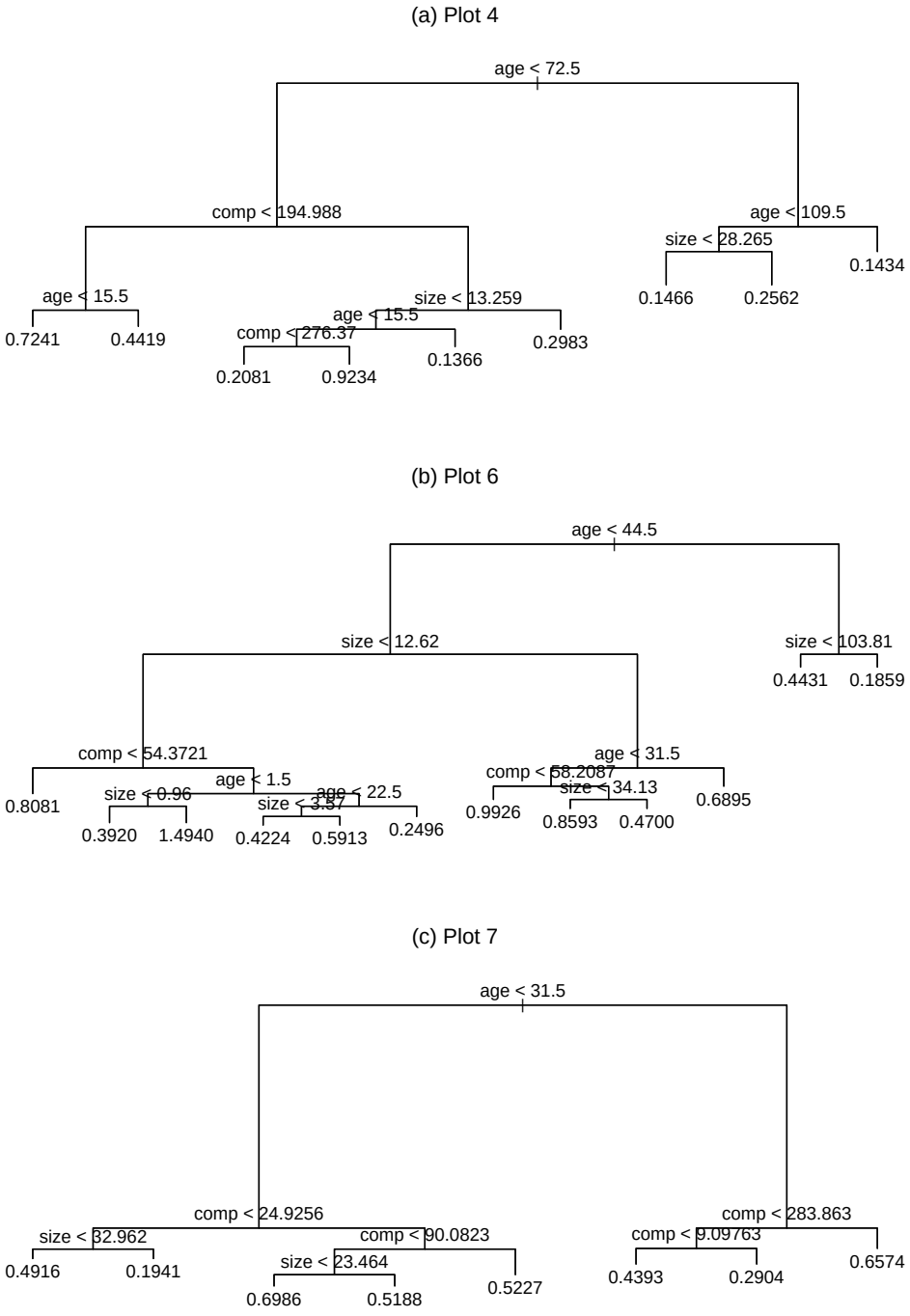

Figure 3.2: Regression trees computed for post 1918 growth increments from each of Rannoch (a) Plot 4 (b) Plot 6 and (c) Plot 7. These seek to identify the primary sources of variation in growth increment, and any interactive effects between them. In each case, age is the most important variable. Plot 5 is omitted due to missing data points.

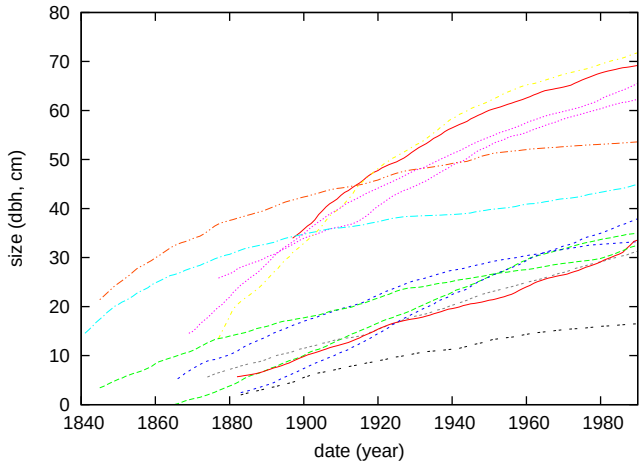

Figure 3.3: Growth curves from a selection of individuals in the Rannoch 4 study plot. Individuals from within one stand have a wide range of apparent asymptotic sizes.

3.4 General growth form

3.4.1 Background

Chapter 2 made the assumption that individual growth is a function of size, and that it follows the Gompertz function. While this is supported by many previous studies of forest trees (Zeide, 1993) and other plants (Schneider et al., 2006), we would like to determine whether this is indeed the most appropriate function for this purpose – Section 3.3 suggested that age dependence may be more appropriate.

That behaviour is characterised solely by a single size measure simplifies model behaviour and makes analysis more tractable, and means that there is no inherent memory in the system. We also have less interest in the age of trees, in terms of the structural characteristics of a forest.

There is some empirical support from other statistical studies that assuming growth dependence upon local interaction and size is the best approach (Larocque, 2002; Martinez-Vilalta et al., 2006). Mencuccini et al. (2005) found that decline in growth often attributed to age can generally be expressed solely with respect to size. Nonetheless, the results from Section 3.3 suggest that the primary factor influencing individual growth is age. This is supported by plotting a selection of individual growth curves extant in Rannoch plots (Figure 3.3). Each curve appears to asymptote (trees approach a fixed size in the long run), but the apparent asymptotic size varies dramatically. Thus, it is important to consider models in which growth asymptotically approaches zero with increasing age as well as (or instead of) increasing size.

In this section, we analyse the properties of individual growth curves. We would like to determine which functions best describe the general form of growth, and identify the level of parametric variation within the population. Size-dependent models are considered first, followed by age-dependent models. The data used for this section are all growth curves from plots 4 and 6 (omitting trees from a 10m wide boundary region in the plots).

The main tool for this section will be *non-linear mixed effects* (NLME) analysis. This entails dividing the data into subsets (in this case, a single individual's growth increments), and fitting a predefined functional form to each using non-linear least squares. This ensemble of curves can then be used to compute the mean, variance and covariance of the parameters for the functions. Full details are given in Appendix A.2.

3.4.2 Analysis

Size-dependent models

The Gompertz equation, used in Chapter 4, relates diameter growth rate to current diameter:

$$\frac{ds(t)}{dt} = s(t)\left(\alpha - \beta \ln(s(t))\right) \tag{3.1}$$

(with an additional term incorporating competitive interactions). This equation is a special case of a more general model developed by Richards (1959):

$$\frac{ds(t)}{dt} = \frac{\kappa}{1-\delta} s(t)\left(\left(\frac{s(t)}{w}\right)^{\delta-1} - 1\right). \tag{3.2}$$

w is the maximum size, and κ is the growth rate parameter. δ controls the position of the point of inflection; taking $\delta \to 1$ gives the Gompertz model (representing Equation 3.2 using a power transform; see Lei and Zhang, 2004). Other commonly used special cases are the *monomolecular* model ($\delta = 0$, with point of inflection at the origin: $ds(t)/dt = \alpha - \beta s(t)$), and the *logistic* model ($\delta = 2$: $ds(t)/dt = s(t)\left(\alpha - \beta s(t)\right)$ (Seber and Wild, 1989).

To assess which of these special cases best describes the general growth form, consider first fitting Equation 3.2 to the available data via NLME analysis (at this stage neglecting interaction between trees). Probability mass functions for each parameter across the population are presented in Figure 3.4.

δ has a population mean of 1.372 and median of 0.675. It takes continuous values, but its modal value (from the mass function with bin width 0.5) is between 0 and 0.5. While there is a reasonably clear peak at zero, the estimated distribution of δ for the population (Figure 3.4b) shows fairly high variance, with a significant density

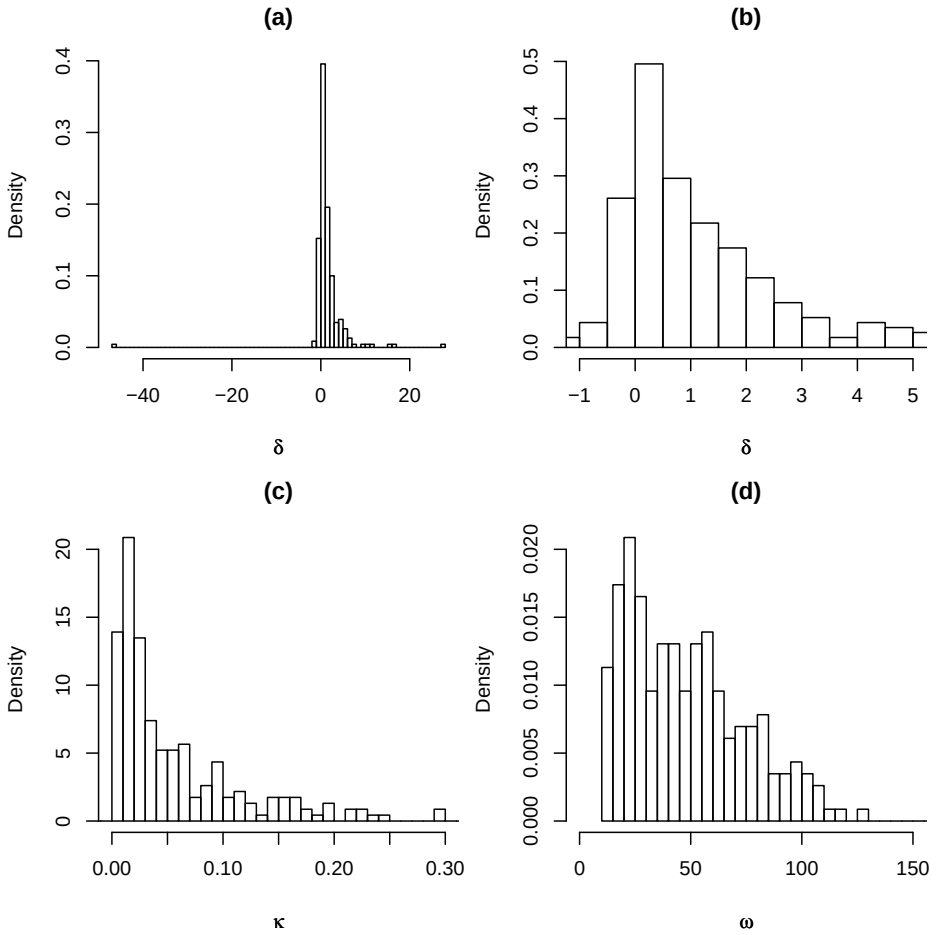

Figure 3.4: Estimated population parameter distributions, fitting the Richards growth model (Equation 3.2) to all available individual growth curves from Rannoch study plots (growth versus size only; no interaction/competition term). (a) δ (b) δ – a more detailed view of the highest density part of the distribution – twice as many bins as (a). (c) κ (d) ω.

across the range characterised by the three proposed special cases. Furthermore, the distribution of all parameters is skewed (there is a discrepancy between mean and modal values) – a non-Gaussian distribution suggesting systematic variation between individuals, not caused by randomness alone.

Fitting instead each special case to the data suggests that the monomolecular model is the most appropriate (though it is not a much better fit than the Gompertz). Table 3.1 presents these results: a lower AIC (Aikake's An Information Criterion, Aikake, 1974) or lower residual standard error (RSE) indicates a better fit to the data (see Appendix A.3).

There are some issues, however, mainly associated with the lack of complete

Table 3.1: *Size-dependent growth model fits* (no interaction/competition term). Estimated parameters for non-linear growth models fitted to data from Rannoch plots 4 and 6 combined (plot 5 and 7 omitted due to missing recent management history; growth curves computed based upon all increments for individuals further than 10m from an edge). Functions fitted are given in Section 3.4.2. The numbers in brackets denote the correlation between the estimated fixed effects parameters: $(\rho_{\alpha\beta})$.

	nlme			
	Fixed (μ)	Random (σ)	RSE	AIC
monomolecular				
α	0.622	0.401	0.119	-10767.69
β	0.00149	0.0169	(0.56)	
Gompertz				
α	0.144	0.104	0.123	-9935.3
β	0.0410	0.0344	(0.983)	
logistic				
α	0.0773	0.0661	0.135	-8035.31
β	0.00331	0.00408	(0.939)	

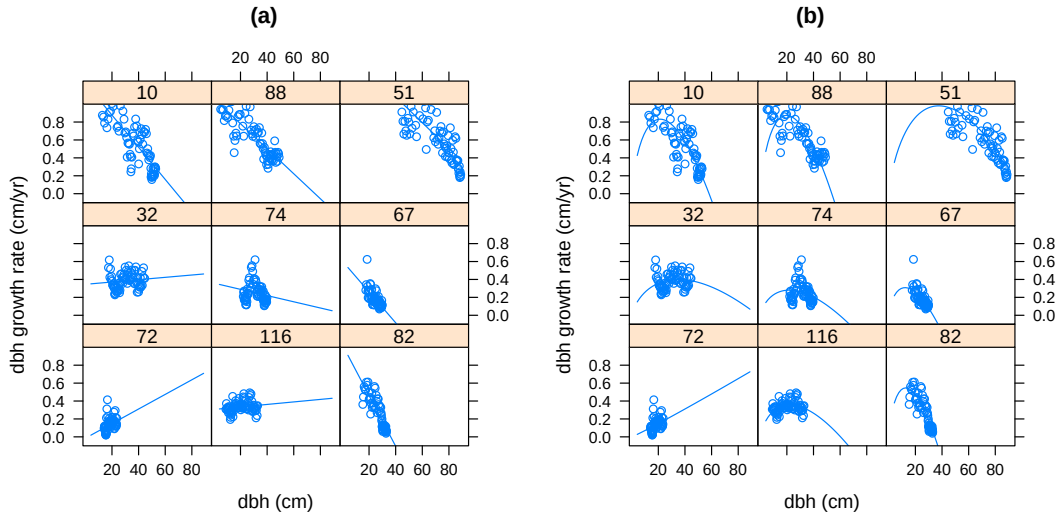

Figure 3.5: A selection of fits to individual growth increment data from Rannoch Plot 4 using the (a) monomolecular and (b) Gompertz models. The number above each curve is a tree's identifier in the stand. Note tree 72, which does not have sufficient data to estimate a biologically realistic growth curve under either model. This problem appears more prevalent with the monomolecular model, and can lead to a negative estimated population mean for β.

data for growth over the life of each tree. In certain circumstances, the data for the growth of an individual may give the impression of, and be best fit by, a biologically

impossible function. Consider, for example, the selection of fits computed in Figure 3.5. Under both the monomolecular and Gompertz models, the best fitting curve for tree 72 gives a growth rate *increasing* with size, rather than approaching zero (β is negative in the estimated growth function). This is clearly impossible; trees do not have the capability to grow without limit. This issue is more prevalent in parameter estimation for the monomolecular model; for example, the best fit for tree 32 in Figure 3.5 is again biologically implausible under the monomolecular model, but is acceptable under the Gompertz model. This negativity is reflected in the parameter estimates in Table 3.1: the fixed effect (population mean) estimate for β is the monomolecular model is very low. Worse still, the fixed effect is found to be negative once interaction has been included in the fitted model (see Section 3.5).

In terms of fit quality (for individual fits) there may be little to choose between the three models, but many of the individual sets of growth increments clearly display curvature, which is impossible to recreate without a point of inflection. Including interaction *could* account for curvature, but a negative second derivative (that is "downward" curvature) would imply that interaction has greater effect on large trees.

Measurement error (and tree asymmetry) means that most trees do not "start" at zero dbh (Figure 3.3). As the main difference between the proposed growth models is the initial curvature in growth rate, it is useful to consider additional data relating to this stage of the life-cycle.

Early growth – sapling section data

Sarah Taylor and Colin Edwards (2007, unpublished) collected age and diameter profiles for young trees (by destructive sampling close to the study plots at the Black Wood of Rannoch and in Glen Affric). The main goal of this work was to determine the amount of time taken to establish by Scots pine and Birch saplings, but the collected data also contains information relevant to the determination of early growth patterns.

Curvature in initial height growth is clearly demonstrated (see Figure 3.7a) and we know that it asymptotes with age, which supports the use of a sigmoidal height growth curve with a point of inflection at $t > 0$. Diameter profiles (diameter measured at height intervals from base to tree tip – Figure 3.7b) show that diameter generally decreases roughly linearly (with the same gradient for most trees, regardless of light conditions) over the height of juvenile trees, with a widening at the base. However, *dbh* growth does not "start" at the same time as height growth. By the time trees are 1.3m tall (breast height), some are entering a period of linear height growth (Figure 3.7a), but others are not. This suggests that for some trees, a monomolecular model would be appropriate, but the annual increment data makes it clear that it is not applicable in all

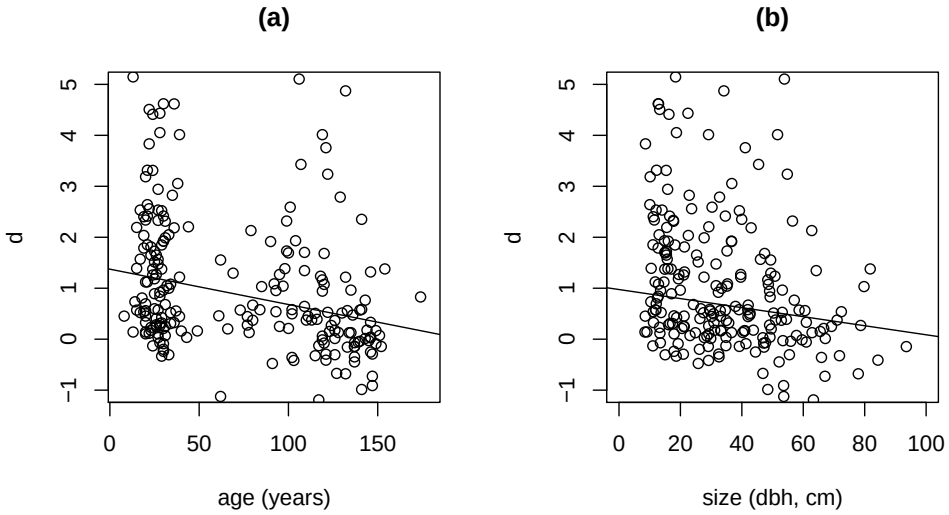

Figure 3.6: Correlation between estimated Richards curvature parameter and tree (a) age (b) size, at 1990. A value of $\delta > 0$ means that the estimated growth curve displays a period over which growth rate is increasing. This type of model (sigmoid) receives more support from available data for young or small trees than that for mature trees.

cases – it is found that juveniles tend to provide more support for sigmoidal growth curves (Figure 3.6). The non-zero point of inflection of the Gompertz growth curve allows greater flexibility in fitting. In practice, curves fitted under NLME could have differently located points of inflection (through random effects), thus more realistically representing particular individuals.

Age-based models

Given results from Section 3.3, we might expect models including age as an explanatory variable to provide a better fit to the observed growth increments. For example, an age-based model analogous to the Gompertz function could be used:

$$\frac{ds(t)}{dt} = t(\alpha - \beta \ln(t)) \tag{3.3}$$

where t is the number of years since birth. A problem in this and other formulations involving a decreasing function of age is that growth can become negative. If a simulated individual survives to $\exp(\alpha/\beta)$ years of age, any further increase in age will induce negative growth. Obviously this does not happen in the size-dependent model: size cannot continue to increase independently of growth! Negative growth might be acceptable if $s(t)$ is viewed as a measure of "health", with trees dying once

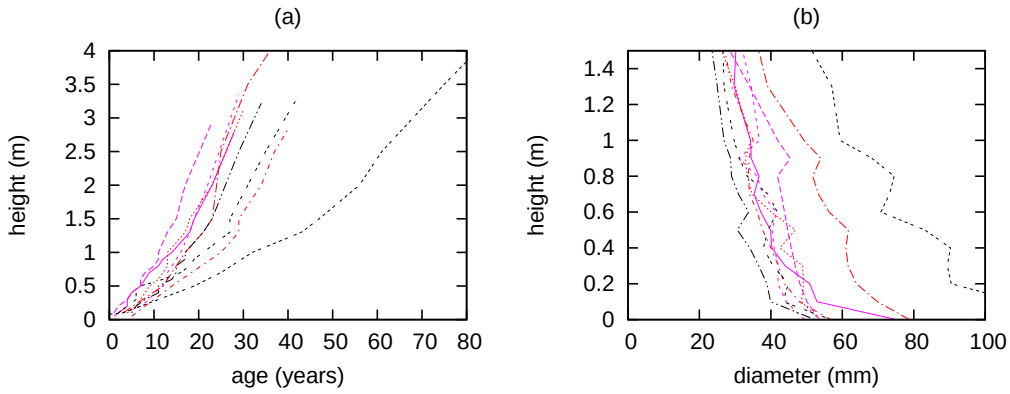

Figure 3.7: *Growth profiles of juvenile trees*. (a) Height growth versus time, for a sample of saplings growing near to the Rannoch study plots, collected and analysed by Taylor and Edwards (2007, unpublished). The curve colour indicates the (roughly categorised) light conditions under which the sapling was found: full overstory (black), canopy gap (red), open (pink). (b) Sapling diameter profiles, measured from ground up to 1.5m, for the same trees. Colours as (a).

$s(t)$ became less than zero. In the simulation model, however, $s(t)$ also determines how a tree interacts with its local neighbourhood. A more desirable option is the use of a function that approaches zero in the limit of old age, for example

$$\frac{ds(t)}{dt} = \beta \exp(-\kappa t). \tag{3.4}$$

The could also be combined with the size dependent model to give a non-negative growth rate that approaches zero, either in old age or at a defined (asymptotic) size:

$$\frac{ds(t)}{dt} = s(t)(\alpha - \beta \ln(s(t))) \exp(-\kappa t) \tag{3.5}$$

Here, the value of κ determines the relative importance of age and size.

The results of fitting each model to amalgamated data (all post-1918 data from plots 4, 6 and 7) are summarised in Table 3.2. The quality of fit is broadly similar to the best of the size-structured models; slightly, but not notably, better. Fitting Equation 3.5 to the data leads to a biologically implausible negative estimate for β. This may reflect the fact that interaction is not explicitly included in the function – large or old trees are likely to experience less interaction than smaller ones. However, as stated previously, replacing size with age as the explanatory variable *can not* directly explain any variability in growth trajectories – only one curve can ever be described by an estimated function. This issue is tackled in Section 3.5.

Table 3.2: *Age-dependent growth model fits* (no interaction/competition term). Estimated parameters for non-linear growth models fitted to data from Rannoch plots 4 and 6 combined (plot 5 and 7 omitted due to missing recent management history; growth curves computed based upon all increments for individuals further than 10m from an edge). The numbers in brackets denote the correlation between the estimated random effects parameters: $(\rho_{\alpha\beta})$ or $(\rho_{\beta\kappa}), (\rho_{\alpha\kappa})$.

	nlme			
	Fixed (μ)	Random (σ)	RSE	AIC
$\frac{ds(t)}{dt} = t(\alpha - \beta \ln(t))$				
α	0.756	0.709	0.119	-10777.34
β	0.0602	0.194	(0.906)	
$\frac{ds(t)}{dt} = \beta \exp(-\kappa t)$				
β	0.611	0.356	0.120	-10806.02
κ	0.00152	0.0168	(0.463)	
$\frac{ds(t)}{dt} = s(t)(\alpha - \beta \ln(s(t))) \exp(-\kappa t)$				
α	0.111	0.728	0.110	-11851.31
β	-0.0689	0.0759	(0.431)	
κ	0.0307	0.0273	(-0.252	-0.930)

3.5 Explaining individual growth variation

The NLME fits detailed in Tables 3.1 and 3.2 display large random effects parameters, while naive regression to size, age and other explanatory variables leaves high levels of unexplained variation. These features illustrate the importance of individuality, but raises a question of how such variation arises.

3.5.1 Interaction

Instantaneous

The spatial nature of real populations is one of the most commonly suggested sources of variation between each individual's experience, and the consequent development of inhomogeneous structure (e.g. Bolker and Pacala, 1999; Law and Dieckmann, 2000; Illian et al., 2008).

Plants exist in a fixed location in space, leading to the idea of a "plant's eye view" of the world (Law et al., 2003). The mathematical treatment of local neighbourhood effects has its origins in theoretical physics (the concept of a "potential") and was later adapted by authors of forestry yield models. These have used "competition indices", descriptors of an individual's local neighbourhood, for several decades (see e.g. Biging and Dobbertin, 1992, 1995 or Pommerening, 2002).

The general idea is that the presence of neighbours in some way influences the ability of a tree to grow, survive or reproduce. Typically, in the realisation of a simulation or empirical model, some integral (containing functions of relative size and location) is computed across the current state of the population, and an additional term is added into the expressions describing individual demographic (e.g. growth, mortality) rates. For an individual i, this term is most simply defined proportional to:

$$\Phi_i(t) = \sum_{j \in \omega_i} F(s_i(t), s_j(t)) G(\vec{x}_i, \vec{x}_j) \tag{3.6}$$

where ω_i is the set of all individuals excluding i. It is most simply included additively. For example, in a monomolecular growth function:

$$\frac{ds_i(t)}{dt} = \alpha - \beta s_i(t) - \gamma \Phi_i(t) \tag{3.7}$$

In this case, growth is slowed, and the asymptotic size taking into account interaction at time t is $s_i^*(t) = (\alpha - \gamma \Phi_i(t))/\beta$, as opposed to α/β in the absence of interaction.

Cumulative

If interaction is instantaneous, removal of competitors at any point during a tree's life means that it can always attain the maximum size possible in the absence of interaction. We should also consider the possibility that suppression has a permanent effect on its future growth potential. Oliver and Larson (1996) describe how conspecific trees starting at the same initial growth rate may reach different asymptotic heights due to competitive stress during the juvenile stage of the life cycle.

This creates mathematical difficulties, particularly in the development of dynamical models, due to the necessity of an integral over time (often referred to as delay effects: the system effectively stores information about its history). However, incorporation into a simulation model is straightforward. $\Phi_i(t)$ in Equation 3.7 is replaced by

$$\Phi_{i,cumul}(t) = \int_0^t \Phi_i(t')dt' \tag{3.8}$$

where $t' = 0$ is an individual's date of birth. Its asymptotic size now changes as it becomes older, dependent upon the level of interaction it experiences:

$$s_i^*(t) = \frac{\alpha - \gamma\Phi_{i,cumul}(t)}{\beta}. \tag{3.9}$$

Since $\Phi_{i,cumul}(t)$ tends to increase, so $s_i^*(t)$ is strictly non-increasing. In a simulation model, the choice of Φ can now have a large effect upon individual growth dynamics – asymptotic size can effectively be determined at an early stage in the life-cycle, or at a small size (Figure 3.8).

Analysis

In this section, the fit of the two best size-dependent growth functions (monomolecular and Gompertz), with both instantaneous and cumulative interaction (with $\Phi_i(t)$ defined as per Equation 2.7 and 2.8) are considered using NLME analysis. The Richards model with an interaction term is not presented here due to numerical issues with the fitting procedure. Two subsets of the amalgamated growth data from the Black Wood of Rannoch (using plots 4 and 6) are considered:

- increments occurring after 1918 ("subset A")
- increments measured in individuals arriving after 1918 ("subset B")

Plots 5 and 7 are omitted due to missing data for some trees. Subset A has the advantage of containing data from trees of all ages, and a much larger number of data points. However, the cumulative interaction data in this subset is unknown and

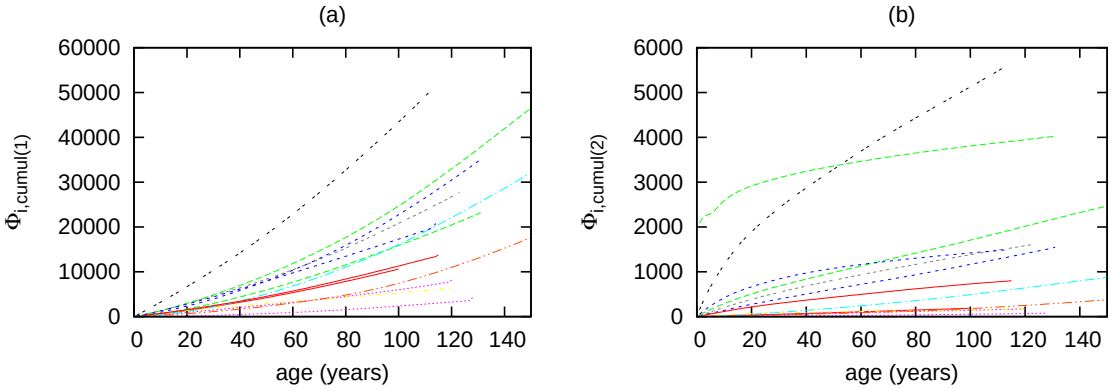

Figure 3.8: *Cumulative interaction against age for two choices of* $\Phi_i(t)$ (for the same sample of individuals as Figure 3.3). This choice alters the time at which interaction has the greatest effect, and the consequent change in individual asymptotic size over time. (a) $\Phi_i(t) =$ Equation 2.7. Cumulative interaction increases at an increasing rate. (b) $\Phi_i(t) = (1/s_i(t))\times$Equation 2.7. The greatest interaction pressure is experienced at smaller sizes, leading to a levelling in the trajectory of cumulative interaction.

likely incorrect, due to the lack of knowledge about stand state prior to 1918. Subset B should allow more accurate determination of cumulative interaction, but is restricted by containing far fewer individuals/data points, and only those pertaining to young individuals. These issues must be borne in mind as conclusions are drawn. Unfortunately, NLME parameter estimates for age-dependent models including interaction did not converge (possibly due to insufficient data) and are hence omitted.

There are various ways of assessing the quality of fit of the models. Firstly we have residual standard error (RSE) and Aikake's An Information Criterion (AIC, Aikake, 1974). See Appendix A.3 for a brief overview; it must be noted that these values are not comparable between fits to different subsets of the data. It is also useful to consider the magnitude of the estimated random effects (population variance in the basic parameters) relative to the estimated fixed effects (population mean of the basic parameters) – lower relative variance implies a better explanation of the data.

Some general features of the fits can be noted from Table 3.3. Firstly, as a rule, the fit of the monomolecular models (as measured by RSE or AIC) appears better. However, its ratio of variance to mean (random effect/fixed effect) for each parameter is actually larger than for the Gompertz model; the estimated mean function (fixed effects alone) explains less of the variance in the data. In all cases (monomolecular/Gompertz and instantaneous/cumulative interaction) random effects are the same order of magnitude as the fixed effects; no function provides a particularly good explanation of the variation between individuals.

Table 3.3: *Fitting growth models including interaction*. Estimated parameters for non-linear growth models fitted by NLME to data from Rannoch plots 4 and 6 combined (plot 5 and 7 omitted due to missing recent disturbance history; growth curves computed based upon (i) subset A – all increments after 1918, or (ii) subset B – increments of individuals arriving after 1918, for individuals further than 10m from an edge). The numbers in brackets denote the correlation between the estimated random effects parameters: $(\rho_{\alpha\beta})$ or $(\rho_{\alpha\gamma}, \rho_{\beta\gamma})$.

	(i) Subset A: Post-1918 increments				(ii) Subset B: Post-1918 arrivals			
	Fixed (μ)	Random (σ)	RSE	AIC	Fixed (μ)	Random (σ)	RSE	AIC
instantaneous interaction								
monomolecular								
α	7.56e-01	5.64e-01	1.10e-01	-8843.7	7.39e-01	3.87e-01	1.87e-01	-377.1
β	-4.30e-03	1.89e-02	(0.298)		-1.62e-02	1.5e-02	(0.870)	
γ	1.56e-03	2.22e-03	(0.666	-0.267)	1.35e-03	7.31e-04	(0.864	0.973)
Gompertz								
α	1.31e-01	1.03e-01	1.16e-01	-8194.0	2.18e-01	9.12e-02	2.02e-01	-189.1
β	3.52e-02	2.86e-02	(0.988)		5.31e-02	2.82e-02	(0.993)	
γ	6.51e-05	6.97e-05	(0.577	0.481)	1.42e-04	8.59e-05	(0.328	0.247)
cumulative interaction								
monomolecular								
α	6.00e-01	4.09e-01	1.12e-01	-8844.9	6.05e-01	3.53e-01	1.87e-01	-371.3
β	-3.62e-03	1.74e-02	(0.458)		-1.92e-02	1.58e-02	(0.859)	
γ	1.57e-05	1.29e-05	(0.325	-0.688)	3.90e-05	1.23e-05	(0.286	0.697)
Gompertz								
α	1.45e-01	9.69e-02	1.15e-01	-8251.0	2.07e-01	9.06e-02	1.97e-01	-188.7
β	4.07e-02	3.09e-02	(0.981)		5.36e-02	2.98e-02	(0.985)	
γ	-6.7e-07	1.00e-06	(-0.885	-0.895)	2.59e-06	9.73e-06	(-0.447	-0.547)

Secondly, the inclusion of interaction into the monomolecular model leads to negative mean estimates for the parameter β in *all* cases (some examples of how this can occur were presented in Figure 3.5). This implies that in the absence of interaction, growth would accelerate as individuals became larger, which is biologically impossible. In such a scenario, the only limit to large individuals' growth is interaction, which is contrary to both intuition and observation. In contrast, the greatest interaction pressure is generally thought to be experienced by juveniles (Oliver and Larson, 1996).

Finally, in the fits computed to subset A, cumulative interaction leads to better fits (as measured by AIC), while in the case of subset B it does not. It is also observed that the fixed effect corresponding to the interaction parameter γ is negative in the Gompertz model fitted to subset A. These two issues are probably linked: the oldest (and slowest growing) trees currently alive have, in general, experienced lower interaction since 1918 than more recent arrivals, which have grown up in their shade and are also growing faster. We might thus surmise that the true factors leading to the limitation of the mature trees' growth occurred before 1918 (resulting in the negative

γ for the cumulative model of all increments). In any case, the lack of sufficient data means that an estimate of γ consistent with the growth of both juvenile and mature trees is impossible to obtain. It is however likely that cumulative interaction does have a role in tree growth – this is investigated in Chapter 4.

The lack of sufficient data to verify the cumulative interaction models, and the inability to fit a biologically realistic monomolecular model to the growth data, means that the simulation model implemented in Chapter 2 uses the Gompertz growth model with instantaneous interaction, slightly tuned from the parameters obtained by fitting to all post-1918 increments. Chapter 4 considers, amongst other alterations, the effect of including cumulative interaction in the simulation model. The remainder of this section deals (somewhat more speculatively) with other possible sources of the observed variation in diameter growth.

3.5.2 Height dependence

Trees do not grow only in diameter, but also in many other dimensions. The most obvious alternative metric is height. Height is less straightforward to measure than diameter, and consequently features less commonly in forest datasets. Tracking its history is also very much more difficult than it is for diameter. Data from the Rannoch study plots includes tree heights, measured at 1994 and 2005.

In consideration of the actual mechanics of competition for light, intuition would suggest that it is height, as opposed to diameter, that plays the major role in competitive interactions between trees (Adams et al., 2007; Strigul et al., 2008). Figure 2.1 demonstrated that useful relationships between these measures exist, but it is also interesting to consider directly the relationship between tree height and diameter growth.

The above mentioned additional data points for each tree allow the consideration of further possible relationships:

- height at 1994 vs dbh growth (g_{dbh}) at 1994
- competition reformulated with height instead of dbh, vs g_{dbh} at 1994
- g_{height} vs g_{dbh} 1994-2005
- competition (dbh based) vs g_{height}/g_{dbh} 1994-2005
- competition (height based) vs g_{height}/g_{dbh} 1994-2005

A reasonably clear trend is observed between height growth and diameter growth (strong trees are growing in both dimensions, Figure 3.9c), and it also appears that

trees under intense competition are more likely to allocate more resources to height than to diameter growth (Figure 3.9d). However, data analysis does not indicate the existence of clearer patterns relating diameter growth to height or height-based competition; no clearer trend is observed, and the data points remain highly scattered.

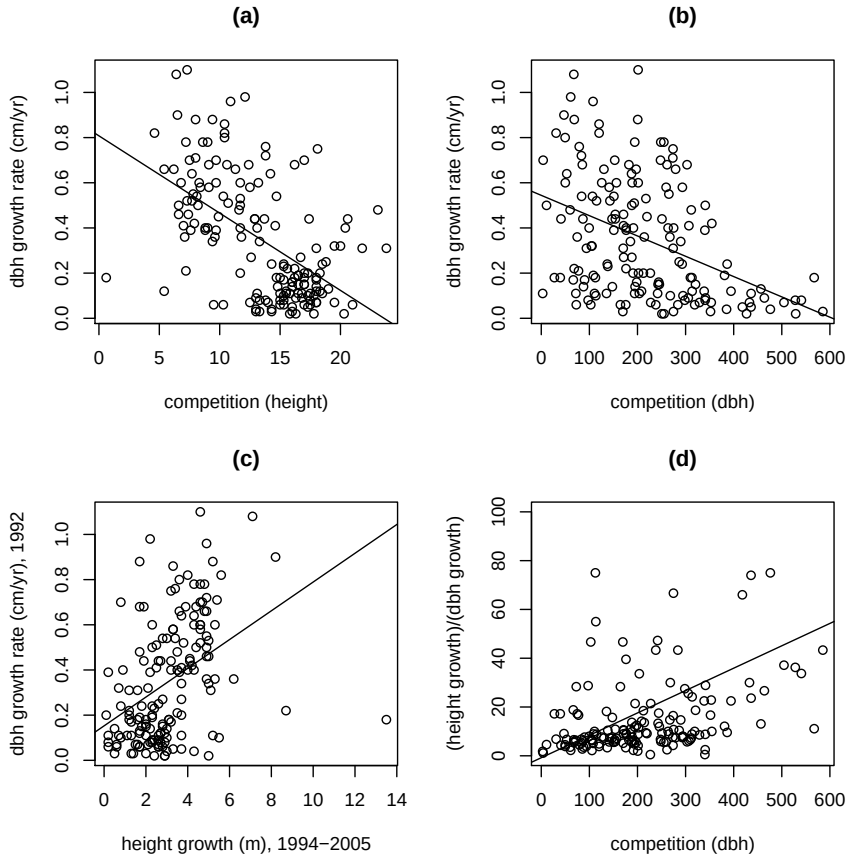

Figure 3.9: *Is height a more important factor in growth than diameter?* Scatter plots of height and diameter-related quantities at a single time point, for all individuals in Rannoch study plots 4, 6 and 7. The line in each plot is that of a significant trend computed using a linear model. (a) Replacing dbh with height in the size component of the competition kernel, at 1992. (b) Original dbh-based competition kernel vs dbh growth, for comparison with (a). (c) Height growth attained between 1994 and 2005, versus diameter growth in 1992. (d) The ratio of height to diameter growth vs competition, showing an increased focus upon height growth under elevated competition.

3.5.3 Intrinsic Variation

The lack of a mechanistic explanation for the observed variation in diameter growth of individual trees raises the possibility of intrinsic variability in a population's characteristics, for example due to genetic heterogeneity. A phylogenetic analysis by Provan et al., 1998 found very large variation, with two distinct subgroups, in a sample from the Black Wood of Rannoch. Such differences could result in certain individuals displaying much slower growth, or higher mortality than others. It is known that different genotypes of Scots pine exhibit different growth characteristics (Rweyongeza et al., 2003), but without specific additional analysis for the data stands, we can only speculate.

3.5.4 Environmental Variation

Environmental variation also plays a role in organisms' life history. Variation is present at many scales: at very large scales, the climate; more locally, the topology and consequent properties of the landscape (slope aspect, elevation, soil structure and so on, which may vary over a scale of many kilometres to just a few metres). It is possible to make inferences on certain aspects using the available data, but not on others.

Very small scale

This is the case of heterogeneity over such scales that can lead to neighbouring trees experiencing very different resource conditions. Examples are soil/rock mixtures and microtopology (small-scale undulation, hummocks and troughs).

Arkle (1996) found that this is likely to be most evident in the survival of seedlings, which has clear implications for the realised point pattern of mature trees. Small scale variation in growth rate was also apparent in the Rannoch plots. The effect of such variation in ground conditions may however be indistinguishable from that of intrinsic variation between trees, and thus requires an assumption that genetic factors do not play a large role. It also requires that competition (and its history) has been properly accounted for. Unfortunately these conditions are not guaranteed with the available data.

Within stands

If the stand is situated on a gradient in, for example, altitude, nutrients, or soil type, it may be possible to observe trends at a stand level. The only stand for which any trend is observed (in age, size or growth rate) is in Plot 6, for growth, which appears

to decrease as the y-coordinate increases. However, interaction also increases with y-coordinate (not shown), as density of trees increases (which may be induced by environmental or previous management effects).

Between stands

We might expect to see more marked differences between stands that are geographically separated, in particular if the sites have widely varied altitude, rainfall or wind speed.

There is no clear difference in single time-point stand statistics (size distributions, spatial correlation functions and so on) between the Rannoch, Glenmore or Glen Affric stands. For example, the current size distribution of Rannoch plot 7 is more different from that of Rannoch plot 4 than plot 4's is from any of the stands from different areas. It thus appears that past management may have a greater effect upon the current size and age distribution than does region.

Annual increment data is not available for stands other than Rannoch, and so it is not possible to compare this directly. Multiple year growth *can* be compared though, as other stands were sampled at least twice. Figure 3.10 is a scatter plot of average dbh growth rate (over 11 years for Rannoch plots, 9 years for Glen Affric). In general higher growth (and greater variation in growth) is observed at Glen Affric, compared to Rannoch. There are also notable differences between the Rannoch plots themselves, plot 4 having the slowest growth of all stands. This may reflect environmental variation, or previous management.

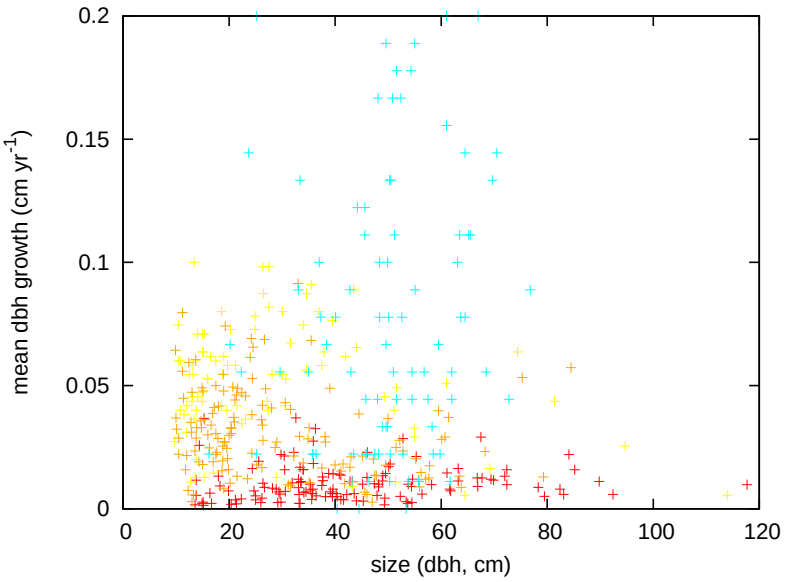

Figure 3.10: *Geographical variation in growth rate*. Dbh growth rate versus dbh for Rannoch plots 4 (red), 6 (yellow), and 7 (orange) (individual means over 11 years) and Glen Affric (cyan – individual means over 9 years).

3.5.5 General Remarks on Variation

Variation is relatively simple to incorporate naively into a simulation model. However, in view of the data analysis carried out, it is difficult to find theoretical justification for drawing particular parameters from certain distributions, while keeping others fixed.

A further issue is that it is impossible to identify whether variation in growth of the mature trees is either intrinsic or environmental, or simply the result of early life suppression, for which data does not exist. As a result of the lack of complete data, a more useful approach is to make qualitative comparisons of the effect of altering model form upon behaviour with the patterns observed in data stands. Various alterations focusing on explaining size variability are described in Chapter 4.

3.6 Summary

As is clear from the sample of growth curves in Figure 3.3, the individual rate of diameter growth in our Scots pine data is not directly related to the individual's diameter. This led to a search for an explanation of the variation in terms of age and local neighbourhood.

Individual growth curves were analysed, and the effect of additional explanatory variables (competition, cumulative competition) upon each tree's growth was considered. These help to explain some inter-individual variation, but a far greater proportion remains, evidenced by the large standard deviation of all parameters in the mixed effects (NLME) analysis. This difficulty in explaining the observed level of variation is likely to be due in part to problems with the model structure, but is greatly complicated by a lack of sufficient data for fitting growth models which include a dependence on the entire life-cycle (through cumulative interaction, for example). This and various other issues that are intractable via data analysis are considered via simulation in Chapter 4.

Of the growth models considered, we ultimately came to the conclusion that it would be sensible to retain the Gompertz model, with instantaneous interaction. This did not obtain the best fit in terms of standard measures of fit quality, but consideration of other factors such as avoidance of biologically impossible parameters point to its use. A sigmoidal curve (with point of inflection at $t > 0$) also seems to be essential to explain the increments of many juveniles (Zeide, 1993). This was demonstrated by plotting the estimated value of δ for the Richards growth model (Section 3.4) against current size/age across all Rannoch plots, both of which display negative correlation (Figure 3.6). However, it is worth bearing in mind that the specific form of very early growth (the only notable difference between the growth models) is unlikely to have any dramatic effect on the overall dynamics of simulated, or real, populations.

Consideration of height seems unlikely to resolve the variation observed between individual growth curves. It is also difficult to determine any particular pattern in the variation of growth over space (there is no trend, only very small scale spatial variation – Figure A.1, Appendix A.1), meaning that variation could have either environmental or genetic causes.

Chapter 4

Understanding population dynamics of Scots Pine using the simulation model

4.1 Introduction

In Chapter 2, a simple individual based model of a forest population was introduced. This model included quantification of both size and space, allowing the study of structural development in each due to successive birth, death and growth events. Chapter 3 made a statistical analysis of growth data, in an attempt to identify the best mechanistic growth model and explain inter-individual variation in unmanaged uneven-aged Scots Pine stands.

As discussed in Chapter 2, the generic behaviour of the simulation model appears to mimic that described by the qualitative stand development models of Oliver and Larson (1996) and Franklin et al. (2002). We would also like to identify how well it replicates patterns seen in populations of a particular species: Scots pine. This chapter first confronts the model with data from plantation and semi-natural Scots pine stands (Section 4.2). Secondly, it considers how any differences might be resolved, and concludes by suggesting an improved model for application to management problems.

Table 4.1: Summary of Scots pine (*Pinus sylvestris L.*) data provided by Forest Research. The Rannoch plots were established in 1948 and maps are available from that time (though sizes were not recorded).

Dataset	Type	Notes/Additional measurements
Glenmore	Plantation (6×1.0ha)	Age 78 years.
Glenmore	Semi-natural (0.8ha)	1930s regeneration experiment (1999, 2005).
Rannoch	Semi-natural (4×0.8ha)	Heights (1983, 1994, 2005). Dbh increments (Chapter 3).
Glen Affric	Semi-natural (1.0ha)	Height, crown radius (1997, 2006).

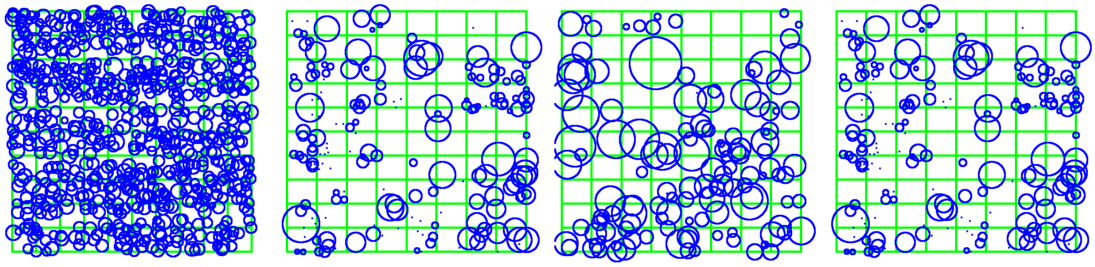

(a) plantation (b) Glen Affric (c) Rannoch 4 (d) Rannoch 7

Figure 4.1: Pictorial representation of forest diameter/location data (collected by Forest Research). Plantation: (a) 78 year old stand at Glenmore (Highland). Semi-natural: (b) semi-natural stand in Glen Affric (Highland, data), (c) Rannoch plot 4, (d) Rannoch plot 7.

4.2 Comparison with empirical data

4.2.1 Data overview

Data from two broad stand types (collected in Scotland by Forest Research, UK Forestry Commission) are available: plantation and "semi-natural" (see Edwards and Mason, 2006; Mason et al., 2007). Point patterns generated from some of these data stands, at the current time, are shown in Figure 4.1. Basic details about the data are given in Table 4.1.

4.2.2 Plantation

Figure 4.2 compares the state of model populations at 80 years from initiation (2m square lattice of 1cm dbh trees, with random variation in individual location of ± 0.5m about each lattice point, 100×100m square arena, periodic boundary conditions) with data from plantation stands at Glenmore.

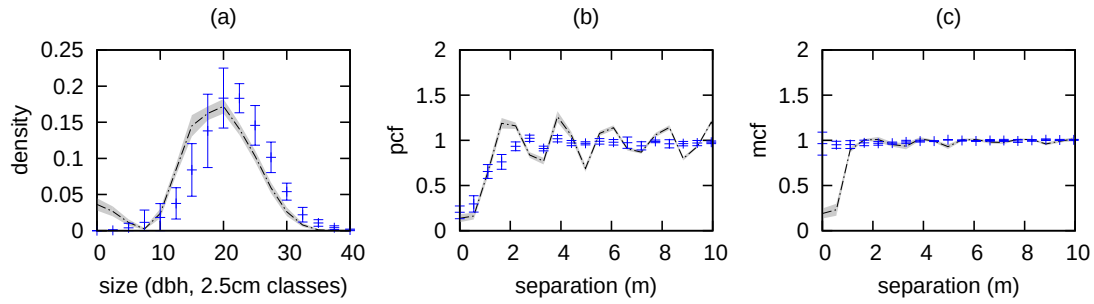

Figure 4.2: *Simulation vs plantation data*. Comparing the model state at 80 years (lines) with data from plantation stands at Glenmore (blue error bars, showing mean and standard deviation calculated from 6 stands). (a) Size density distribution (b) PCF (c) MCF.

Density and basal area (not shown in Figure)

The simulated density of model populations is fairly close to that of plantation stands at Glenmore (simulated at 80 years vs. dataset: 0.09063 vs 0.08523 individuals per m^2). However, basal area is notably underestimated (29.22 vs 36.67$m^2 ha^{-1}$).

Size distribution

The reason for the low basal area noted above is apparent in Figure 4.2a; at 80 years, the mean/modal size of trees is lower. The growth parameters estimated from semi-natural data alone (in Chapter 3) produce insufficient growth in the simulated population.

There are also too many juveniles in the simulation at 80 years – regeneration has not occurred in the data stands. This may indicate problems with the model birth process, or poor deer control at the Glenmore plantations (which is not accounted for in the model).

Pair correlation function

The simulated PCF at 80 years displays two key features: a reduced density of pairs with small separations ($<$ 2m), and a distinct lattice pattern. The first of these is mirrored in the plantation data, the second is not.

The PCF computed from Glenmore plantation data (Figure 4.2c, error bars) does not show the signature expected of a 2m square lattice, rather a fairly homogeneous pattern at long ranges. In data collection, locations of trees were measured relative to several posts, each with location accurate to $\pm$0.5m, which may conceal the lattice structure. Another possibility is that the apparent non-regularity is a result of non-alignment of (and larger than expected spacing between) rows. Two types of random

variation in simulation initial conditions were investigated, to attempt to match early spatial correlation (not shown):

- Set lattice points at corners of 2m sided squares. Allow uniform or Gaussian random variation about these. This subdues the lattice "peaks", but does not alter their spacing.
- Planting "a row at a time". Allow a small random lateral variation when choosing the location of each subsequent tree in a row. Select the location of each new row using 2m as a minimum and add a random amount. This leads to a reduced density of trees and alters the location of the correlation function peaks.

In each case, a very large amount of random variation is required to remove the lattice signature from the correlation function, to the point that the pattern created does not appear visually to be a lattice. It seems likely that the data collection method at least partially conceals the expected regular lattice structure. Thankfully, the model's long run dynamics do not depend on the precise details of early spatial structure.

Mark correlation function

Overall, the early pattern of the simulation model displays a greater level of size inhibition (reduced MCF) at short ranges than does plantation data (Figure 4.2c). Figure 4.3 shows the mark correlation of juvenile/mature subsets of the stands, and their cross correlation (computed in R using a smoothing kernel). Mature trees ($\geqslant$ 15cm dbh) alone appear to display greater size inhibition at very short ranges in the real stand than the simulation (Figure 4.3b). However, the sharp did in the appears to be partly related to the smoothing applied here, and is not representative of patterns observed in general plantation stands (in which there is little or no signal of inhibition at this stage of development; see Figure B.1, Appendix B). There also appears to be strong negative correlation in the location of juvenile ($<$ 15cm dbh) and mature trees in both the simulation and the data (Figure 4.3c). Juveniles themselves do not have a clear pattern, due to their low density (Figure 4.3a), but their relatively high density in the simulation model at early times appears to explain the difference in overall MCF.

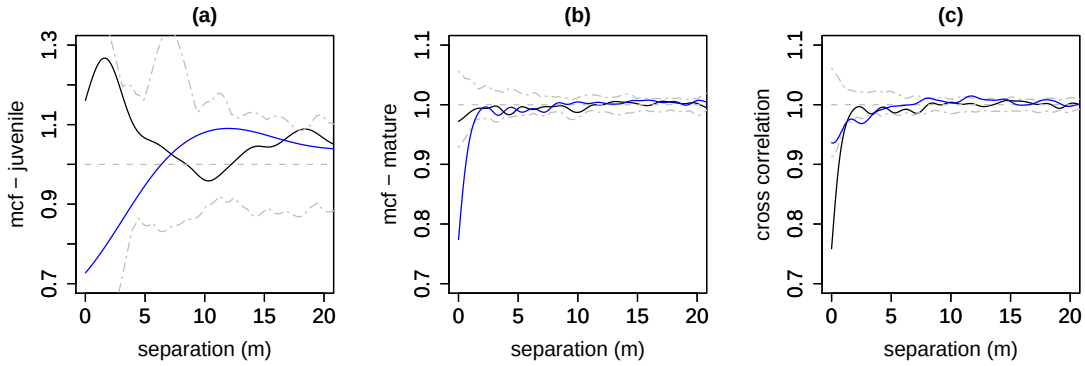

Figure 4.3: *Plantation MCF comparison*. The mark correlation function computed for a simulated population at 80 years (black line), compared with that of a single plantation data stand (blue line). Grey dash-dot lines indicate 98% bounds generated from 100 randomly generated patterns, grey dashed that *expected* of a spatially random pattern. (a) Juveniles ($<$ 15cm dbh) only. (b) Mature ($\geqslant$ 15cm dbh) trees only. (c) Cross-correlation of juveniles and mature tree location.

4.2.3 "Semi-natural" data

We would also like to identify whether the model is able to mimic the behaviour of unmanaged forests, and here compare its long-run behaviour with non-plantation data.

Almost all forested areas (in the UK at least) have at some point been subject to management. For this reason they must be referred to as "semi-natural"; their current state reflects both natural processes and human intervention. As a result, dramatic differences may exist between stands (even locally), and it is often unclear how close a given forest is to "true old-growth" or "equilibrium". The data stands (identified in Table 4.1: Glenmore non-plantation, Rannoch, Glen Affric) display high variability, but similar signatures are seen:

- Size distribution has wide spread and a "canopy" peak at a moderate size (Figure 4.4c)
- PCF (Figure 4.4a) shows clustering of individuals
- MCF (Figure 4.4b) displays inhibition of growth/size at short ranges

Management history for the semi-natural data stands is known from 1918 onwards, but some educated guesses regarding previous management can be made. For example, we know that the best trees were removed from many forests (and certainly the Rannoch plots) during the First World War (1914-1918). Additionally, the state of the Rannoch stands may (in part) be deduced using the individual growth/age data from the annual increment cores discussed in Chapter 3. Working back from the current (actual) diameter, the size of each tree at 1918 can be estimated, and consequently the total basal area (in 1918) of the trees still present today (plot 4: 11.6m^2, plot 6: 2.1m^2 (small area missing), plot 7: 3.3m^2). There is known to have been low mortality in these stands over this period (the study plots were established in 1948).

To attempt to replicate the data stands' history (and for the comparison presented in Figure 4.4) we run the model to equilibrium, remove trees from the largest 60% to reduce the basal area to 10m^2, and run for a further 80 years. The properties observed in this scenario are fairly similar to the model's actual steady state. More specific managements were implemented, but these did not assist further in understanding particular features of the data.

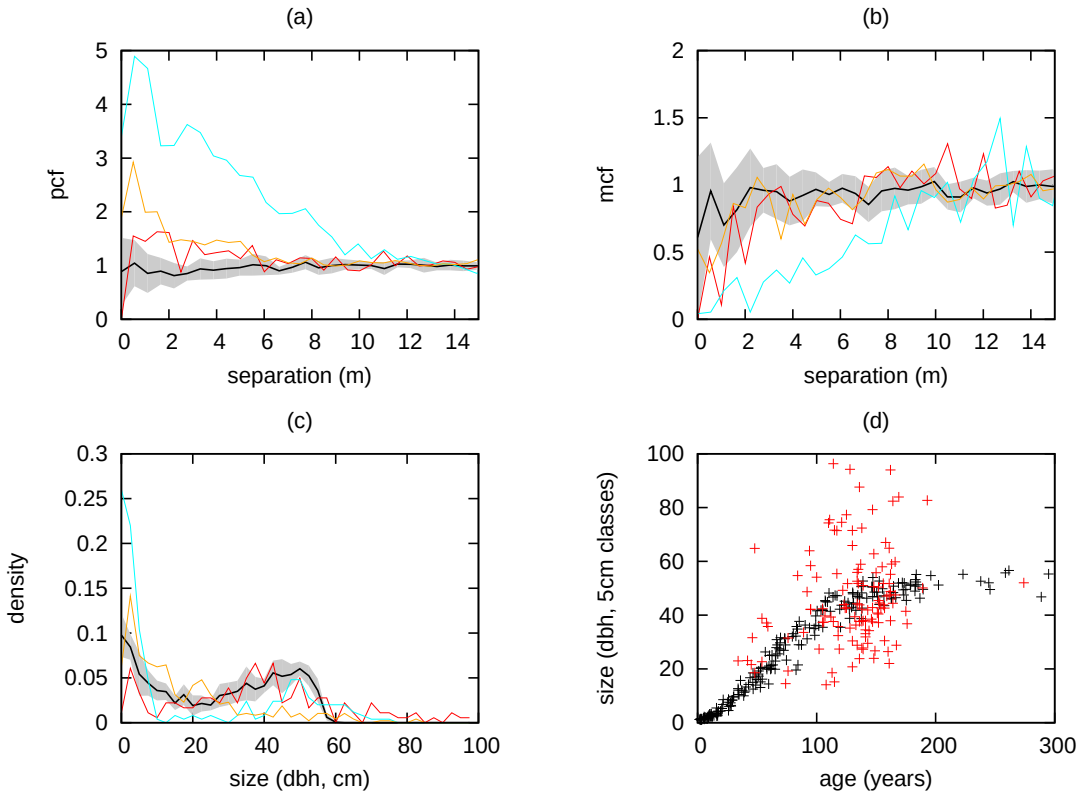

Figure 4.4: *Simulation vs "semi-natural" data*. The data plots were heavily managed prior to 1918; we approximate this here by running a model stand to equilibrium, thinning to 10m^2 basal area (removing trees randomly from the largest 60%), and running for a further 80 years (see Section 4.2.3). Solid line and grey envelopes in (a),(b) and (c) are simulated results. Data: Rannoch plot 4 (red), Rannoch 7 (orange), Glen Affric (cyan). Spatial correlation functions display a similar signature for all stands - (a) clustering of individuals, and (b) inhibition of growth/size at short ranges. (c) Size distribution varies between the plots, probably in part reflecting their management history. (d) shows the variability in size attained at a given age present in the data (data only available for Rannoch stands – plot 4 shown (red)), compared with the simulation 80 years after the intervention (black).

Density and basal area

Simulated steady state density is similar to that of semi-natural data (0.0265 vs 0.019-0.0495 individuals per m^2). Basal area, on the other hand, is on the lower limit of that observed (22.5 vs 23.7-31.6m^2ha^{-1}). Recalling the plots' low mortality over the past 50 years, it is also unclear whether the current basal area of the data plots is above or below a steady state; basal area trajectories (calculated by summing the sizes of all currently living trees) for the Rannoch plots (Figure 4.5a) show a monotonic increase.

Density of currently surviving mature trees (the number of individuals present at a particular date, determined by the presence of growth rings: Figure 4.5b) has not increased exponentially over the data duration, as one would expect with constant average population birth and death rates. Instead, it has remained roughly constant over long periods, with step increases. Plots 6 and 7 see a step increase during the 1960s, and all stands see a step increase in density between 1994 and 2005: regeneration appears to have been much higher over this period. Current size distributions for all semi-natural stands show a high density of small trees (Figure 4.4c). Such a result is suggestive of a change in reproductive capability or regeneration success, or a high turnover (mortality) of juveniles.

Figure 4.5b shows how high mortality of juveniles could explain their larger than expected current density (blue lines: μ_1 and μ_2 increased $\times 5$ for individuals < 10cm dbh). However, it cannot explain a step change of the type seen during the 1960s. A change in regeneration conditions (due to browsing pressure, for example) from 1940 onwards thus appears likely, and ties in with a change in ownership (the Forestry Commission taking responsibility for the area in 1946; Colin Edwards, personal communication).

Parameter sensitivity analyses suggest that the low basal area may be remedied by increasing the growth parameters α and β (Section 2.5). This and the issues relating to size are tackled in Section 4.4.

Size distribution

Size distribution of the data is generally characterised by a wide spread and a "canopy" peak at a moderate size (Figure 4.4c). This is similar to the simulation output, but there are two important issues.

Firstly, the estimated growth parameters limit the asymptotic size at $\exp(\alpha/\beta) = 62.9$cm, meaning that the few very large trees observed in data cannot be created by the model. Secondly, data displays a wide range of sizes for a given tree age, while simulated individuals of a given age are relatively homogeneous in size (Figure 4.4d). Both issues are tackled in Section 4.4.

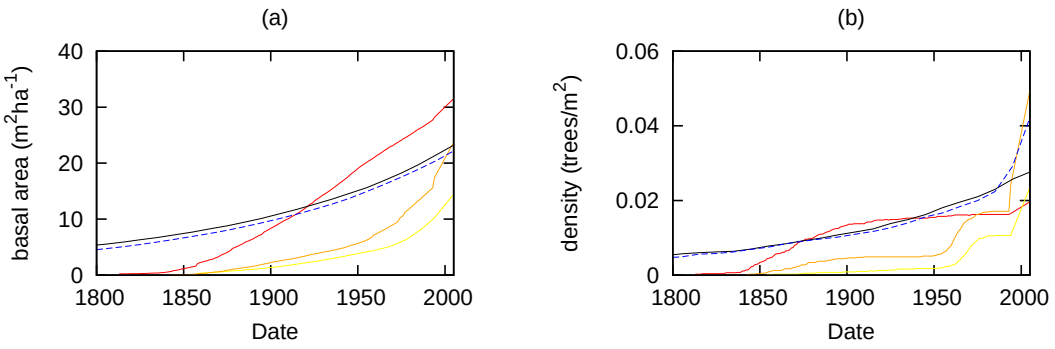

Figure 4.5: The trajectory of (a) basal area and (b) density of currently surviving trees in Rannoch plots 4 (red), 6 (yellow) and 7 (orange). Equivalent data generated using the basic simulation model are shown by black solid lines, and with an increase in juvenile ($<$ 10cm dbh) mortality, blue dashed lines (mortality parameters $\times 5$, f $= 1$).

Pair correlation function

Comparing the spatial correlation functions produced by the model with those of the semi-natural data is quite revealing of the model's inadequacies. In data stands, the pair correlation function (PCF) displays the signature of a clustered pattern (increased density of close pairs), whereas that of simulated stands is fairly homogeneous, but displays slight inhibition at short ranges (Figure 4.4 and 4.6). This is a result of birth at random locations, the establishment probability (Equation 2.6), and the dependence of death upon local interaction (Equation 2.4).

Clustering can only be created in the model by the birth process (local dispersal), beneficial interactions between trees, or environmental heterogeneity. Alterations to the birth process are considered in Section 4.3.

Mark correlation function

Using the parameters estimated from the Rannoch increment data, the long-run behaviour of the model displays local inhibition in growth (reduced MCF), which is qualitatively correct in comparison with semi-natural data. Figures 4.3 and 4.7 provide little evidence that the effect of competition on individual growth of established is incorrectly modelled in general (apart from Glen Affric, the effect is only slightly more distinct in the data).

In addition to displaying the strongest growth inhibition, Glen Affric displays a somewhat unique pattern. Trees are very much clustered (Figure 4.6), and the presence of mature trees appears to be far more influential upon the existence and survival of juveniles than at Rannoch, where deviations in the cross-correlation of juvenile and mature tree locations from random are indiscernible (Figure 4.7c).

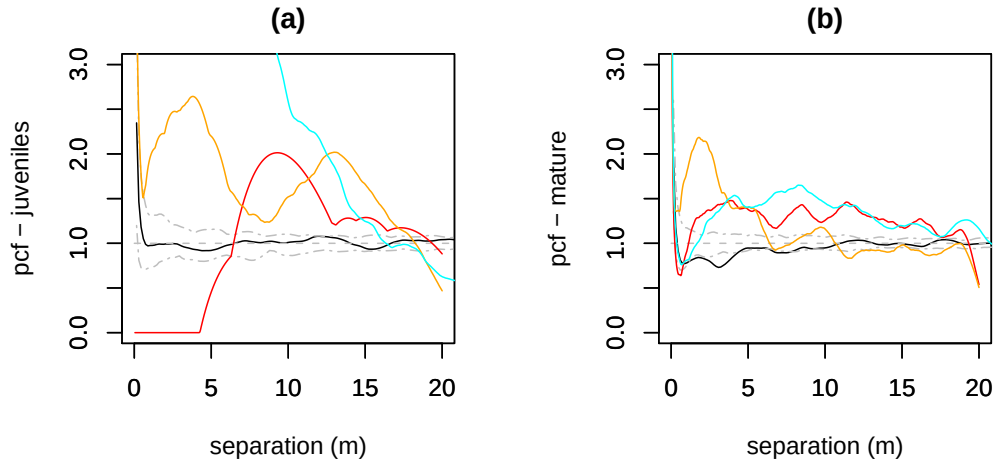

Figure 4.6: *Steady-state PCF comparison*. The pair correlation function computed for a simulated population at 880 years, compared with that of semi-natural data stands (black: simulated, red: Rannoch 4, orange: Rannoch 7, cyan: Glen Affric). Grey dash-dot lines indicate 98% bounds generated from 100 randomly generated patterns, grey dashed that *expected* of a spatially random pattern. (a) Juveniles only (b) Mature trees only.

However, the MCF of mature trees alone is almost indistinguishable between any of the data stands, or the model steady state (Figure 4.7b).

The contrasts with the situation seen in the simulated plantation, in which the overall MCF was too inhibited at very short ranges. However, at early times simulated populations display *more* regeneration (juveniles) than data stands, while in the long-run, they display relatively *less* regeneration than the data stands (Glen Affric in particular). The relative density of juveniles in data stands appears to correlate directly with the level of size inhibition at short ranges as measured by the MCF.

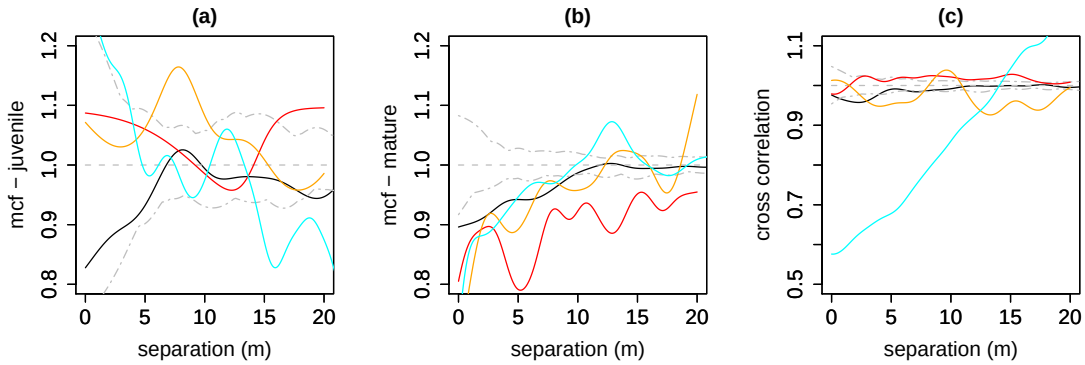

Figure 4.7: *Steady-state MCF comparison*. The mark correlation function computed for a simulated population at 880 years, compared with that of semi-natural data stands (black: simulated, red: Rannoch 4, orange: Rannoch 7, cyan: Glen Affric). Grey dash-dot lines indicate 98% bounds generated from 100 randomly generated patterns, grey dashed that *expected* of a spatially random pattern. (a) Juveniles ($<$ 15cm dbh) only (b) Mature trees ($\geqslant$ 15cm dbh) only. (c) Cross-correlation of location of juveniles and mature trees.

4.2.4 Summary

In many respects, the simulation model compares well with data from Scots pine forests, in both young (plantation) and old (semi-natural) stands. However, there are several features that are not matched well. The most important of these are:

- slightly inhibited, as opposed to clustered, overall pattern of tree locations (PCF)
- inability to consistently replicate observed regeneration level (number/spatial pattern of juveniles) with respect to established trees
- low basal area at all times
- size of trees at a given age is too homogeneous.

The first two points are considered in Section 4.3, while Section 4.4 presents possible solutions to the latter two. Figures in the remainder of this section do not include any real stand data, but consider the qualitative effects of altering various defining features of the model.

4.3 Refining the birth model

4.3.1 Background

In real populations, many processes combine to determine whether the seed of a particular mature tree reaches 1cm diameter at breast height (the state of individuals on their entry into the model). In contrast, the reproductive mechanism implemented in the simulation model is very simple.

In the model, the birth process primarily affects the form of the PCF (only birth and death affect this statistic directly). The model's overall PCF (4.4a) displays some inhibition, barely distinguishable from that of a random pattern. The semi-natural data tend to show more clustered patterns in general. However, the juveniles themselves appear to be clustered (especially in the Glen Affric plot, Figure 4.6b). Furthermore, their locations are either negatively (Glen Affric) or not correlated (Rannoch) with those of the mature trees (Figure 4.7b). This suggests that recruitment may be limited by local density of large trees (the case of clustered juveniles, negatively correlated with large tree locations), or by environmental heterogeneity (the case of clustered juveniles, not necessarily correlated with large trees).

The birth process also affects the MCF, stand density, basal area and the size distribution, insofar as governing the ultimate number of surviving seedlings. The most obvious refinements to the birth model are and their effect upon model dynamics are investigated below.

4.3.2 Local dispersal

Background

In reality, pine seeds are distributed via cones, with greater numbers falling from larger trees. We might thus more realistically consider the arrival of individuals resulting from the dispersal of seed from a particular tree, with a distance computed using a *dispersal kernel*. Dispersal kernels are generally difficult to estimate empirically. Malcolm et al. (2001) suggest that most seed falls within 1-2 tree heights, and that this decay is exponential. Another estimate is that 80% of seed fall within 2.5 tree heights (Colin Edwards, personal communication). However, many forms are in common use, and for consistency with the interaction function introduced in Chapter 2, a Gaussian kernel is used here:

$$B(r) = \frac{k_b}{\pi} \exp(-(k_b r)^2). \tag{4.1}$$

Dispersal direction is chosen uniformly at random.

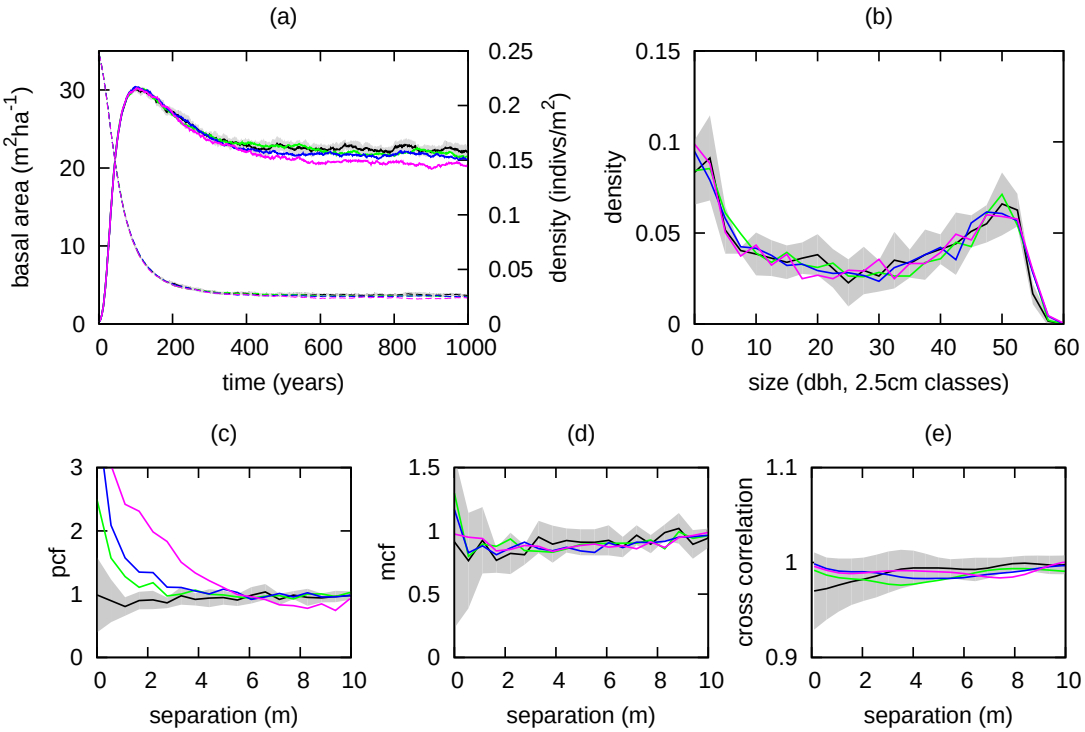

Figure 4.8: *Local dispersal*. The black lines with grey standard deviation intervals show the mean behaviour of the model with random dispersal (original results presented in Figure 2.4). Coloured lines show mean behaviour of the model as dispersal becomes more local (k_d =0.075 (green), 0.15 (blue), 0.25 (magenta)). (a) basal area (solid line), density (dashed line), (b) size density distribution at 800 years, (c) PCF at 800 years (d) MCF at 800 years. (e) Cross-correlation of juvenile and mature individual locations at 800 years. Local dispersal leads to a clustered distribution of individuals, but clouds the signature of local growth inhibition in the MCF. No difference in plantation (80 year) statistics is observed (not shown).

Results

Adding a dispersal kernel with the same scale as the interaction kernel into the model immediately corrects the qualitative difference between the data and simulated PCF (see Figure 4.8c), the level of clustering being affected directly by the scale of dispersal.

The increase in parent-offspring close neighbours created by local dispersal also leads to a slightly heightened MCF and cross-correlation at short ranges. Other statistics are unaffected. It is worth noting that dispersal is the only mechanism in the model that can lead to clustering (there is no spatial inhomogeneity).

Bolker and Pacala (1999) found that species' relative scale of dispersal affects their ability to invade one another. As described above, altering the scale (distance $1/k_b$) of dispersal relative to the interaction kernel affects the spatial structure of the population. In more competitive populations (for example, increasing μ_2 by one order of magnitude), longer range dispersal allows offspring to escape the shade of their parents, and consequently increases both individual density and stand basal area (as found by Bolker and Pacala (1997) – see Figure B.4, Appendix B).

4.3.3 Establishment probability

Background

The basic birth model (Section 2.2.4) defines a probability of establishment for seedlings:

$$\mathbb{P}_e(x,t) = \left(1 - (\mu_1 + C\mu_2\Phi_{seedling}(x,t))\right)^y \tag{4.2}$$

C alters the effect of neighbourhood upon establishment, and was fixed at 1 in previous simulations. An increase may explain the segregation of juvenile and mature trees, as observed at Glen Affric (Figure 4.7c) and Glenmore (regeneration study data – see Edwards and Rhodes (2006)).

Results

The result from simulations performed using altered values of C, with a corresponding change in f such that $f\mathbb{P}_e$ is held constant (assuming the original equilibrium mean competition value), are shown in Figure B.2, Appendix B. The effect upon density, basal area and the size distribution is minimal. There also does not appear to be a strong signal in the spatial correlation functions.

Increasing C while holding f fixed leads to clearer changes (Figure 4.9): seedlings have increasing difficulty in establishing in regions occupied by large individuals. This effect is directly observable in the stand density and basal area, which decrease.

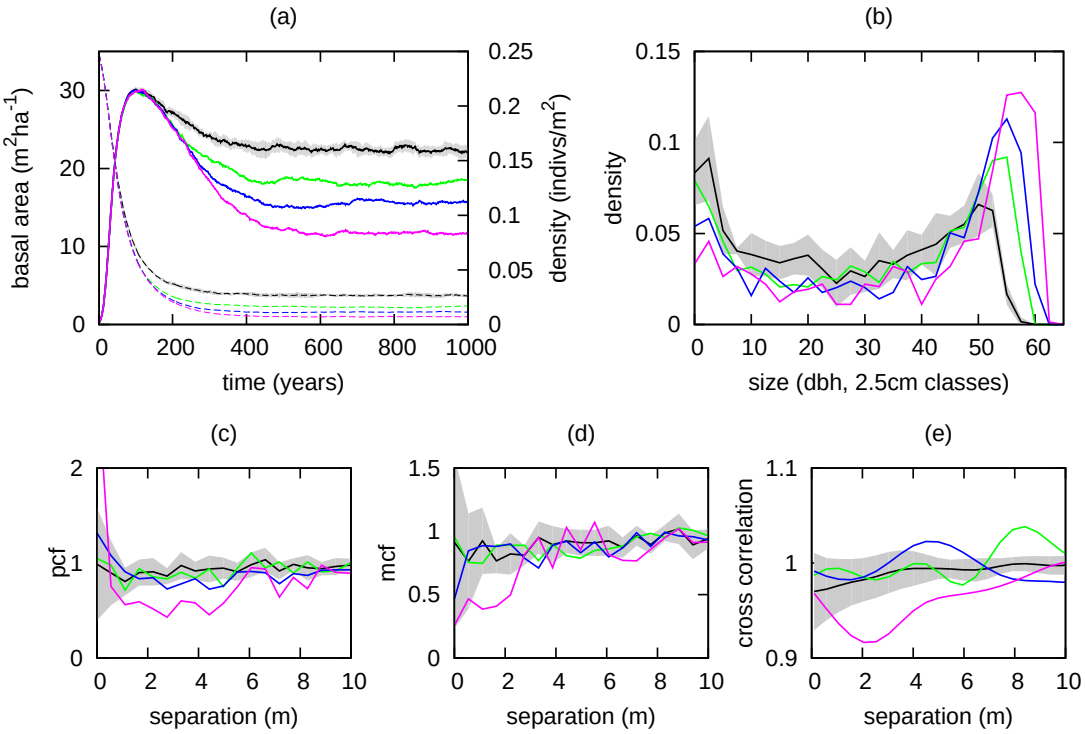

Figure 4.9: *Altering establishment dependence on interaction*; with f $= 0.15$, the basic rate used in Chapter 2. C=5 (green), 10 (blue),20 (magenta). (a-e) as for Figure 4.8.

Both the PCF and the MCF display depression at short ranges. The short range cross-correlation is significantly affected only at very large values of C.

4.3.4 Basal area dependent establishment

Background

The strong negative correlation between mature and juvenile trees seen in the Glen Affric plot could reasonably be attributed to neighbour-dependent establishment. However, the locations of juveniles in the Rannoch plots do not display any signal of correlation (positive or negative) with the locations of mature trees (Figure 4.7c). Plot 7 has low basal area, and high regeneration; Plot 4 has higher basal area, and low regeneration. The two stands have fairly similar spatial structure (Figures 4.4a,b). This suggests that basal area might be as important, if not more important, than local competition in determining the level of regeneration.

Strict basal area dependence is equivalent to applying a mean-field interaction kernel to establishment, a transition from local dependence being available by gradually reducing k_d, as described below.

Results

Figure B.3 (Appendix B) shows that reducing k_d in the establishment probability actually has minimal effect on simulation model behaviour. The effect of a broader kernel only becomes evident in simulations where the kernel has become so broad that its integral over the simulated arena decreases, meaning that more can establish (that is, only a finite population area effect occurs – magenta line in Figure B.3a,b).

Simulations with stronger interaction dependence in the establishment probability ($C = 5, 10$) also produce little change in behaviour (not shown). It is also impossible for this formulation of establishment probability to lead to increased clustering – regeneration becomes *less* dependent upon local spatial structure.

4.3.5 Growth rate of seed/saplings

The establishment probability defined above assumes that trees take a fixed amount of time to reach the initial size used in the model. However, local competition affects seedling growth, as well as mortality. For this reason, those inhabiting shaded areas take longer to reach a given size than those in full sunlight. Table 4.2 summarises Scots pine sapling growth data collected and analysed by Sarah Taylor in Autumn/Winter 2007.

Table 4.2: *Results from juvenile growth data collected and analysed by Sarah Taylor*. Mean time to reach a particular diameter at 1.5m height is given, with standard deviation in brackets. Open grown trees reach breast height most rapidly (see also Figure 3.7a), and small tree growth (between zero and 10cm diameter) is much faster under high light conditions. Trees from two of the light categories were not collected from both plots; these columns are omitted. Trees from the "Erosion" light category were subject to an "open" light environment.

Light		Erosion	Open (unshaded)		Gap	Overstory (shaded)	
Plot		GA	GA	BWR	BWR	GA	BWR
time to	0cm	10.5 (1.29)	21.5 (10.6)	18.7 (4.6)	25.4 (5.8)	26.3 (9.0)	27.8 (11.4)
	7cm	23.7 (4.6)	54.3 (14.9)	45.8 (13.6)	54.3 (6.7)	68.9 (20.2)	69.4 (16.2)
	10cm	29.3 (6.9)	68.4 (16.8)	57.5 (18.0)	66.7 (7.5)	87.2 (32.5)	87.2 (18.5)
sample size		4	2	15	5	4	8

As light level increases, juvenile trees spend less time at heights smaller than 1.5m (height growth curves from the same data are shown in Figure 3.7a). Ground disturbance also appears to have an important effect upon early growth (and indeed regeneration success, see Edwards and Rhodes, 2006), another factor unaccounted for in the model.

The establishment probability might be altered to incorporate an interaction dependent "time" component (the exponent):

$$\mathbb{P}_e = (1 - (\mu_1 + C_1\mu_2\Phi_i(t)))^{C_2\Phi_i(t)}. \tag{4.3}$$

That is, the duration spent in the establishment period is altered by neighbourhood, as well as the probability of mortality per unit time. However, several issues must be considered. Firstly, the ratio of variation in the time to reach 0cm dbh *within* light condition categories to that *between* them (in Table 4.2) is very high – it is the later growth that is more clearly correlated with light level. Secondly, C_1 and C_2 are difficult to estimate from data, and indeed must be given very different values to account for the patterns observed in different natural stands. Finally, the incorporation of the additional parameter C_2 does not achieve any fundamental difference in behaviour versus simply varying C_1. It would thus seem prudent to retain the existing formulation.

4.3.6 Scenarios derived from semi-natural data

Background

The regeneration observed in the semi-natural data stands varies substantially, both in magnitude and pattern relative to the locations of mature trees. Rannoch 4 and

Glen Affric display a sharp peak of trees in the smallest size classes, while Rannoch 7 has a more established component of small trees, and looks to have achieved more consistent regeneration over the last 50 years. The locations of juveniles in the Rannoch plots are relatively random with respect to the mature trees, while juveniles at Glen Affric (Figure 4.1b) and the Glenmore regeneration experiment plot (not shown in figures in this chapter) are strongly negatively correlated.

Despite implementing various mechanisms aimed at altering regeneration behaviour, it seems difficult to account for these differences in behaviour by consideration of the simulation model steady state – only fairly subtle changes occur. However, all the above results assume identical initial conditions, which do not necessarily correspond to the data. It is perhaps more appropriate to consider model behaviour under the different regeneration scenarios, using the data to provide initial conditions. We are searching for a single regeneration model that is able to explain the regeneration patterns seen in all three stands, given the structure of the mature trees.

In the case of the Rannoch plots, the past state may be inferred using the tree ring data. Management prior to 1918 is unknown. The Forestry Commission acquired the site in 1946, and it is thought that deer browsing pressure may have been higher during the 50 years preceding this date (Colin Edwards, personal communication). The inferred state at 1945 is taken as an initial condition below; the model is then run for 60 years for comparison with the (known) state at 2005. For Glen Affric, historical data is not available, but the estimated growth function may be used to compute a *very rough* estimate of trees' sizes at previous dates. Since the plot was established around the same time as the Rannoch plots, growth of current trees is "reversed" for 60 years using Equation 2.1 to generate an initial condition. The same procedure of running the model forward, with reproduction, is then performed. In generating the initial conditions, it is assumed that no mortality has occurred during the intervening period.

Results

Using the procedure described above to infer the data plots' previous state, it was not possible to find that a single birth model that recreates the current patterns seen in *all* three stands. The general results are described qualitatively below.

For Rannoch plot 4, the steady recruitment over the period up to 1990 is reasonably well matched, regardless of the precise form of establishment probability. The overall clustered pattern is observed only when local dispersal is included. It is worth noting that local dispersal has an apparently negligible effect on the cross-correlation, leaving it effectively random, as observed in the Rannoch plots.

In Rannoch plot 7, stronger regeneration in the period from 1950 onwards is observed. Its basal area at this time was likely far lower than that of plot 4. Altering the strength of dependence upon interaction (C) does not account for the difference. Making establishment more dependent upon basal area than local effects (decreasing k_d) does not appear to account for the difference either, even when C is increased concurrently. Reproduction appears to have occurred at a higher rate in this plot, independently of the difference in structure/density.

No birth model tested replicates the extremely strong negative cross-correlation between juveniles and mature trees in the Glen Affric stand. The mature trees display a clustered pattern. Using the birth model incorporating local dispersal and increased local inhibition of establishment, some inhibition is observed in the simulated cross-correlation function (but not as much as in the data – this would require almost totally excluding establishment in the neighbourhood of existing trees).

A final point is that under no birth model configuration is the apparently increasing birth rate of the data stands (Figure 4.5) accounted for by the simulations. This raises a problem of explaining these trees' presence. If mortality rate is identical for all trees, and is constant over time, the patterns in the semi-natural data should not be observed. Of course, if small trees (say $<$ 10cm dbh) experience higher mortality rates (Taylor and MacLean, 2007), the patterns are easier to understand. Another explanation is improved deer control over the study period, leading to heightened recruitment of seedlings.

4.3.7 Summary

This section had various motivations. The first was that the PCF displays clustering in all semi-natural data, but not in simulated populations. Secondly, a high degree of variation in regeneration patterns is observed between the semi-natural stands, both in density and in the degree of apparent inhibition by established trees (as measured by the cross-correlation).

In general, alterations to the establishment process led to weaker effects than might have been expected. Particularly notable is the weak effect of any of the considered formulations upon the cross-correlation between juvenile and mature trees. Even at levels of establishment inhibition which cause density to be substantially reduced, or with highly localised dispersal, cross-correlation is fairly unresponsive. An identical analysis was carried out using a smaller cut-off size between the two categories (5cm), and the results obtained were no clearer.

In simulation output, the PCF of juveniles only did not display clear effects, instead being subject to very high levels of variation under a given parameterisation

(and indeed between the data stands). The reason for this is the small number of individuals upon which the calculation is based. It was not included in figures presented in this section, due to the difficulty in making inferences based upon it.

Local dispersal has a clear positive effect on the PCF, providing a better match with the data. However, it also increases the MCF at short ranges (which as a result no longer matches the data very well), suggesting that clustering *could* be partly due to environmental heterogeneity.

4.4 Growth and size

4.4.1 Basic Issues

Growth rate

At early times (plantation, 80 years) the mean size of trees and basal area in the model is too low (Figure 4.2). As can be seen in Figure 4.10, the estimated Gompertz curve (black line) is clearly too "slow" to account for most juvenile trees in the Rannoch data. The majority of the growth increment measurements used for estimation are necessarily taken from older trees (many of which have grown surprisingly slowly, Chapter 3).

Ignoring interaction for the moment, there are two parameters that control the instantaneous growth rate of an individual in the model. Recall the Gompertz function:

$$\frac{ds}{dt} = s\,(\alpha - \beta \ln(s)) \tag{4.4}$$

At small sizes, the growth rate is dominated by α. At the initial size $s = 1$, the first term on the right hand side (αs) is positive, while the second ($\beta s \ln s$) is zero. Differentiating the equation also tells us that the growth rate is increasing until $(\alpha - \beta)/\beta = \ln s$, while the asymptotic size is $\exp(\alpha/\beta)$. Initial growth rate can thus be increased by increasing α, without affecting asymptotic size (provided β is increased accordingly).

Increasing α and β increases the peak plantation basal area (closer to the observed plantation), as the mean size of individuals at 80 years is slightly larger (Figure 4.11). The evolution of density is not affected by the parameter changes, nor are the steady state PCF and MCF (even when the growth competition parameter γ is increased).

Two parameter alterations are presented in Figure 4.11, and the smaller of the two produces slightly more favourable results. However, it is difficult to discount the possibility that even higher parameters should be used; despite a worsening in the plantation size distribution fit, many juveniles in the semi-natural stands have grown faster than is possible with these parameters (see again Figure 4.10). Furthermore, in Scots pine plantations it has been observed that when removing trees from a stand of around $35 m^2 ha^{-1}$ basal area, the drop in basal area is very rapidly refilled (Colin Edwards, personal communication), which does not occur with the lower grow parameters (see Chapter 6). Increasing γ in addition to (α, β) can lead to a similar mean size at 80 years, but a slight alteration to mortality parameters is required, for example, to match density and variance in size correctly.

The use of different growth functions was also considered. For example, an equivalently parameterised monomolecular growth function gives faster juvenile

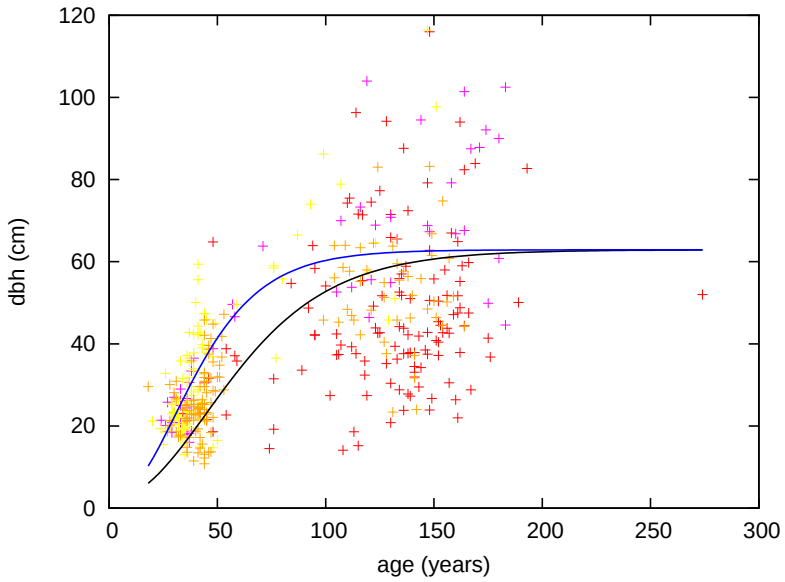

Figure 4.10: Plot of size (dbh) against age for all Rannoch study plot data in 1990, which demonstrates the breadth of sizes of individuals of a certain age (crosses, Rannoch plots: 4 (red), 5 (magenta), 6 (yellow), 7 (orange)). Superimposed over this are two Gompertz growth curves: that used in Chapter 2 (black), and another with the same asymptotic size, but faster initial growth rate ($\alpha = 0.19$, $\beta = 0.04587$: blue). These datasets were discussed in more detail in Chapter 3.

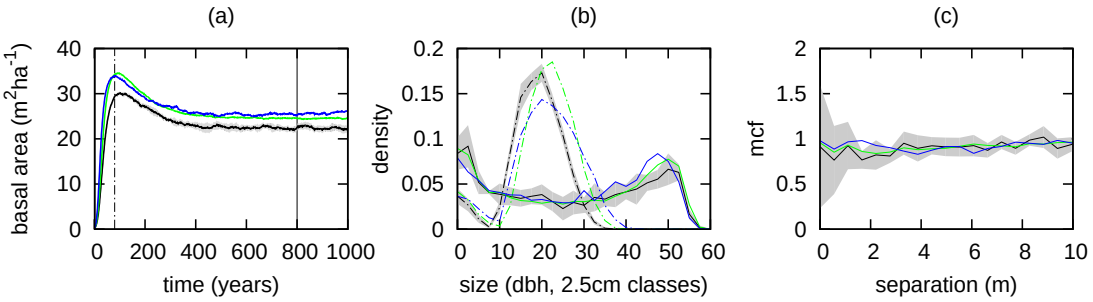

Figure 4.11: *Faster growth.* The effect of increasing growth parameters (α, β, γ) to (0.15, 0.03622, 0.00005) (green) and (0.19, 0.04587, 0.00007) (blue). For comparison, original results (as Figure 2.4) use black curves. (a) Evolution of density (dashed) and stand basal area (solid line), averaged over 10 simulations of a 1ha plot. (b) Size distribution at 80 (dash-dot) and 800 (solid) years. (c) Mark correlation function – time/line style as (b).

growth than a Gompertz function. However, this leads to populations with a very low density of juvenile trees in the steady state (Appendix B, Figure B.5), requiring large alterations to birth and mortality rates for equivalent behaviour of the size distribution. It is not considered further here.

Maximum size

In the long-run, individuals accumulate in the upper size classes, close to the asymptotic size. This behaviour occurs regardless of the actual magnitude of the asymptotic size, and is only dependent upon non-extinction of the population. The semi-natural datasets display different behaviour, being characterised by a canopy "peak" in density at an intermediate size and a very low, but non-zero, density of much larger trees – the variance of sizes of canopy trees is very large. The low density "tail" observed in the data is never recovered by the model.

Life-history variation

More importantly, in the data, old trees of a similar age vary widely in size. This is made clear in Figure 4.10, which shows age against size for all Rannoch data plots, with the implemented model growth curve superimposed for comparison. This variation is not explained (statistically) by altering the interaction kernel form, or making growth rate dependent instead upon age or height (see Section 3.5).

Explaining the patterns seen in the data is complicated by its incomplete nature; the basic problem being that the trees which are very small for their age (a large proportion of the old trees) are the same trees for which early life neighbourhood data is unavailable. Simulation is therefore a useful tool in exploring the effect of various changes to the manner in which individual tree growth is determined:

- changes to interaction form
- cumulative interaction
- age dependence
- individual variation

Each intended solution presents new behavioural issues for consideration.

4.4.2 Altering basic aspects of interaction

Background

A great deal of work has been produced on the subject of competition indices, in both the forestry (Biging and Dobbertin, 1992; Bollandsas et al., 2008; Mailly et al., 2003; Pommerening, 2002) and more general population dynamics (Purves and Law, 2002; Schneider et al., 2006) literature. It is now generally accepted that the inclusion of spatial interactions is important in explaining patterns in real communities (Pacala and Deutschman, 1995; Turnbull et al., 2007), but some studies have found that changes to the precise form of spatial dependence do not necessarily have a great effect on explanatory power (Purves and Law, 2002; Canham et al., 2004). It has also been found that strong competitive size-asymmetry can reduce the effect of spatial aspects of interaction (Hara and Wyszomirski, 1994; Weiner et al., 2001). Given the relatively weak coefficient of the effect of interaction on growth (γ), the minimal difference between the mean-field and spatial models observed in Section 2.6 is hardly surprising.

In the basic simulation model, competitive interaction is not totally asymmetric; regardless of their size, individuals always experience *some* interaction with neighbours (though this tends to decrease with size). Complete asymmetry is approached as $k_s \to \infty$. Altering this and the other interaction parameters (k_d, γ), and the interaction kernel form, is thus the first line of enquiry.

Results

Simulations were performed using a variety of spatial kernel forms operating over a similar spatial scale, but (in accordance with the studies noted above) no major differences in behaviour were found. Analysis of the Rannoch growth data, as detailed in Chapter 3 was also made using the same suite of kernels, but none performed notably better than any other (not shown).

The effect of altering parameters k_d, k_s and γ was documented in Section 2.5. Altering size asymmetry (k_s) has little effect on any of the computed statistics except the variance of the early size distribution. The spatial extent of competition (k_d) primarily affects spatial structure and basal area (as interaction becomes increasingly local, the population becomes "more dense" due to the mean size of trees being larger). However, the shape of the plantation size distribution is adversely affected under such a change.

Furthermore, in the current model, no basic parameter change is able to account for the variation of tree sizes at a given age observed in Figure 4.10. This requires

fundamental changes, such as those outlined below.

4.4.3 Cumulative interaction

Background

The notion of cumulative interaction was introduced in Section 3.5.1. However, incomplete data meant that no improvement in statistical fits was made using this formulation.

It was noted (Figure 3.8) that under cumulative interaction, the level of size asymmetry could have a fundamental effect on the dynamics of individual growth, and population size structure. As competition becomes increasingly asymmetric (k_s increases), asymptotic size is determined earlier in individuals' lives (that is, when they are smaller). Variation in growth behaviour as described by Oliver and Larson (1996, pg. 37) (that is, determined by early inhibition) may thus be implemented in the model.

The dynamical effects of cumulative interaction are explored below using the simulation model.

Results

Owing to the difficulty in accurately identifying parameters for the cumulative interaction growth model (Section 3.5.1), the growth parameters presented in Table 3.3 are not used for the simulations shown below. For clearer comparison of the two competitive scenarios, the basic growth parameters α and β remain the same as in Chapter 2. γ is set at 1×10^{-6}, and μ_2 is 5×10^{-7}. All other parameters remain unchanged. The specific competitive interaction scenarios presented in Figure 4.12 are:

- Symmetric ($k_s = 0$)
- Asymmetric ($k_s = 1.2$)
- Highly asymmetric ($k_s = 20$)

Comparison of the "cumulative model" with the "basic model" (instantaneous competition) shows some similarities, and some distinct differences. Qualitatively, the evolution of individual density (not shown) and basal area (Figure 4.12a) is similar. However, steady state basal area is much lower under cumulative interaction.

Relatively low accumulated interaction at early ages means that juveniles generally grow faster in the cumulative model than the basic model (seen in the steeper

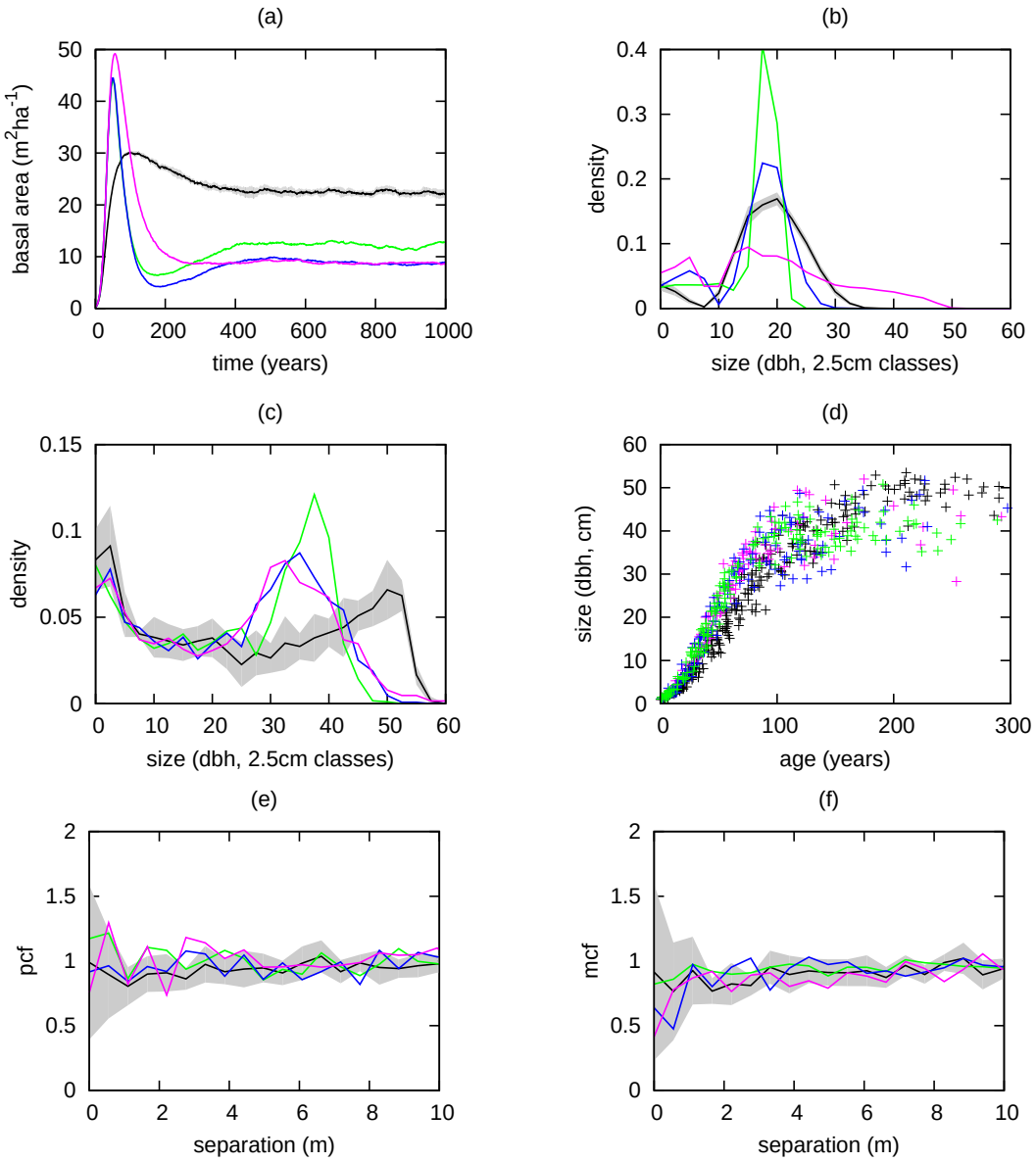

Figure 4.12: *Cumulative interaction*. Reformulating competition so that it accumulates through individuals' lifespans (Equation 3.8) leads to a change in behaviour. Results from the basic model are shown in black/grey, other lines are generated with cumulative competition with (α,β,γ)=(0.1308,0.03158,1E-06), varying k_s (= 0 (green), 1.2 (blue), 20 (magenta)). (a) stand basal area (b) size density distribution at 80 years (c) size density distribution at 800 years (d) size vs age at 800 years (e) PCF at 800 years (f) MCF at 800 years.

initial slope in size vs age in Figure 4.12d). This results in a higher peak in basal area, and at an earlier time (4.12a). Cumulative interaction also means that individuals grow more slowly when they are mature, leading to a smaller average asymptotic size

(apparent in 4.12c,d), which causes the lower steady state basal area.

Another effect of cumulative interaction is that variation in individuals' neighbourhoods over the course of their lives leads to variation in their asymptotic size, an effect that increases with size asymmetry (Figure 4.12d). It is also apparent that deviations in competitive asymmetry under the cumulative model (as for the basic model) lead to large shifts in the variance of the early size distribution (Figure 4.12b). In all cases, the steady state size distribution is believable in comparison with data stands (though maximum size clearly remains limited). The PCF is not greatly affected (4.12e), but the MCF shows clearer short range depression at higher levels of asymmetry (4.12f).

However, there remains somewhat less heterogeneity in growth under any of the presented scenarios (Figure 4.12d) than is observed in the data stands (Figure 4.10). Furthermore, steady state density and basal area are very low using the cumulative model. Increasing fecundity has a weak effect on these quantities, and comes at a cost of an unrealistic high density of juvenile trees in simulated plantations (not shown). Reducing the mortality rate also has a fairly minimal effect on the steady state basal area.

Size asymmetry is often cited as a driving factor in the population dynamics of plants (e.g. Weiner et al., 2001). It is interesting that altering the level of asymmetry did not greatly affect the steady state behaviour of the basic instantaneous competition model (Figure 2.5), but when competition is allowed to accumulate, changes become apparent. These results suggest that in real populations, a lasting effect of competition is seen in the growth of individuals, even after the source of competition has been removed. However, this is insufficient to account for the variability observed, and does not account for the few very small/large old trees observed in the semi-natural Scots pine data.

4.4.4 Age dependence

Background

An alternative mechanism that allows interaction at early life stages to affect future growth prospects is to include age dependence in the growth function. For example:

$$G_i(t) = \exp(-k_a a_i(t)) s_i(t) \left(\alpha - \beta \ln(s_i(t)) - \gamma \Phi_i(t)\right) \tag{4.5}$$

where $a_i(t)$ is individual age. Individuals effectively lose the ability to grow as they become old, and intense competition at an early age thus means that they remain small for the duration of their lifespan. The model populations' variation in competitive

neighbourhood can thus be expected to result in a range of asymptotic sizes.

Results

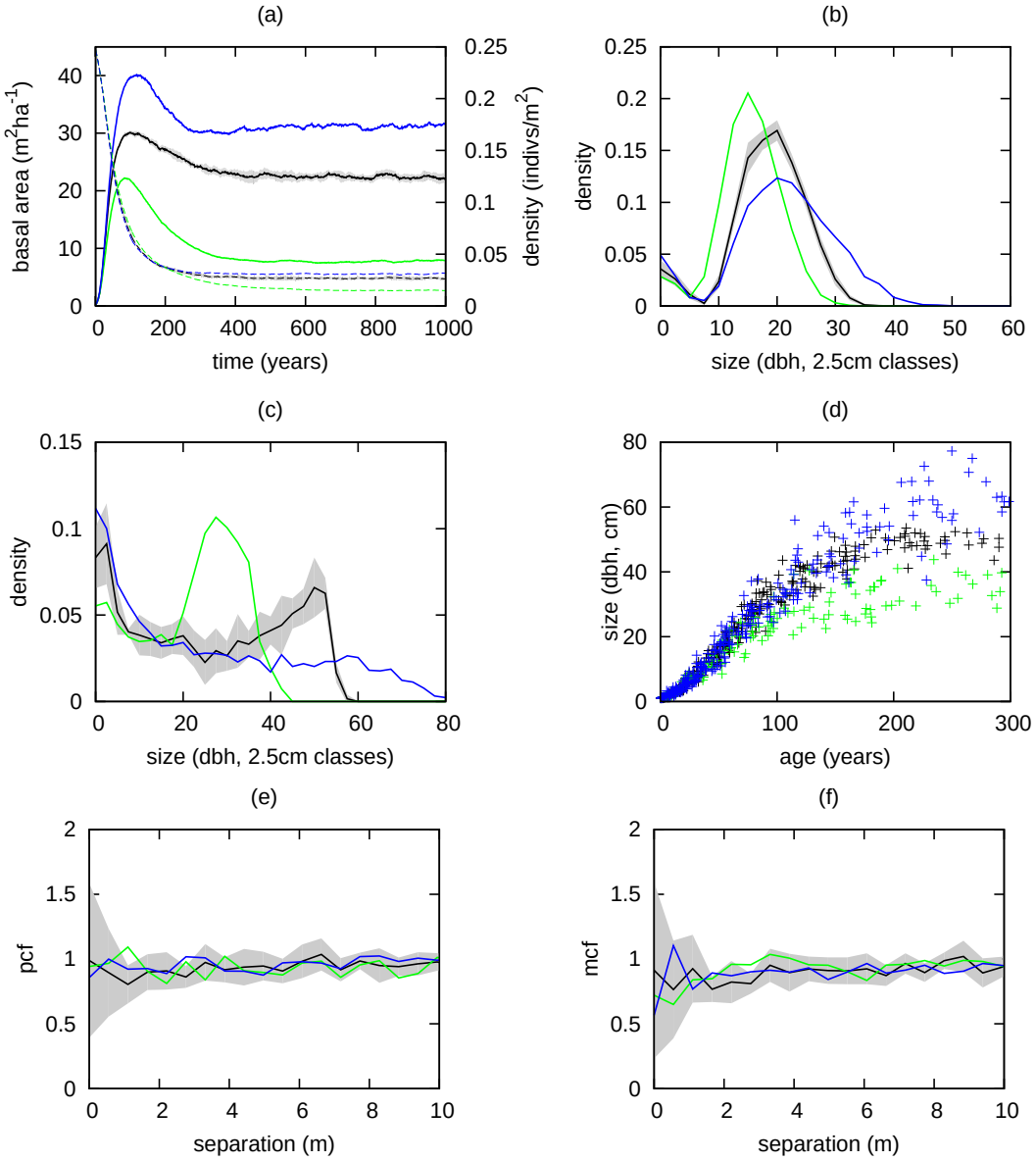

Figure 4.13: *Age-dependent growth*. Formulating growth rate such that it decays with age (Equation 4.5) leads to increased variability in the steady-state size distribution and size at a given age. (α,β,γ)=(0.137,0.0274,0.00005). (a-f) as for Figure 4.12. In (a), solid lines show basal area and dashed lines show individual density. Using parameters estimated in Table 3.2 (κ_a =0.02, green) leads to very low density and basal area. Reducing the age dependence parameter as detailed in the text (κ_a =0.01, blue) produces more amenable behaviour.

Two scenarios were simulated: (1) $k_a \in [0.01, 1]$, with all other parameters as in the basic model, and (2) the same range of k_a, but with the parameters (α,β,γ)=(0.137,0.0274,0.00005) (computed using a NLS fit to all datapoints at once, which would give a larger asymptotic size in the absence of the age dependent term).

Using the original parameters, only simulations using $k_a = 0.01$ survive the simulated period of 1000 years; when k_a is larger, the possibility for growth decays so rapidly with age that no individuals reach the larger size classes. Moreover, the spread of size vs age under this parameterisation does not come close to that of the semi-natural data (not shown).

Using the alternative growth parameters obtains more realistic results, which are presented in Figure 4.13. The larger asymptotic size imparted by the altered α and β means that age dependence does not prevent initial growth into the moderate (30–50cm) size classes. An increased level of variation in size at a given age is observed, but with this parameterisation basal area is too low, and the long-run size distribution is notably stunted (Figure 4.13c). Reducing the rate of growth decay with age to $k_a = 0.01$ leads to a larger individual asymptotic size and consequently higher basal area, with no noticeable reduction in size-age variation.

4.4.5 Individual growth variation

Background

There are two possible causes of the discrepancy between the model and data size and size/age distributions. Firstly, the difference may be induced by fundamental failings in the construction of the model, for example in its characterisation of competition and growth. Secondly, it may be due to intrinsic or environmental variation between the growth of the trees in real stands.

The results of NLME analysis presented in Table 3.3 have very large standard deviations for all estimated parameters, of the same order of magnitude as the corresponding mean values. An identical analysis of simulated data (where the simulated individuals have fixed and identical parameter values) recovers the growth parameters used accurately and with low standard deviation, throughout stand development (Table 4.3), and with a range of different parameters (not shown). In each time "window", the NLS estimates and fixed effects of the NLME are almost identical. At later times, the relative quality of fit of the NLME model improves, and variability in neighbourhood leads to increased random effects. However, these remain (at most/worst) one order of magnitude less than the fixed effects, in contrast with the very large random effects observed in the real data, which suggest true heterogeneity, or omission of variables from the growth model.

Table 4.3: *Computing NLS and NLME fits to simulated data.* Estimates for the growth parameters α, β and γ are made using individual growth data from three different periods of stand development. Note that estimates are made with lower RSE in the first period, due to the very low variability in growth trajectories at this time. RSE is Residual Standard Error (Equation A.10), Appendix B, AIC is Aikake's An Information Criterion (Equation A.8 – not comparable with data fits in Chapter 3 due to different number of data points) and values in brackets are correlations between the random effects, $(\rho_{\alpha\beta})$ and $(\rho_{\alpha\gamma}, \rho_{\beta\gamma})$.

	nls			nlme			
	LS Estimate	RSE	AIC	Fixed (μ)	Random (σ)	RSE	AIC
0-100 years							
α	1.308e-01	2.9e-07	-421189.1	1.308e-01	3.528e-12	2.9e-07	-421177.1
β	3.158e-02			3.158e-02	2.190e-23	(0)	
γ	5.000e-05			5.000e-05	2.741e-15	(0	0)
100-500 years							
α	1.298e-01	8.3e-03	-91480.17	1.298e-01	4.794e-03	5.3e-03	-99436.9
β	3.130e-02			3.134e-02	1.153e-03	(1.000)	
γ	4.970e-05			4.949e-05	2.480e-06	(0.983	0.980)
500-1000 years							
α	1.256e-01	2.0e-02	-64794.59	1.282e-01	8.627e-03	7.8e-03	-84044.2
β	3.028e-02			3.099e-02	1.966e-03	(0.998)	
γ	4.662e-05			4.742e-05	8.234e-06	(0.951	0.935)

In the absence of such explanatory variables, we can try incorporating the variation estimated from the data directly into the model, and assess the robustness of behaviour to this. Various approaches are considered below:

1. α,β from a bivariate Normal distribution (estimates from Table 3.3)

2. allowing β alone to vary, using estimates from Table 3.3

3. sampling $\exp(\alpha/\beta)$ from the sizes of mature trees in the data, fixing α

In each case γ is allowed to vary proportionally to the asymptotic size of an individual, such that $\exp(\alpha/\beta)/\gamma = 62.9/0.0157 = 4007.6$ (the value of this ratio using the initially estimated parameters).

Results

Simulations performed selecting α,β from the bivariate Normal distribution estimated by the analysis presented in Section 3.3 (with estimated correlation $\rho = 0.988$, approach (1) above) obtain good steady state behaviour, but there is excessive size variance at age 80 years (Figure 4.14b). The variability inferred from the semi-natural

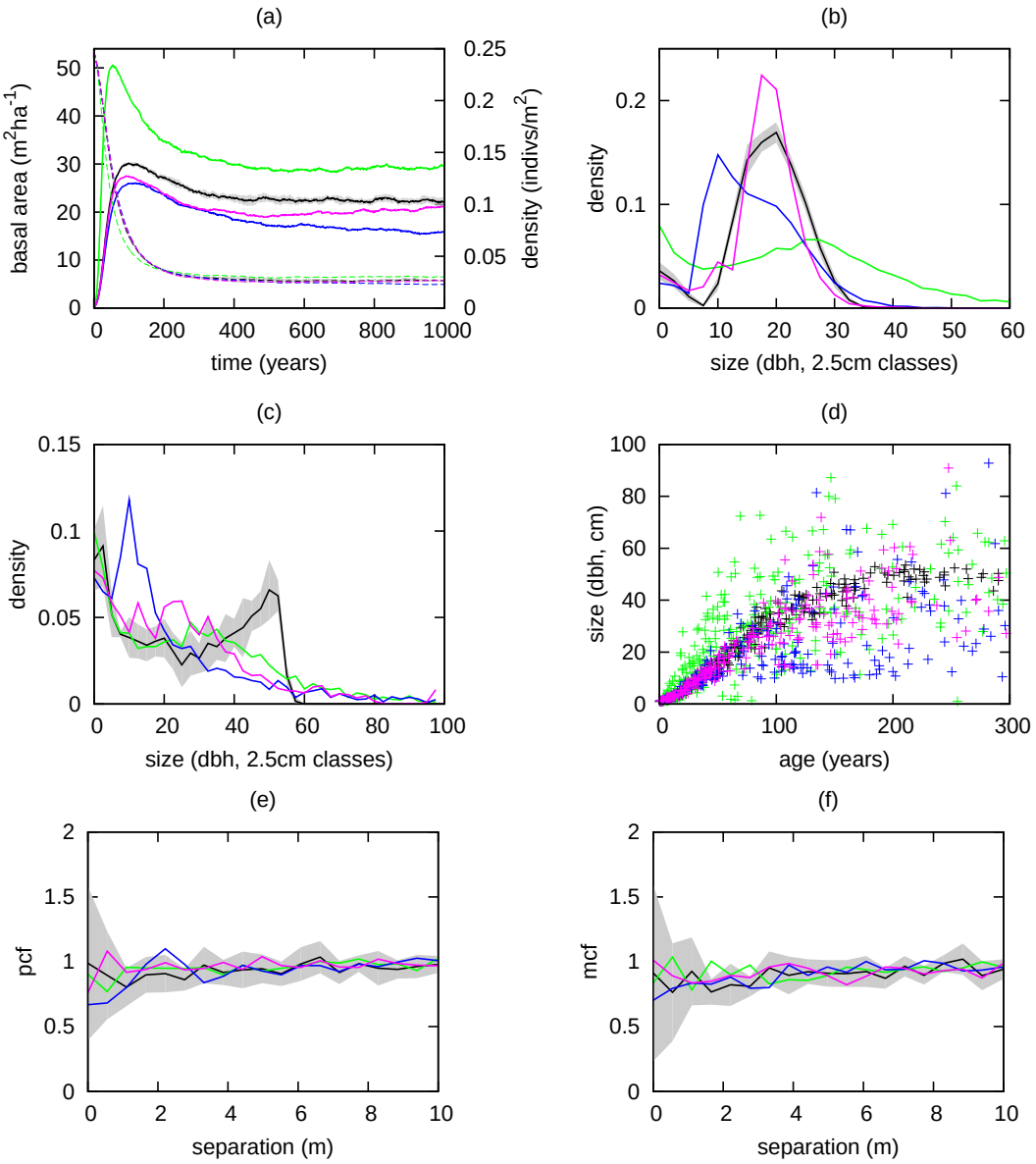

Figure 4.14: *Variable growth*. Allowing heterogeneity in individual growth parameters, as described in Section 4.4.5 also leads to a change in behaviour. Results from the basic model are shown in grey. α, β from bivariate normal (green, "1" in main text), β from normal distribution (blue, "2"), $\exp(\alpha/\beta)$ sampled directly from individuals over 100 years old in Rannoch plot 4, with α fixed (magenta, "3"). (a) stand basal area (b) size density distribution at 80 years (c) size density distribution at 800 years (d) size vs age at 800 years (e) PCF at 800 years (f) MCF at 800 years.

data appears to be inconsistent with the plantation data, where initial growth rate is relatively uniform across individuals.

In Equation 2.1, α controls the initial growth rate, while α/β determines asymptotic size. This suggests approaches (2) and (3) above: fixing α at the mean from the NLME analysis, while either allowing β alone to vary, or drawing $\exp(\alpha/\beta)$ (asymptotic size) from the observed sizes of individuals greater than 100 years old in the data stands. Both methods produce similar evolution of basal area, and obtain a more realistic plantation size distribution. However, (2) causes too many trees to remain very small for their entire lifespan (4.14c), while (3) obtains a better overall match with size and joint age-size distributions. It can also be sampled directly from a target stand. Spatial correlations are not affected by any choice of heterogeneity considered here (4.14e,f; though explicit environmental heterogeneity, for example, would affect these).

4.4.6 Summary

Parameter adjustments in the basic model were generally unable to account for its discrepancy with the available data (obtaining a good match for one statistic leading to the loss of accuracy in another). However, fundamental changes, such as cumulative competition, or age dependence, while not providing a complete explanation, nonetheless help to understand the importance of history, maturity and variability in real stands.

It is perhaps somewhat naive to assume that all variability in the individual growth data could be explained by recourse to mechanistic processes. Ultimately, the inclusion of explicit individual variation in growth rates was necessary to explain this variation. This can represent genetic (Provan et al., 1998) or environmental (Arkle, 1996) heterogeneity. Past management may also have increased the apparent heterogeneity: if for example it favoured removal of the best trees (which is highly likely), the remaining older trees may not have displayed typical growth rates.

The relatively small size of the datasets and the lack of genetic or environmental/soil data preclude determination of any specific source of heterogeneity. However, it is safe to say that competition (both instantaneous and cumulative), age dependence, and heterogeneity all have a role to play in the structure observed in real populations.

4.5 Summary

4.5.1 Overview

This chapter described various attempts to account for data variability using mechanistic processes. The basic model introduced in Chapter 2 displayed notable failings by way of comparison with data from Scots pine populations at various stages of development. Alterations to the basic components of the model (birth and growth; due to its limited scope in structure generation death was not tackled in any further detail here) were able to account for some patterns seen in the data, such as a clustered pattern of trees, or some variability in the growth rate or size of trees at a given age.

However, it was not possible to explain accurately all behaviours observed in the data, notably the strong differences seen in regeneration patterns between the semi-natural data stands, apparent step increases in density through time, and the full extent of variation in growth in the Rannoch stands. These features of the data may be indicative of the extent to which individuals, and the soil/environmental conditions in which they grow, vary over very small scales, and temporal/local variation in browsing pressure on regeneration. Determination requires additional data, which is not currently available for these stands.

4.5.2 An improved model for application

In light of the analysis presented in this Chapter, it is possible to suggest an improved model for the population dynamics of Caledonian pine stands. The most important alterations to the original model are:

- Local dispersal (on the same scale as interaction – Section 4.3.2)
- Increasing early growth speed (new growth parameters $(\alpha, \beta) = (0.15, 0.0362)$ – Section 4.4.1)
- A mechanism for growth variation

There was no clear indication that alteration to the establishment mechanism would produce improved dynamics, though in application of the model in Chapter 6, robustness to such alteration is considered. Dispersal and increased growth rate can be implemented simply, as detailed in their respective sections. However, the mechanism for growth variation is unclear. Accepting that variation exists, Chapter 6 also considers the robustness of management recommendations to the inclusion of growth variation, incorporated by approach (3) from Section 4.4.5.

Chapter 5

Mathematical moment approximation of the simulation model

5.1 Introduction

Individual based microscopic simulation models (hereafter IBMs) have proved very useful in ecology, forestry, physics and chemistry. Nevertheless, scientists have also sought to describe the bulk properties of their study systems using mathematical equations (macroscopic models). Statistical physics was originally developed with the goal of describing the overall behaviour of large numbers of fluid particles (such as the early work of Boltzmann, Fermi), but the philosophies and methods of the pioneers have also been very useful to scientists from other disciplines.

From an analytical perspective, macroscopic models have several advantages. IBMs are defined by rules which affect dynamics at a small scale, and it is often unclear how these dynamics scale to affect the overall properties of a system or population. On the other hand, macroscopic models can provide an explicit description of overall behaviour, which is defined in terms of the same individual parameters. In some cases, macroscopic models are analytically tractable, meaning that an exact solution for certain properties can be obtained. More frequently, simplifying assumptions are required to obtain such results, or they are not possible to obtain. Nevertheless, the derivation of macroscopic differential equations (ordinary or partial: hereafter ODEs and PDEs) often provides insights even when analytical solutions cannot be found. Furthermore, carefully constructed numerical integration schemes can often provide a solution. In lower dimensional systems these allow rapid computation of behaviour,

though this is rapidly lost as the dimensionality of summary measures increases, as will be seen.

This chapter deals with dynamical mathematical models of (single species) population dynamics. A differential equation approximating a mean-field birth-death model is described first, followed by its extension to include size and spatially structured dynamics. This allows identification of the differences between behavioural properties. All but the simplest models are, in general, analytically intractable, and so the results of numerical integration of the equations are also presented.

5.2 Mean-field models

In the context of population dynamics, "mean-field" is an umbrella term for models in which the dynamics are not dependent upon spatial structure – the basic modelling premise being that each individual in a population has an identical experience. In such models, the rates applying to individuals might be dependent only upon the total number of individuals, total biomass, or in the case of a size structured model, the distribution of individual sizes. Such an approximation allows one to move directly from the analysis of individual level effects, to the behaviour of the population as a whole.

5.2.1 A density dependent birth-death process

As an example, consider a population in which the number of individuals at time t, $N(t)$, is the result of just two processes, reproduction by existing individuals (birth), and death. Assume that each individual in the population reproduces at a constant rate b_1. The total rate of reproduction is thus $B(t) = b_1 N(t)$. Assume further that mortality of existing individuals occurs at a baseline rate, d_1, increased by increasing population size. The total mortality rate is thus $M(t) = N(t)(d_1 + d_2 N(t))$. The dynamics of the $N(t)$ are thus described by a differential equation,

$$\begin{aligned} \frac{dN(t)}{dt} &= B(t) - M(t) \\ &= (b_1 - d_1)N(t)\left(1 - \frac{d_2}{b_1 - d_1}N(t)\right) \end{aligned} \tag{5.1}$$

(each rate being multiplied by the population size to give the total rate of change). This is the logistic equation, postulated by Verhulst (1838), and rediscovered by Pearl and Reed (1920) who used it to describe human population growth in the United States of America. The equation is often presented in the form $dN(t)/dt = rN(t)\,(1 - N(t)/K)$.

Here, $K = (b_1 - d_1)/(b_2 + d_2)$ is the maximum sustainable population size (the "carrying capacity", which implies a fixed habitat size for the population), and $r = b_1 - d_1$ is the so-called *Malthusian parameter*, the maximum rate of population growth. Alternatively, the equation can be written in terms of density $n(t) = N(t)/A$, where A is the total habitat area.

5.2.2 A model with size structure

The importance of size-structuring of populations was recognised long ago by several authors. The best known model for age and size structuring of populations was introduced by von Foerster (1959). This approach was developed further by (amongst others) Sinko and Streifer (1967), who discussed a more general model that includes von Foerster's as a special case. More recent work has looked explicitly at the effects of size-dependence of physiological traits (for example DeRoos et al., 2003).

Ignoring age structure for now, let $N(s,t)$ be the number of individuals of size s at time t. The total number of individuals between sizes s_1 and s_2 is then $\int_{s_1}^{s_2} N(s,t)ds$. Setting $n(s,t) = N(s,t)/ds$, and letting $ds \to 0$, the behaviour of the system can be described by a partial differential equation

$$\frac{\partial n(s,t)}{\partial t} = -\frac{\partial}{\partial s}\left[n(s,t)G(s,t)\right] - M(s,t)n(s,t), \tag{5.2}$$

where $G(s,t)$ and $M(s,t)$ are the growth and mortality rates of individuals of size s at time t, respectively. Sinko and Streifer (1967) derive the more general case including age dependence for each term, and an additional term, $\partial n(s,a,t)/\partial a$, on the left hand side of the equation (where a is age).

An initial condition – the size distribution at time zero, $n(s,0)$ – must be specified. Additionally, Equation 5.2 does not include a birth term. We thus define a boundary condition $B(s,t)$, which describes an additional input to the density $n(s,t)$, and may be included directly in the right hand side of Equation 5.2. Sinko and Streifer (1967) point out that in many situations (and this is certainly true in the case of forests – see Chapter 2), this is best defined as an integral over the existing population. Thus, in line with Chapter 2, we can define

$$G(s,t) = \max\left(s\left(\alpha - \beta\log(s) - \gamma\Phi(s)\right), 0\right) \qquad \text{(growth rate)} \tag{5.3}$$

$$M(s,t) = \mu_1 + \mu_2\Phi(s) \qquad \text{(mortality rate)} \tag{5.4}$$

$$B(s,t) = P_e I(s=1)\int_0^\infty \frac{f\pi(s')^2}{4} n(s',t)ds'. \qquad \text{(birth rate)} \tag{5.5}$$

where the indicator function $I(s=1)$ means that birth only occurs in size $s = 1$; we

could equivalently define this as $B(1,t)$, omitting the indicator function. As in Chapter 2, $B(s,t)$ includes the establishment probability, but here it is a direct multiplier $P_e = (1 - M(1,t))^{20}$. Various options are available for the interaction function Φ, resulting in a range of mean-field models. For example:

$$\Phi(s) = \begin{cases} \int_0^\infty n(s',t)ds' & \text{density-dependent} \\ \int_0^\infty s'^2 n(s',t)ds' & \text{basal area dependent} \\ \int_0^\infty F_1(s,s')n(s',t)ds' & \text{size-structure dependent} \end{cases} \tag{5.6}$$

where $F_1(s,s')$ defines the strength of interaction imposed by an individual of size s' upon an individual of size s (see Chapter 2 for a more in-depth description). Only the third of these is actually dependent upon the size s. For ease of comparison (parametrically) with the stochastic IBM presented in Chapter 2, it is this form that is used for the numerical results presented in Section 5.2.4.

5.2.3 Solution to a simple case

Unfortunately, the density-dependent integral definitions of interaction (Equation 5.6) mean that we have not found an analytical solution for $n(s,t)$. However, setting the interaction term to be zero in Equations 5.3 and 5.4 allows some progress, and the form of the equilibrium density to be determined.

Computing the size derivative, we have that

$$\frac{\partial n(s,t)}{\partial t} = -s(\alpha - \beta \ln(s))\frac{\partial n(s,t)}{\partial s} - n(s,t)\left(\alpha - \beta(1 + \ln(s)) + \mu_1\right) \tag{5.7}$$

The steady-state solution can be obtained directly by setting $\partial n(s,t)/\partial t = 0$ in Equation 5.7, and $n(s,t) = \hat{n}(s)$, giving

$$\frac{\partial \hat{n}(s)}{\partial s} = -\hat{n}(s)\left(\frac{1}{s} + \frac{\mu_1 - \beta}{s\left(\alpha - \beta \ln(s)\right)}\right). \tag{5.8}$$

Separating variables and integrating over the range $[1, s']$, ultimately gives

$$\hat{n}(s') = \hat{n}(1)\frac{1}{s'}\left(\frac{\alpha - \beta \ln(s')}{\alpha}\right)^{\frac{\mu_1 - \beta}{\beta}} \tag{5.9}$$

where $\hat{n}(1) = B(1,t)$ is the boundary condition (Equation 5.5); As this is an integral, we cannot analytically solve the equation. Furthermore, Equation 5.9 describes an equilibrium only when $\hat{n}(1)$ is constant. The other terms give the form of the density, which is bimodal (at the initial and maximum sizes), and qualitatively matches the

results of both numerical integration and "mean-field" IBM results (see Section 5.2.4).

In the case that interaction is included and is a simple function of size, setting $\partial n(s,t)/\partial t = 0$ gives

$$\frac{\partial \hat{n}(s)}{\partial s} = -\hat{n}(s)\left(\frac{1}{s} + \frac{\mu_1 + \mu_2\Phi(s) + \gamma s\frac{d\Phi(s)}{ds} - \beta}{s\left(\alpha - \beta\ln(s) - \gamma\Phi(s)\right)}\right). \tag{5.10}$$

We cannot solve this equation in general, but the inclusion of interaction leads to additional terms in the right-hand fraction, and affects the value of $\hat{n}(s)$ in two ways. Assuming that $\Phi(s)$ is positive: i) the additional term in the denominator means that the singularity seen at the asymptotic size ($\exp(\alpha/\beta)$) in the absence of interaction occurs at a smaller size (as seen in Figure 5.1), and ii) the relationship between the two additional terms govern the extent to which $\hat{n}(s)$ decays faster at small sizes (resulting in a decreased total population size).

5.2.4 Numerical integration

Given the difficulty in obtaining analytical results, we now take a different approach. In Equation 5.2 we can write the derivatives as *finite differences* to give

$$\begin{aligned}\frac{n(s,t+\Delta t) - n(s,t)}{\Delta t} = &-\frac{n(s,t)G(s,t) - n(s-\Delta s,t)G(s-\Delta s,t)}{\Delta s}\\ &- M(s,t)n(s,t) + B(s,t)\end{aligned} \tag{5.11}$$

which can be rearranged to give an update rule for $n(s,t)$:

$$\begin{aligned}n(s,t+\Delta t) = n(s,t) + \Delta t\Bigg(&-\frac{n(s,t)G(s,t) - n(s-\Delta s,t)G(s-\Delta s,t)}{\Delta s}\\ &-M(s,t)n(s,t) + B(s,t)\Bigg).\end{aligned} \tag{5.12}$$

The original differential equation is defined in the limit $\Delta t \to 0$ and $\Delta s \to 0$. However, using $\Delta t \neq 0$ and $\Delta s \neq 0$ in Equation 5.12 allows us to directly compute the development of $n(s,t)$ (defined at discrete values of s) through time. This is an example of a "finite difference scheme".

Holmes (2006) provides a very readable and informative introduction to many aspects of the construction and implementation of finite difference schemes for differential equations, and before proceeding, certain points must be noted. The approximations used for the derivatives in Equation 5.11, which give the update rules, are some of the simplest of many possible approximations. The current time update depends only upon a single previous value, and is generally referred to as *forward*

Euler (a first-order, forward difference approximation). Other more complicated methods are sometimes used, the principal benefits being greater stability of the algorithm and reduced *truncation error* (the error introduced by assuming that a derivative can be represented by a finite difference equation) (Holmes, 2006), but for our purposes first order schemes will suffice.

This size derivative could also be computed using other methods. In Equation 5.2 (an example of an *advection equation*), waves travel in one direction only (in increasing s), and so Equation 5.11 uses an *upwind difference* scheme – that is, the value at $(s, t + \Delta t)$ is dependent upon the values at (s, t) and $(s - \Delta s, t)$ only. Again, many other more complicated methods are available, but this is implemented here for its simplicity and known stability properties. Holmes (2006) states that, in the form $n(s, t + 1) = (1 - \Delta t/\Delta s)n(s, t) + (\Delta t/\Delta s)n(s - 1, t)$, behaviour is stable conditional on $\Delta t/\Delta s \leqslant 1$). This is not so straightforward to determine in Equation 5.12, as some terms include additional quantities that vary ($g(s, t)$ and $\mu(s, t)$). Instead, the two following conditions must be satisfied:

$$\frac{\Delta t}{\Delta s} G(s - 1, t) \leqslant 1, \tag{5.13}$$

$$\left(1 - \frac{\Delta t}{\Delta s} G(s, t) - \Delta t M(s, t)\right) \geqslant 0. \tag{5.14}$$

This applies to all values of s except s_0, at which birth also occurs. The inclusion of the growth function extends the region of stability, as it always takes values which are less than 1. Numerical tests seem to validate the applicability of Equation 5.13: behaviour does not become unstable until $\Delta t \approx 1.5 \times \Delta s$ (Appendix C).

Generally speaking, one might expect the accuracy of the method to improve as the increment sizes decrease, but this is subject to the satisfaction of 5.13 and 5.14. A "best case" is presented in Figure 5.1, together with mean-field IBM results for comparison. The size distribution at 80 years does not match perfectly. Better matches to this statistic were obtained, but at the expense of accurate long run behaviour. In fact, all aspects of the presented statistics are affected by the choice of Δs and Δt. In general, coarse graining of the size distribution causes inaccurate behaviour at early times, while very fine graining leads to issues later on. Reducing Δs relative to Δt leads to improved accuracy up to a point, but causes poor long run behaviour, and ultimately instability of the procedure as it is reduced further (Appendix C).

5.2.5 Summary

Complicated conditions for stability mean that the ultimate choices for the increments Δs and Δt must be made in an ad-hoc fashion. However, it was found that the

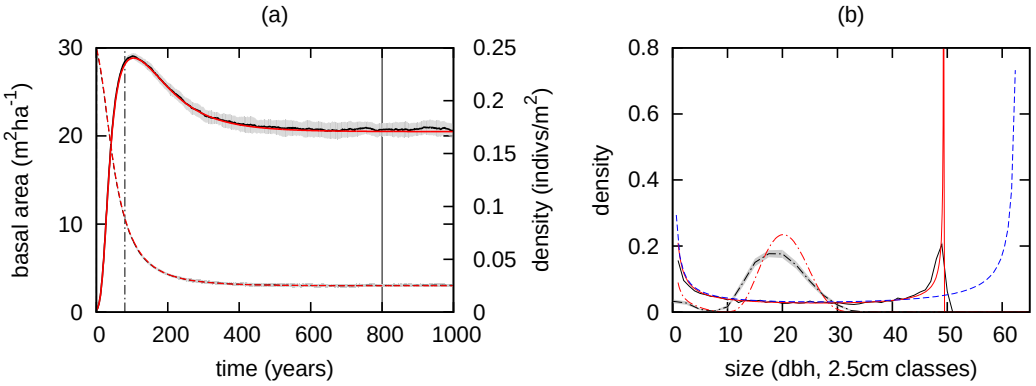

Figure 5.1: *Mean-field models: comparing results from numerical integration (PDE) and the mean-field IBM*. These results use $\Delta s = 0.085cm$ and $\Delta t = 0.125y$ (a) Evolution of basal area (solid) and density (dashed) through time. (b) Size distribution at 80 (dash-dot) and 800 (solid) years. IBM results are shown in black/grey, and PDE in red. In the long run, behaviour is almost identical (the IBM size distribution at 800 years is averaged over 10 plots, and has a coarser resolution (0.5cm) than the PDE). The blue dashed line is the solution of the equilibrium size distribution in the absence on interaction (Equation 5.9).

behaviour of $n(s,t)$ as computed by numerically integrating Equation 5.12 becomes close to that of the mean-field IBM presented in Chapter 2 as the size increment becomes small, and $\Delta t \approx 1.45 \times \Delta s$. Even using very small increments, Equation 5.12 is very quick to compute in comparison with the IBM. Both these features support the use of such an approach. We now turn attention to the development of an equivalent model incorporating explicit spatial interactions.

5.3 Spatial models

As authors moved towards the study of more complex populations, the inadequacy of mean-field models became more apparent. The use of increasingly complicated stochastic models helped shift the focus of study onto the effects of *individual* properties upon community structure. Small population sizes increase the relative effect of stochasticity, reducing the applicability of the perfect mixing assumption. Random fluctuations about a homogeneous equilibrium of interacting species in a spatial arena can lead to the development of stable spatial structure (Turing, 1952). Some problems, such as the population dynamics of plants, are explicitly spatial. Plants are sessile (non-moving), and consequently have their neighbourhood determined from the moment they become established. This led to the development of a class of models referred to as *birth-death-interaction* processes (in continuous space, or on a lattice).

5.3.1 Spatial birth-death processes

An important turning point in spatial ecology was the work of Matsuda et al. (1992), who discussed an extension of the Lotka-Volterra model onto a lattice. The birth and mortality rates at a location x on the lattice are proportional to $n(x)$, the proportion of occupied nearest-neighbour sites to x. This leads to a model describing the evolution of the overall density n_i of sites containing an individual of a particular species i, and the evolution of *pair densities*, that is, the density of pairs of neighbouring sites containing individuals of species i and j, n_{ij}. This formed the basis for much work in varied aspects of biology (e.g. Ellner, 2001; Filipe and Maule, 2003).

A continuous-space equivalent was developed more recently: the single species case being first discussed by Bolker and Pacala (1997), and developed further by Law and Dieckmann (2000). Call the density of individuals at location x at time t $n(x,t)$. Individuals in the population with location x'' produce offspring at location x at a rate:

$$B(x,x'') = fm(|x-x''|) \tag{5.15}$$

where $m()$ is a *dispersal kernel*, the probability that an offspring lands a certain distance from its parent. The mortality rate of an individual at location x is given by

$$M(x) = \mu_1 + \mu_2 \int_{x'} F_2(|x-x'|)n(x',t)dx' \tag{5.16}$$

where $F_2()$ is an *interaction kernel* which describes the (usually deleterious) effect of interaction with a neighbour located a certain distance away (see Chapter 2).

Interaction and dispersal are assumed to be rotationally symmetric; only separation distance is of importance to the dynamics.

Constructing a master equation for $n(x,t)$, assuming spatial homogeneity (averaging across space), and some algebra, leads to the differential equation of the *first moment* of the population, $n_1(t)$:

$$\frac{dn_1(t)}{dt} = (f-\mu_1)n_1(t) - \mu_2 \int F_2(r)n_2(r,t)dr, \tag{5.17}$$

where $r = |x-x'|$. $n_2(r,t)$ is the density of pairs of individuals with separation r (the *second moment*). The dynamics of the first moment are thus dependent upon the current first- *and* second moments.

Repeating the procedure for the second moment (with more algebra), dynamics are found to be dependent upon moments up to and including $n_3(r,r',t)$, the third moment, or "triplet density":

$$\begin{aligned}\frac{dn_2(r,t)}{dt} =& 2fm(r)n_1(t) \\ &+ f\int m(r')n_2(r+r',t)dr' + f\int m(r')n_2(-r+r',t)dr' \\ &- 2\mu_1 n_2(r,t) \\ &- m_2\int \Phi(r')n_3(r,r+r',t)dr' - m_2\int \Phi(r')n_3(r,r',t)dr' \\ &- 2\mu_2\Phi(r)n_2(r,t).\end{aligned} \tag{5.18}$$

This equation describes the combined effects of dispersal and interaction in the development of spatial structure, which consequently impacts the realised global individual density, $n_1(t)$ (which may be larger or smaller than that of a mean-field population).

If one were to derive an equation for the dynamics of $n_3()$, it would be found to depend upon moments up to and including $n_4()$: in general $dn_i/dt = f(n_1,...,n_{i+1})$. This hierarchy is infinite, and in practice, must be truncated at some point. This is the problem of *moment closure*. The basic approach is to approximate higher order densities (the "moments" of the spatial process) with functions of lower ones. Order two is generally considered a useful point at which to truncate, as it is the simplest level at which spatial information can be included. Densities of triplets (and larger groupings) are also difficult to visualise conceptually (Law et al., 2003; Murrell et al., 2004). Several studies compared the basic behaviour of these "moment models", closed at second-order, with the individual-based stochastic models they attempt to summarise (Bolker and Pacala, 1997, 1999; Law and Dieckmann, 2000; Law et al.,

2003), but it was not until the work of Murrell et al. (2004) that a comprehensive comparison of the available closures (third-moment approximations) was made. Broadly, Murrell states, these are one of three types (dependence on t is dropped here):

$$n_{3(ijk)}(r,r') = \frac{1}{b}\left(a n_{1(i)} n_{2(jk)}(r'-r) + b n_{1(j)} n_{2(ik)}(r') + c n_{1(k)} n_{2(ij)}(r) - (a+c) n_{1(i)} n_{1(j)} n_{1(k)}\right) \quad \text{"Power-1"} \tag{5.19}$$

$$n_{3(ijk)}(r,r') = \frac{1}{a+c}\left(a\frac{n_{2(ij)}(r) n_{2(ik)}(r')}{n_{1(i)}} + b\frac{n_{2(ij)}(r) n_{2(jk)}(r'-r)}{n_{1(j)}} + c\frac{n_{2(ik)}(r') n_{2(jk)}(r'-r)}{n_{1(k)}} - b n_{1(i)} n_{1(j)} n_{1(k)}\right) \quad \text{"Power-2"} \tag{5.20}$$

$$n_{3(ijk)}(r,r') = \frac{n_{2(ij)}(r) n_{2(ik)}(r') n_{2(jk)}(r'-r)}{n_{1(i)} n_{1(j)} n_{1(k)}} \quad \text{"Power-3"} \tag{5.21}$$

where a, b and c can be used to weight particular terms in the closure (though this violates certain intuitive requirements, see Murrell et al. (2004)).

This body of work was broadly successful in helping to understand many basic questions in ecology, including, amongst others: the drivers of population spatial structure (Bolker and Pacala, 1997; Law et al., 2003), the outcome of interaction between species (sometimes different in spatial communities compared with mean-field behaviour Law and Dieckmann, 2000), and the benefits of adopting particular life-history strategies (Bolker and Pacala, 1999). However, no published study incorporates the effect of size- in addition to spatially-structured interactions. This leaves an important gap in knowledge, due to the perceived importance of both structural aspects to the dynamics of real communities.

5.3.2 Combining size and spatial structure

A model of neighbour-dependent growth of plants was outlined by Law et al. (unpublished manuscript), defining the dynamics of the relevant first and second moments. However, no closure was defined for the third moment, and as a consequence no numerical integration of the derived partial differential equations was computed, preventing comparison of the moment model with stochastic simulation results.

The derivation described below is based upon that of Law et al., but includes additional birth and mortality terms. The equations themselves allow insight into the drivers of population dynamics: how size and spatial structure affect first-order properties, and how spatial structure develops. Approximations for the third moment

based upon those of Murrell et al. (2004) are presented, and a basic comparison of their properties is presented.

Moments/densities

The quantities of interest are densities dependent upon both size and separation. Consider small boxes of area $dx \times ds$ about a point in size and space (x, s). We consider the number of individuals $N(x, s)$, and its rate of change within these small boxes (dx and ds are sufficiently small that $N(x, s) \in 0, 1$. To simplify notation, dependence of t is assumed and not shown for the remainder of this section. The first-order density (hereafter "first moment") is

$$n_1(s) = \mathbb{E}\left(\frac{N(x, s)}{dxds}\right) \tag{5.22}$$

where $N(x, s)$ is the number of individuals at (x, s). Integrating over s obtains the first moment of the non size-structured model. The second moment (pair-density) is

$$n_2(r, s, s') = \mathbb{E}\left(\frac{N(x, s)(N(x + r, s') - \delta(r)\delta(s' - s))}{(dxds)^2}\right) \tag{5.23}$$

This is a function of separation and the sizes of each member of the pair (delta functions remove "self-pairs"). However, integrating over s and s' recovers the unnormalised pair density from the non size-structured model. That is,

$$n_2(r) = \int_s \int_{s'} n_2(r, s, s')ds'ds \tag{5.24}$$

($PCF(r) = n_2(r)/(\int n_1(s)ds)^2$). The unnormalised mark-correlation function can also be obtained by a simple integration:

$$g_{mm}(r) = \frac{1}{\bar{s}^2} \int_s \int_{s'} ss' n_2(r, s, s')ds'ds \tag{5.25}$$

($MCF(r) = g_{mm}(r)/(\int n_1(s)ds)^2$). Correspondingly, the third moment is given by

$$\begin{aligned} n_3(r, r', s, s', s'') =& \mathbb{E}\left(\frac{1}{(dxds)^3} N(x, s)(N(x + r, s') - \delta(r)\delta(s' - s))\right. \\ & \left. \times (N(x + r', s'') - \delta(r')\delta(s'' - s) - \delta(r' - r)\delta(s'' - s'))\right). \end{aligned} \tag{5.26}$$

Again, delta functions remove the "self" triplet case, where any one of the three members has the same location/size as any other.

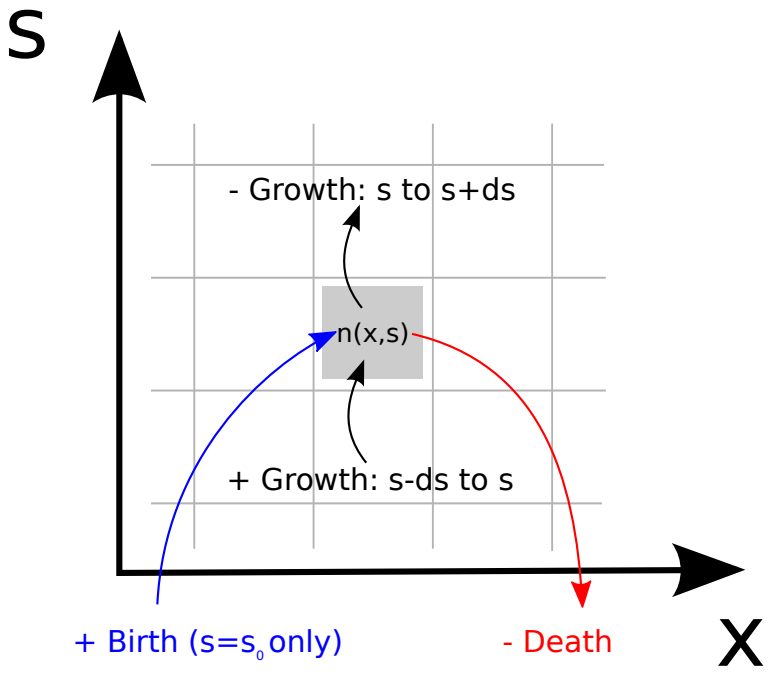

Figure 5.2: *Events affecting the value of the first moment*. For computation, the moments must be discretised. The first moment $n(x,s)$ is increased by birth, and growth from the size below, and is decreased by mortality and growth into the size above. In Equation 5.34, this is averaged over space.

First moment

Figure 5.2 shows the events that cause changes in the first-order density within a small box at location x and size s, $N(x,s)$.

Growth of an individual can cause an increase in this density (growth "into" the box) or a decrease (growth "out of" the box). The change in density is described by the contributions (the rate of attainment of small size increments δs by an individual, multiplied by the density of individuals at the size/location):

$$G_1(x,(s-\delta s)\rightarrow s) = \left[g(s-\delta s) - \gamma \sum_{i\in\omega} \Phi(r_i, s-\delta s, s_i) N(x_i,s_i)\right] N(x,s-\delta s)\frac{1}{\delta s} \tag{5.27}$$

$$G_1(x,s\rightarrow(s+\delta s)) = \left[g(s) - \gamma \sum_{i\in\omega} \Phi(r_i, s, s_i) N(x_i,s_i)\right] N(x,s)\frac{1}{\delta s} \tag{5.28}$$

x_i and s_i are the locations and sizes of other individuals in the population ω (which contains n individuals), $r_i = |x - x_i|$, and $g(s)$ is a function of size that describes the growth rate of an individual in the absence of competition. $\Phi(r,s,s_i)$ describes the

competitive effect (upon an individual of size s) of a neighbour of size s_i located a distance r away.

Mortality of an individual causes a decrease in density at x and s (similarly to Equations 5.16 and 5.4):

$$D_1(x,s) = \left[\mu_1 + \mu_2 \sum_{i\in\omega} \Phi(r_i, s, s_i) N(x_i, s_i)\right] N(x,s). \tag{5.29}$$

Birth causes an increase in density (similarly to Equations 5.15 and 5.5). The birth rate at x and s is:

$$B_1(x,s) = \int \delta(s-1) P_e \left[\sum_{i\in\omega} \frac{f\pi s_i^2}{4} N(x+r_i, s_i).m(|r_i|)\right] ds \tag{5.30}$$

The complication in the spatial model is that the establishment probability, P_e, is also dependent on an integral over space, meaning that we must consider its effect, combined with that of the dispersal kernel, in the calculation of the first moment. To simplify analysis, assume that the establishment probability is a decreasing linear, as opposed to non-linear, function of local interaction:

$$P_e(x) = 1 - \mu_B \sum_j \Phi(r_j, 0, s_j) N(x+r_j, s_j). \tag{5.31}$$

The birth rate then becomes

$$\begin{aligned} B_1(x,s) = \int \delta(s-1)\frac{f\pi}{4} \Bigg[& \sum_{i\in\omega} s_i^2 N(x+r_i, s_i) m(|r_i|) \\ & -\mu_B \sum_{j\in\omega}\sum_{i\in\omega} s_i^2 m(|r_i|) \Phi(x+r_j, 0, s_j) N(x+r_i, s_i) N(x+r_j, s_j) \Bigg] ds. \end{aligned} \tag{5.32}$$

The total change in density $N(x,s)$ (at time t) is given by

$$\Delta N(x,s) = \Delta t \left[G_1\left(x, (s-\delta s) \to s\right) - G_1\left(x, s \to (s+\delta s)\right) - D_1(x,s) + B_1(x,s)\right] \tag{5.33}$$

Dividing through by Δt, taking expected values in small regions of space (substituting $N(x,s)$ with $N(x,s)/dxds$), and taking the limit as $dx \to 0$, $ds \to 0$ and $n \to \infty$, leads to an equation for the dynamics of the average density across space (calculated by

Law et al. (unpublished manuscript) for the growth only case):

$$\begin{aligned}\frac{\partial n_1(s)}{\partial t} =& -\frac{\partial}{\partial s}\left[g(s)n_1(s) - \gamma\int\int \Phi(r', s, s')n_2(r', s, s')dr'ds'\right] \\ & - \mu_1 n_1(s) - \mu_2\int\int \Phi(r', s, s')n_2(r', s, s')dr'ds' \\ & + \int \delta(s-1)\frac{f\pi}{4}\left[\int s'^2 n_1(s')ds' \right. \\ & \qquad \left. -\mu_B\int\int\int\int s'^2 m(|r'|)\Phi(r''-r', 0, s'')n_2(r'', s', s'')ds'dr'ds''dr''\right] ds.\end{aligned} \tag{5.34}$$

Spatial structure plays a role here in determining growth and mortality terms. It also alters the boundary condition (source/birth term) of the equation: the final term of Equation 5.34 combining the effects of dispersal and interaction kernels, in respect of the relative location of parents and competitors to their offspring (see also Bolker et al., 2000).

Comparison with mean-field equation

It is possible to decompose the integrals in Equation 5.34 to give "mean-field" and "spatial" terms. We have that

$$\mathbb{E}\left[N(x, s)N(x+r, s')\right] = \mathbb{E}\left[N(x, s)\right]\mathbb{E}\left[N(x+r, s')\right] + Cov(r, s, s'). \tag{5.35}$$

The second term on the right hand size is the *covariance* between $N(x, s)$ and $N(x+r, s')$: it is greater than zero when they are correlated (that is, if the number of pairs of individuals with given separation and sizes is higher than the global average), and less than zero when the converse is true. Rescaling to densities ($\div(dxds)$: $N \to n$ and

$\mathrm{Cov} \to c$) and substituting into Equation 5.34 allows the following decomposition:

$$\begin{aligned}
\frac{\partial n_1(s)}{\partial t} = &- \frac{\partial}{\partial s}\Big[\, g(s)n_1(s) \\
&* \quad -\gamma\left(\int F_1(s,s')n_1(s)n_1(s')ds\right. \\
&\dagger \quad \left. +\int\int \Phi(r',s,s')c(r',s,s')dr'ds'\right)\Big] \\
&- \mu_1 n_1(s) \\
&* \quad -\mu_2\left(\int F_1(s,s')n_1(s)n_1(s')ds\right. \\
&\dagger \quad \left. +\int\int \Phi(r',s,s')c(r',s,s')dr'ds'\right) \\
&+ \int \delta(s-1)\frac{f\pi}{4}\left[\int s'^2 n_1(s')ds'\right. \\
&\quad -\left(\int\int s'^2 F_1(0,s'')n_1(s')n_1(s'')ds'ds''\right. \\
&\dagger \quad \left.\left. +\int\int\int\int s'^2 m(|r'|)\Phi(r''-r',0,s'')c(r'',s',s'')ds'dr'ds''dr''\right)\right] ds.
\end{aligned} \tag{5.36}$$

It is clear that (in comparison with the mean-field model) when the spatial terms (marked with a †) are greater than zero, overall mortality will be greater, and the growth rate at all sizes will be lower. The birth rate will also be lower (the penultimate line in Equation 5.36 giving the reduction in birth rate pertaining to the mean-field establishment probability). The knock on effect in this case is that the global average density is lower than that of the mean-field model. When these integrals are less than zero, global density is heightened. But under what scenarios does each effect occur?

In populations where the pattern is strongly clustered, the spatial integrals will be greater than zero, while those that exhibit reduced pair density at short ranges are likely to have a higher density than they would in an equivalent mean-field model. Computing the interaction integrals in Equation 5.36 directly from simulated IBM populations (at equilibrium) yields a "mean-field integral" (second line) $= 6.58$ and a "spatial" integral (third line) $= -0.11$. The spatial integral is indeed negative, allowing density to increase, but only a tiny fraction (the magnitude of its value is $\approx 1.8\%$ that of the total mean-field interaction). This explains the minimal difference in steady state density observed in the IBM (Figure 2.8).

More generally, the differences between mean-field and spatial model predictions presented in Figure 2.9 can now be explained directly. It was found that increasing μ_2, γ, or decreasing (α, β) in tandem increase the gap in density and basal area between

the mean-field and spatial models (with the latter's being greater). The reason for this is clear from Equation 5.36: increasing the interaction multipliers increases the effect of the difference between the two integrals. Decreasing the growth rate also increases the relative importance of the interaction kernel in determination of the density. It was also found in Section 2.6.3 that when f is very low, or μ_1 very high (around an order of magnitude), the density of the mean-field model becomes much greater than that of the spatial model: this is the situation when the basic mortality term ($\mu_1 n_1(s)$) dominates the behaviour.

Second moment

The events determining the behaviour of the second moment are identical to those of the first moment (Figure 5.2), except that they may occur at either "end" of a pair. For example, death of either individual reduces the number of pairs with given sizes and separation by one. Either individual may grow, and a new pair may be created by a birth at either end of the pair.

Events that increase the number of pairs of individuals with sizes s and s' and separation r ($N(x,s)N(x+r,s')$), with their contributions, are "growths in", and births. First, growth:

$$\text{Growth at } (x,s): \left[g(s-\delta s) - \gamma \sum_{i\in\omega} \Phi(r_i, s-\delta s, s_i) N(x+r_i, s_i) \right] \times N(x, s-\delta s) N(x+r, s') \frac{1}{\delta s} \tag{5.37}$$

$$\text{Growth at } (x+r,s'): \left[g(s'-\delta s) - \gamma \sum_{i\in\omega} \Phi(r_i - r, s'-\delta s, s_i) N(x+r_i, s_i) \right] \times N(x, s) N(x+r, s'-\delta s) \frac{1}{\delta s}. \tag{5.38}$$

Second, birth (using the simpler establishment probability, Equation 5.31):

$$\text{Birth at } (x,s): \left[\int \delta(s-1)\left(\sum_{i\in\omega}\frac{f\pi s_i^2}{4}N(x+r_i,s_i)m(|r_i|)\right)\right.$$
$$\left.\times\left(1-\mu_B\sum_j \Phi(r_j,0,s_j)N(x+r_j,s_j)\right)ds\right]N(x+r,s') \quad (5.39)$$

$$\text{Birth at } (x+r,s'): \left[\int \delta(s'-1)\left(\sum_{i\in\omega}\frac{f\pi s_i^2}{4}N(x+r+r_i,s_i)m(|r_i|)\right)\right.$$
$$\left.\times\left(1-\mu_B\sum_j \Phi(r_j,0,s_j)N(x+r+r_j,s_j)\right)ds'\right]N(x,s). \quad (5.40)$$

Events that decrease the number of pairs are "growths out", and deaths/mortality. First, growth:

$$\text{Growth at } (x,s): -\left[g(s)-\gamma\sum_{i\in\omega}\Phi(r_i,s,s_i)N(x+r_i,s_i)\right]$$
$$\times N(x,s)N(x+r,s')\frac{1}{\delta s} \quad (5.41)$$

$$\text{Growth at } (x+r,s'): -\left[g(s')-\gamma\sum_{i\in\omega}\Phi(r_i-r,s',s_i)N(x+r_i,s_i)\right]$$
$$\times N(x,s)N(x+r,s')\frac{1}{\delta s}. \quad (5.42)$$

Second, death:

$$\text{Death at } (x,s): -\left[\mu_1+\mu_2\sum_{i\in\omega}\Phi(r_i,s,s_i)N(x+r_i,s_i)\right]N(x,s)N(x+r,s') \quad (5.43)$$

$$\text{Death at}(x+r,s'): -\left[\mu_1+\mu_2\sum_{i\in\omega}\Phi(r_i,s',s_i)N(x+r+r_i,s_i)\right]N(x,s)N(x+r,s'). \quad (5.44)$$

Here, $\Delta(N(x,s)N(x+r,s')) = (5.37+...+5.44)\times\Delta t$. Dividing through by Δt, taking expectations in small regions of space and taking the limits $dx \to 0$, $ds \to 0$ and $n \to \infty$ leads to the following differential equation for the behaviour of the second

moment of the model, $n_2(r, s, s')$.

$$
\begin{aligned}
\frac{\partial n_2()}{\partial t} = & -\frac{\partial}{\partial s}\Big[\, g(s) n_2(r, s, s') \\
& \quad -\gamma \int\int \Phi(r'', s, s'') n_3(r, r'', s, s', s'') dr'' ds'' \\
& \quad -\gamma \Phi(r, s, s') n_2(r, s, s') \,\Big] \\
& -\frac{\partial}{\partial s}\Big[\, g(s') n_2(r, s', s) \\
& \quad -\gamma \int\int \Phi(r'' - r, s', s'') n_3(r, r'', s, s', s'') dr'' ds'' \\
& \quad -\gamma \Phi(r, s', s) n_2(r, s', s) \,\Big] \\
& -\mu_1 n_2(r, s, s') \\
& \quad -\mu_2 \int\int \Phi(r'', s, s'') n_3(r, r'', s, s', s'') dr'' ds'' \\
& \quad -\mu_2 \Phi(r, s, s') n_2(r, s, s') \\
& -\mu_1 n_2(r, s, s') \\
& \quad -\mu_2 \int\int \Phi(r'' - r, s', s'') n_3(r, r'', s, s', s'') dr'' ds'' \\
& \quad -\mu_2 \Phi(r, s', s) n_2(r, s', s) \\
& +\int \delta(s' - 1) ds' \frac{f\pi}{4} \Big[\int\int s''^2 m(r'') n_2(r'' + r, s, s'') dr'' ds'' \\
& \quad -\int\int\int\int s''^2 m(r'') \Phi(r''', 0, s''') n_3(r + r'', r + r''', s, s'', s''') dr'' ds'' dr''' ds''' \\
& \quad +\int s^2 n_1(s) ds - \int\int m(r) \Phi(r'', 0, s'') n_2(r + r', s, s'') dr'' ds'' \Big] \\
& +\int \delta(s - 1) ds \frac{f\pi}{4} \Big[\int\int s''^2 m(r'') n_2(r'' - r, s', s'') dr'' ds'' \\
& \quad -\int\int\int\int s''^2 m(r'') \Phi(r''', 0, s''') n_3(r'' - r, r''' - r, s', s'', s''') dr'' ds'' dr''' ds''' \\
& \quad +\int s'^2 n_1(s') ds' - \int\int m(r) \Phi(r'', 0, s'') n_2(r' - r, s', s'') dr'' ds'' \Big] \qquad (5.45)
\end{aligned}
$$

While daunting in appearance, remember that Equation 5.45 describes the combined effect of just three processes: growth, mortality and birth. As the terms are additive, each process can (if desired) be considered and modelled in isolation. There are two terms for each of these three processes, as each can occur at "either end" of a pair. Thus, the terms are arranged into six groups, of three lines each. The first line is the basic term, independent of interaction. The second line for each event describes the effect of neighbourhood interaction on that event. The third line is an adjustment,

including (in the case of growth and mortality) the additional impact of interactions within the pair itself, and (in the case of birth) the effect of reproduction "within a pair" (that is, the case that one of the members of the pair is an offspring of the other).

The source of spatial structure

Variation in the value of $n_2(r, s, s')$ with r indicates the existence of spatial structure. Each of the processes includes a spatial element. Spatial structure in individual location (PCF) arises directly through the birth and mortality terms (which create or destroy individuals in the population). Spatial structure in relative size arises through the growth terms only. However, no process operates in isolation and so changes in (for example) growth do cause indirect changes in the pattern on individual locations.

Whether the population displays a clustered pattern depends upon the relative impact of dispersal, establishment limitation, and interaction induced mortality. Mortality always increases segregation. If the second line of each of birth terms (the spatial convolution of the dispersal and interaction kernels) is less than zero at a given separation, the density of pairs at that separation will tend to decrease further, giving a more segregated pattern. In the opposite case, birth leads to clustering, but competes with mortality in the determination of spatial pattern.

The equations describing the dynamics of $n_1(s)$ and $n_2(r, s, s')$ cannot be solved analytically. The construction of a finite difference scheme for the coupled Equations 5.34 and 5.45 is more intricate than the mean-field case, but identical principles apply. However, at the time of writing, the integration scheme has not been implemented satisfactorily. This is the topic of ongoing work, but no results will be presented here.

Moment closure

As in Section 5.3.1, the dynamical system theoretically involves an infinite hierarchy of moments. If we wish to curtail calculations of higher-order moments, we must choose some method of closure for the system. The most obvious method is to use closures analogous to the power-1, 2, and 3 closures for the non-size model (Equations 5.19-

5.21) as approximations for $n_3(r, r', s, s', s'')$. That is:

$$n_3() = \frac{1}{b}\left(a n_1(s) n_2(r' - r, s', s'') + b n_1(s') n_2(r', s, s'')\right. \quad \text{"Power-1"}$$
$$\left. + c n_1(s'') n_2(r, s, s') - (a + c) n_1(s) n_1(s') n_1(s'')\right) \quad (5.46)$$

$$n_3() = \frac{1}{a + c}\left(a \frac{n_2(r, s, s')(r) n_2(r', s, s'')}{n_1(s)} + b \frac{n_2(r, s, s') n_2(r' - r, s', s'')}{n_1(s')}\right. \quad \text{"Power-2"}$$
$$\left. + c \frac{n_2(r', s, s'') n_2(r' - r, s', s'')}{n_1(s'')} - b n_1(s) n_1(s') n_1(s'')\right) \quad (5.47)$$

$$n_3() = \frac{n_2(r, s, s') n_2(r', s, s'') n_2(r' - r, s', s'')}{n_1(s) n_1(s') n_1(s'')} \quad \text{"Power-3"}$$
$$(5.48)$$

As these criteria are direct analogues of those discussed by Murrell et al. (2004), they could be expected satisfy most of the criteria (D1-D6) discussed there, albeit with n (overall density) replaced by $n(s)$, $n(r)$ replaced by $n(r, s, s')$ and so on. However, several relabelling criteria are given (partitioning the population – randomly or non-randomly – into subpopulations) that depend critically on the assumption that kernels and parameters of the subpopulations are identical. In our size structured populations this is not the case: the level of interaction between two individuals also depends upon their sizes.

The value of two approximations to the third moment from simulated point patterns at early stages of development (100 years) and the steady state (800 years) are shown in Figure 5.3. The "power-3" closure always underestimated the true value observed in these point patterns, while Law and Dieckmann (2000)'s closure ($n_3() = n_2(r, s, s') n_2(r', s, s'')/n_1(s)$) provides a much more accurate approximation in both transient and steady state point patterns. In general, closures which include terms involving the "third pair of the triplet" (the third n_2 in the power-3 closure, omitted in Law and Dieckmann (2000)'s closure) did not perform well here, while a "mean-field" closure ($n_3() = n_1(s) n_1(s') n_1(s'')$) always overestimated the true value (not shown). The apparent structure in the power-3 approximation (Figure 5.3a,c) is difficult to interpret, and does not depend in a clear manner on any of the variables included (size or space). It is however pleasing to see how accurate the simplest spatial closure (i.e. Law and Dieckmann, 2000) is when extended to include size structure.

The lack of complete numerical results means that it is not possible to assess the impact of these findings on the behaviour of the first and second moments, as investigated for the "spatial-only" case by Murrell et al. (2004).

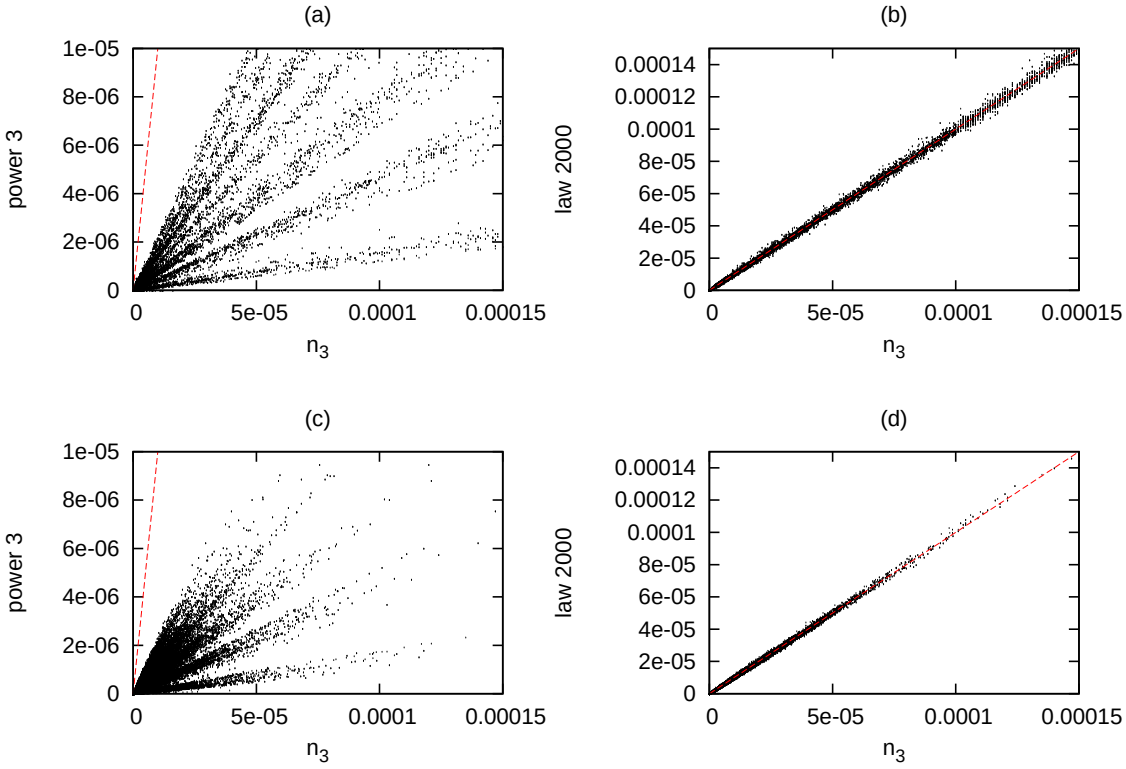

Figure 5.3: *Approximation of* n_3 *using lower order moments* n_1 *and* n_2. Moments were computed from IBM point patterns at 100 years (top row) and 800 years (bottom row), with 10 bins for each size and space index. True values are shown on the x-axis, and approximations on the y-axis. (a) Power-3 closure (Equation 5.48), 100 years. (b) Closure implemented by Law and Dieckmann (2000), extended to account for size, 100 years. (c) As (a), at 800 years. (d) As (b), at 800 years. In each case the dashed red line shows the best outcome, $n_3 =$ approximation.

5.4 Summary

This Chapter has presented differential equation "moment" models that aim to approximate the behaviour of stochastic individual based simulations. The mean-field moment model (Equation 5.12) is both rapid to simulate and, given appropriate choice of time/size increments, obtains accurate transient and long run behaviour, in comparison with IBM results. The "full" size-space moment model proved much more difficult to implement correctly; although no results are presented here, this work is ongoing.

Within the region of stability, steady-state behaviour is insensitive to the choice of size and time step. However, accurate transient behaviour is contingent on the use of small increments in time and size. This is manageable in the mean-field model, in which the integrals are two-dimensional (and are computed for each element in a one-dimensional array $n_1(s)$), but simulation of $n_2(r, s, s')$ in the spatial model requires a two-dimensional integral to be computed for each point in a three-dimensional array. At the level of resolution required for accurate transient behaviour computation would be incredibly slow (slower than the IBM). Furthermore, the amount of memory required for the third moment would be prohibitive at high resolutions.

Nonetheless, the equations presented in this chapter summarise the bulk effects of individual birth, growth and mortality, and as a consequence do help in identifying the drivers of population dynamics. It is hoped that the derivations presented here will provide stimulus for further investigations, especially a more comprehensive investigation into the simulation of a moment model for a population structured in both size and space, and any simplifications that may make it implementation viable.

Chapter 6

Application of models to uneven-aged silviculture: transformation and continuous-cover forestry

6.1 Introduction

In Chapter 2, a simulation model was introduced. Parameterisation for, and applicability to, Scots pine populations was then considered in Chapters 3 and 4. This chapter considers the application of the simulation model to forest management. In line with the overall goals outlined in Chapter 1, these will have primarily ecological motivations, though as will be seen, this need not be considered entirely separately to timber production. The main topics of this chapter are:

- *Transformation* – assisting and accelerating the transition from plantation to old-growth structure.
- *Continuous-cover forestry* – managing a forest stand for both timber output and ecological value.

Both of these objectives entail *uneven-aged* management: the stewardship of stands consisting of trees of diverse age and size, often in irregular spatial patterns. The mechanistic changes incurred by more complex stand structures are not easily understood using traditional approaches, which were developed with *even-aged* stands in mind (O'Hara, 2001). Renshaw et al. (2009) and Comas (2005) studied some thinning and planting strategies using individual-based spatial simulation models. To

date, however, silviculture for transformation or continuous-cover management has not been studied comprehensively using such an approach, though various authors have suggested that it might be a promising route to new insights (McIntosh, 2006; Mason et al., 2007). Hopefully, the results can provide predictive information to guide conservation-oriented management programmes, such as those of Edwards and Mason (2004).

The model detailed in Chapter 2 (with the alteration suggested at the conclusion of Chapter 4) is used here for the purposes of stand simulation. This allows the study of changes in stand structure through time, both visually and by means of summary statistics (density, basal area, size density distribution, age distribution, pair and mark correlation functions).

6.1.1 Transformation

Over a period of several millennia, the extent of natural forests in the British Isles has steadily diminished (Rackham, 2001); this is particularly true of the Caledonian pinewoods, which are estimated by some to cover approximately 1% of their former extent (Colin Edwards, personal communication). While this decline may in part be due to climatic changes, man has also played a large role, grazing animals, growing food, timber and so on (Bennett, 1995). The area covered by man-made forests (plantations) has seen a dramatic increase over several centuries, but a current reduced demand for timber means that there is now some redundancy (McIntosh, 2006).

While these man-made stands do not account entirely (in terms of area) for the natural habitat lost, an appealing approach to conservation of species dependent upon the naturally occurring habitat type is to attempt to convert existing plantations to a state close to that of natural stands, rather than clearing land and waiting for a forest to establish naturally, which may take hundreds of years. This process of conversion is referred to as *transformation*.

Various options are available to forest managers wishing to influence the structure of a stand. Of these, the most direct are *thinning* (the removal of trees) and *planting*, which alter the number and distribution of individuals in the stand. Other methods include the *pruning* of existing trees to alter light conditions in the understory, and the application of *ground treatment* in order to improve the chances of successful seedling establishment (Edwards and Rhodes, 2006). Thinning and planting are investigated using the simulation model in Section 6.2.

6.1.2 Continuous-cover forestry

It may be desired to manage a forest stand for multiple purposes. In order to finance its operations, forestry must produce timber, or obtain revenue by some other method. Rather than simply clear-felling the stand once productivity begins to decline *continuous-cover* forest management aims to achieve a continuous yield of timber, but also to enable the forest to naturally regenerate what is removed in harvesting. As such, a more considered analysis of population dynamics (and the impact of management upon them) is required. The complicated size- and spatially-structured nature of uneven-aged forest populations makes this type of management a prime candidate for investigation using an individual-based approach, as considered in Section 6.3.

6.2 Transformation: accelerating old growth

6.2.1 Background

Stands possessing appealing characteristics are not necessarily naturally formed (see e.g. Edwards and Mason, 2004). Is the desired output of transformation activities the same as the old-growth state described here? The "sustainable irregular condition" (Schutz, 2001) has certain expected qualities (Malcolm et al., 2001; Mason et al., 2007):

- Full representation across the size classes: high variance of size in the canopy, and many trees in smaller size classes
- Non-regular spatial distribution
- High recruitment (large numbers of successful seedlings)

Each of these features is found in the long term state discussed in Section 2.4.3 (with the additional inclusion of a dispersal kernel), but precisely the opposite of each is seen in (both simulated and real) plantation stands.

What are the main factors in achieving such a state? Natural regeneration is key, and might be encouraged by thinning the existing canopy. Thinnings are often *size-structured*, made on the basis of canopy status of individuals (that is, their size relative to neighbours and other members of the stand). Less commonly, thinnings may be *spatially structured*, or focus on assisting selected individuals (Edwards and Mason, 2004). More specific examples of such regimes are:

- Removal of dominants e.g. 60-100% size classes
- "Shelterwood" thinning e.g. removal of 20-80% size classes

- Clearance of patches
- Removal of major competitors to selected trees

Active planting of seedlings is also a potentially useful tool in attaining particular structures quickly (McIntosh, 2006), but is more commonly used to establish new woodlands. Its utility in the transformation process requires thinning to take place, to enable successful establishment and of, and sufficient growing space for, the planted trees. Planting is likely to be made in patches cleared specifically for the purpose, or under a low density canopy (creating a "shelterwood" stand, see Nyland, 2002, pg. 327).

Attention is focused on treatments applied to a plantation that are intended to bypass or escape the period of unnaturally high basal area, remove the lattice spatial pattern, and create suitable conditions for the generation of a high-variance size structure; in summary, accelerating attainment of the steady state. The initial condition for presented results is that of one of the plantation stands ("plot 1") at Glenmore, as considered by Edwards and Mason (2004). We assume that the model's steady state is a reasonable reflection of "old growth", and to assess performance of the treatments, we compare the dynamics of managed stands with those of unmanaged stands, using the unmanaged steady state as a target.

6.2.2 Assessing stand development

The state of simulated (and real) populations is well characterised by

- individual density (ρ)
- total basal area (BA)
- size density distribution ($n(s)$)
- pair and mark correlation functions ($PCF(r)$,$MCF(r)$)

In order to assess the similarity between two different forest stands, we define a measure of "similarity between stands" of the form

$$\begin{aligned} D_{12}(t) =& d_1\Delta_{12}\rho(t) + d_2\Delta_{12}BA(t) + d_3\Delta_{12}\int n(s,t)ds \\ &+ d_4\Delta_{12}\int PCF(r,t)dr + d_5\Delta_{12}\int MCF_{12}(r,t)dr \end{aligned} \tag{6.1}$$

where $\Delta_{12}(S(t)) = |S_1(t) - S_2|$ is the absolute value of the difference between in values of a statistic S computed for each stand. Similarity measure comparisons in this

chapter are made with reference to an "equilibrium" stand 2, in this case the "old growth" state, which is assumed to be equivalent to be the model's equilibrium state. As a default, we might wish to give each statistic equal importance; for example, the d_i can be set such that they normalise the differences $\Delta_{12}(S)$, where stand 1 is an unmanaged model stand after 100 years:

$$\begin{aligned} 1 = d_1\Delta_{12}(\rho) = d_2\Delta_{12}(BA) = d_3\Delta_{12}\left(\int n(s)ds\right) \\ = d_4\Delta_{12}\left(\int PCF(r)dr\right) = d_5\Delta_{12}\left(\int MCF(r)dr\right) \end{aligned} \tag{6.2}$$

These differences, and corresponding values for d_i (with the Glenmore initial condition), are given in Table 6.1. The measure could be extended to take into account, for example, total stand growth increment over a period, to assess the trade-off between structure and output for continuous cover forestry purposes. With parameters defined as in Table 6.1, the similarity measure of an unmanaged model stand would take a value very close to 5 after 100 years, and 0 in the steady state.

The value of Equation 6.1 (and each of its terms) – hereafter referred to as the *similarity measure* – can be tracked through time, identifying the rapidity of approach to the steady state. With parameters defined as in Table 6.1, an unmanaged model stand has $\mathbb{E}(D_{12}(100)) = 5$, and $\mathbb{E}(D_{12}(800)) = 0$ (by 800 years, a steady state has been reached). Throughout this chapter, analyses are made using the unnormalised size distribution (a simple count of individuals in each size class), as this allows a more straightforward visual comparison of different stands than the size density distribution.

Table 6.1: Differences between values of statistics used in the similarity measure (Equation 6.1) at model equilibrium (800 years) and those at 100 years in an unmanaged stand, with corresponding values for d_i, calculated as in Equation 6.2.

S	$\Delta(S)$	d_i
ρ	0.009756	102.5
BA	5.108	0.1958
$\int PCF(r)$	1.533	0.6524
$\int MCF(r)$	0.8096	1.235
$\int n(s)$	569.1	0.001757

6.2.3 Thinning

Thinning alone is considered first, and several generic types are applied to simulated stands. Variation between thinning regimes is in one of four aspects:

- number of interventions
- inter-intervention time
- thinning criteria (e.g. size range, spatial constraint)
- target basal area/intensity

Below, each thinning is compared to the model steady state (solid black line throughout this chapter), and also to the dynamics of an unmanaged model population (dotted black line throughout). A comparison/overview of the management procedures using the similarity measure is made in Section 6.2.5.

Clearcut and regrowth

To introduce the application of management using the simulation model, let us consider first the most basic possible thinning treatment, a clearcut. Removing *every* tree in a simulated population will make the population extinct, as immigration/birth depends on the presence of other trees. The removal of 95% of all trees, under two reproductive scenarios, is shown in Figure 6.1: (i) reproduction proportional to the basal area of remaining trees, as stated above (ii) maintaining birth at the rate imparted by the model's steady state (in reality, this could be due to immigration from neighbouring stands).

In case (i), where reproduction is determined solely by the trees currently present in the stand, the population is very slow to re-equilibrate. After 100 years, the basal area of the stand is around 1/4 of the equilibrium. In case (ii), the population is much quicker to recover, nearing the equilibrium basal area after around 150 years. In both cases, however, the state is of a greatly diminished forest in the period following management, in comparison with other thinning strategies (and see Section 6.2.5).

Number of interventions

Simulations were carried out with 1, 2, 5 and 10 identical criteria thinnings (criteria: remove trees from the largest 40%, reducing density by a maximum of 20% at each thinning, to a minimum basal area of $20 \mathrm{m}^2 \mathrm{ha}^{-1}$) performed with a fixed period of 5 years (Figure 6.2).

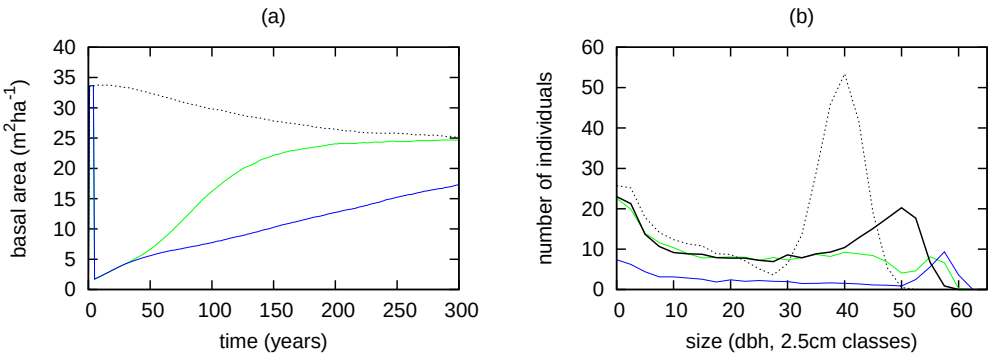

Figure 6.1: *The effect of a clear cut*. The stand is slow to re-establish following a clearcut, taking many centuries to reach equilibrium. The assumption made regarding birth (immigration) into the population has a large effect on the rate of equilibration. Two scenarios are shown: assuming reproductive rate fixed at the equilibrium level (green), and with the rate proportional to the basal area (blue). The dotted black line shows the behaviour of an unmanaged stand.

Increasing the number of interventions leads to a more permanent reduction in basal area, faster reduction in density, and a size distribution closer to the steady state. This effect is robust to thinning criteria or period.

Inter-intervention time

Simulations were carried out with 5 identical criteria thinnings (criteria as above), with a period (inter-intervention time) of 1, 2, 5 and 10 years.

Increasing the period has a similar effect to increasing the number of interventions (see Figure D.1, Appendix D.1) – both have the effect of lengthening the overall period of management, meaning that by the end of the management regime, the mean size of the remaining trees is larger, and they are approaching a period of slower growth. Provided that thinning is sufficiently frequent to cause a net reduction in basal area, these results are robust.

Thinning size criteria

A selective thinning requires criteria in order to determine the trees to be removed. A traditional approach, used in even-aged stand management, is to select trees for removal based on their dbh, with respect to the other trees in the stand. In this way a thinning can, for example, give more growing room to the most successful (largest) trees, or reduce pressure on sub-dominant trees, to allow them to achieve their full growing potential – the choice depending on the state of stand development and the desired outcome.

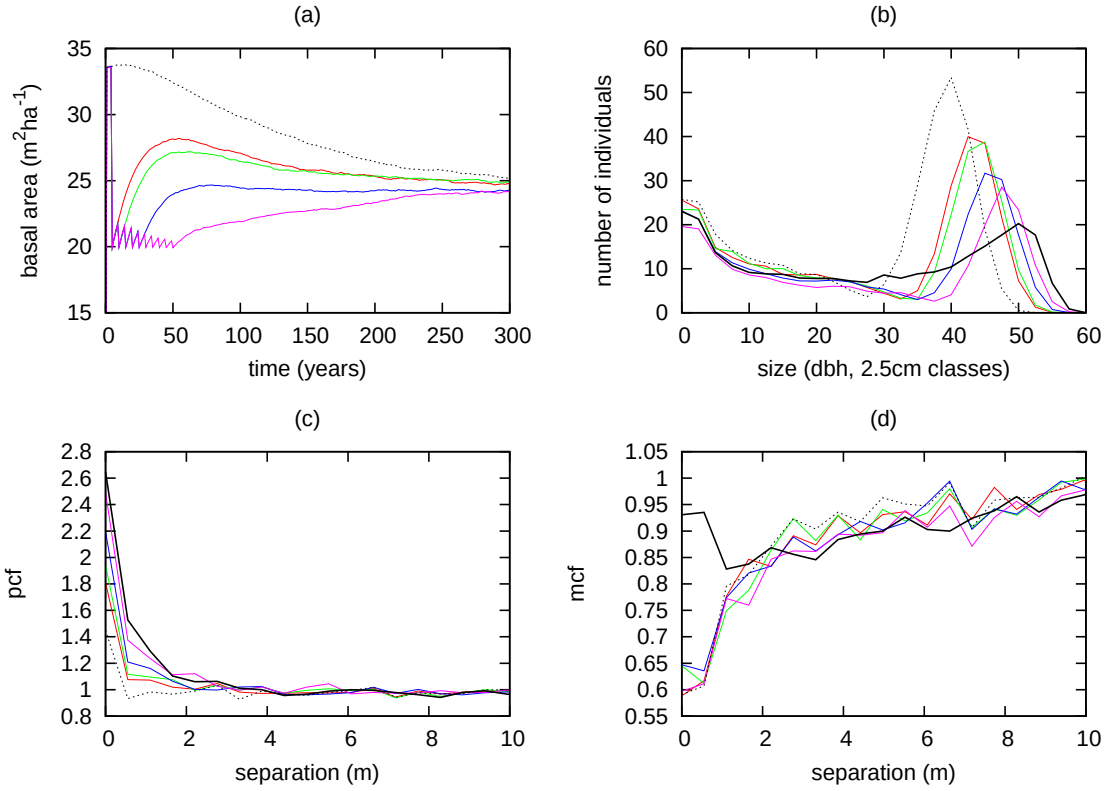

Figure 6.2: *Number of interventions*: 1 (red), 2 (green), 5 (blue) and 10 (magenta). (a) Basal area evolution (b) size distribution at 100 years (c) PCF at 100 years (d) MCF at 100 years. The dotted black line shows the behaviour of an unmanaged stand, the solid black line shows the model steady state.

Thinnings were made selecting trees randomly from different percentile ranges of the size distribution: $0-40\%$, $20-60\%$, $40-80\%$, $60-100\%$, $0-100\%$ (entire size distribution), with identical interval, number of thinnings, and target basal area (Figure 6.3). For a given target basal area, thinning from a lower percentile range of the size distribution implies removing more individuals to reach that target, leading to a reduced individual density following management. The other main effect of altering the size range from which removals are made is upon the subsequent growth of remaining individuals, and the trajectory of basal area. The implemented Gompertz growth function gives the highest growth rate at intermediate sizes, with a maximum at 23.2cm, meaning that removing individuals with smaller sizes imposes the greatest limitation on future basal area increase. Thinning by selecting randomly from the entire size distribution gives intermediate behaviour (Figure 6.3a).

Another consequence of altering the size criteria for thinning is the resulting size distribution. Removing individuals from intermediate size classes results in a low variance "canopy peak" after 100 years, relative to that produced by thinning from the largest individuals. The effect on spatial structure is comparatively negligible.

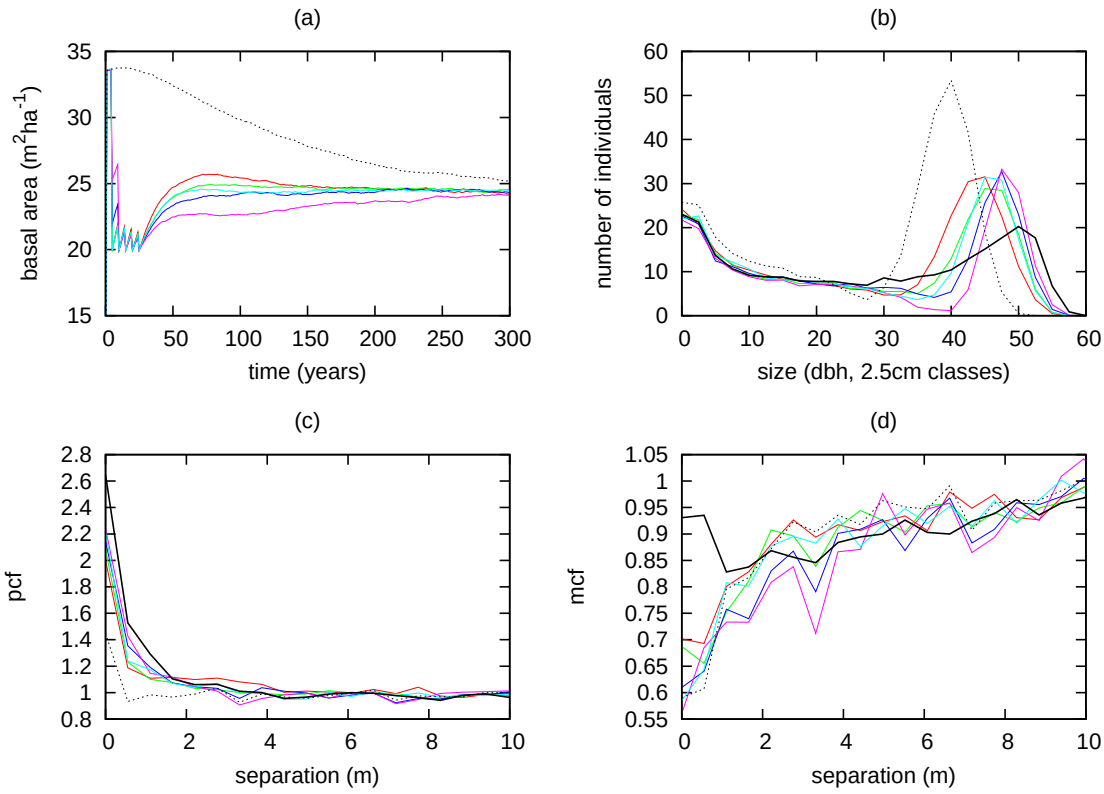

Figure 6.3: *Size criteria*. Removing trees from different portions of the size distribution, to a target basal area of $20 m^2 ha^{-1}$: $0-40\%$ (magenta), $20-60\%$ (blue), $40-80\%$ (green), $60-100\%$ (red), $0-100\%$ (cyan). (a) Basal area evolution (b) size distribution at 100 years (c) PCF at 100 years (d) MCF at 100 years. The dotted black line shows the behaviour of an unmanaged stand, the solid black line shows the model steady state.

Target basal area

As noted in Chapter 4, basal area is thought to affect the possibility for regeneration; when it is high, overall levels of light beneath the canopy are generally low. Treatments aimed at encouraging regeneration thus often reduce it to a target level (Hale, 2001; Edwards and Rhodes, 2006). This target level has an effect on dynamics.

Decreasing the target basal area of thinning does not alter the qualitative comparison of altering thinning size class, or patch size. Intense thinnings (that is, with a low target basal area) do however cause a permanently low density stand. As a result, interaction between individuals is lower and those remaining grow larger than they would have following a less intense thinning. Not only is the maximum size of trees larger, but the variance of the canopy peak is smaller.

In the implemented model configuration, the rate of immigration (a product of birth rate and establishment probability) is dominated by the basal area (and consequently birth rate), meaning that the rate of reproduction is low following an intense thinning.

More intense thinnings also produce a more clustered pattern (heightened short-range PCF) 100 years after management has begun (Figure 6.4), a result replicated whether the thinning is size- or spatially-structured. The MCF displays no effect of such changes. The greater the proportion of the stand area cleared the more rapid is the subsequent regrowth (Figure D.2, Appendix D.1). However, in all cases a similar duration of rapid regrowth occurs. Following this, the released trees no longer grow at an increased rate, and changes in basal area are subject to interaction-limited birth, growth and mortality, as before.

For reasons of structural stability of the remaining trees (Colin Edwards, personal communication, and for example, windthrow risk, Quine and Gardiner, 2007), it is sometimes considered undesirable to reduce the standing basal area or individual density by large steps in a single intervention, even though intense thinnings may be more cost effective. In model simulations, no difference was seen between the behaviour of stands thinned rapidly (and maintained at a low basal area), and stands that were thinned gradually to the same ultimate basal area.

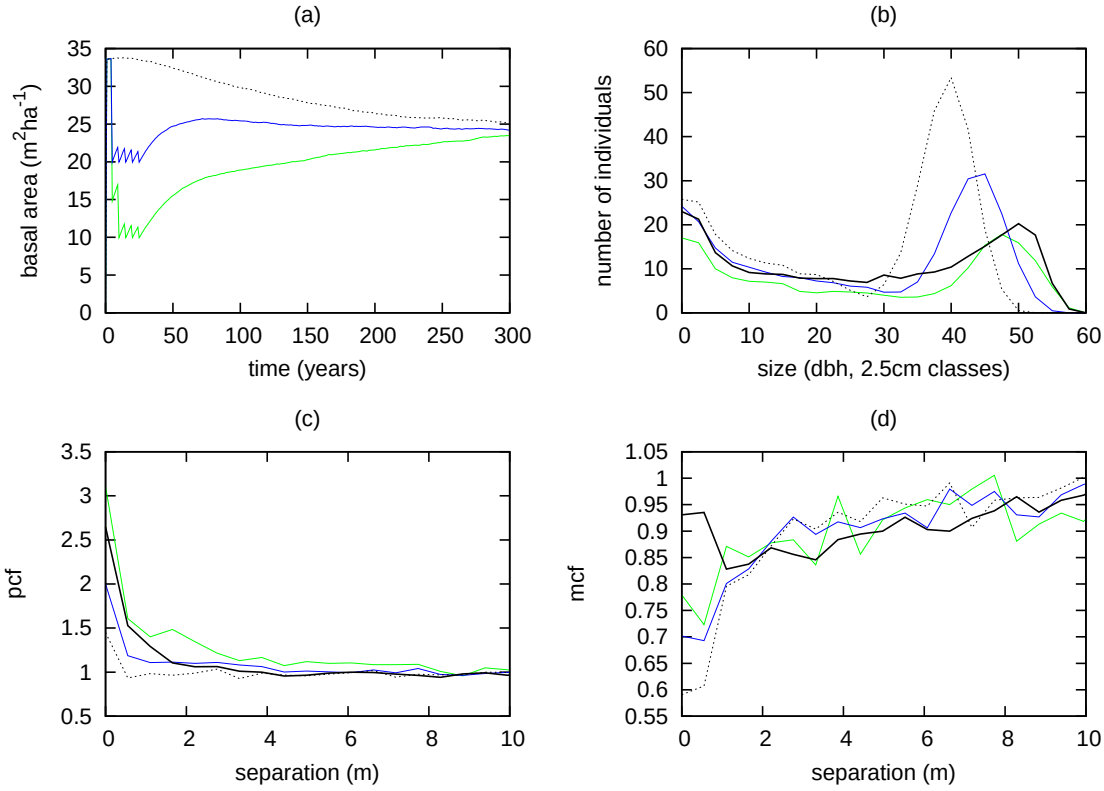

Figure 6.4: *Target basal area* of thinning. $10 m^2 ha^{-1}$ (green), $20 m^2 ha^{-1}$ (blue). (a) Basal area evolution (b) size distribution (c) PCF (d) MCF. The dotted black line shows the behaviour of an unmanaged stand, the solid black line shows the model steady state.

Thinning patch criteria

Thinnings may also be spatially structured. Patch thinnings using square patches to clear 1/8 (or 1/4, or 1/2) of the arena area were carried out, using 2/5/10 patches with area (side) 500 (22.4), 250 (15.8), 125 (11.2)m^2 (m) respectively (or 5/10/20, or 10/20/40).

In general, patch thinnings lead to slower growth of remaining individuals (and slower basal area increase) than do size structured thinnings of the same intensity (resultant basal area) (Figure 6.5). This is because the individuals removed by a size structured thinning are randomly located in the stand, so density reduction is fairly homogeneous. This contrasts with patch thinning, which creates regions of high (unchanged) and low (almost, if not completely, empty) density. Except those on patch edges, the remaining individuals experience roughly the same level of interaction as they did prior to thinning.

A second notable effect of the spatial inhomogeneity of patch thinning, in comparison with non-spatially determined ones, is that the individuals away from patch edges are relatively slow growing, increasing the variance in the canopy peak of the size distribution after 100 years.

The magnitude of both the effects described above is related to the patch size: as patch size increases, the thinning becomes more inhomogeneous, and thus increasimngly different from a spatially random thinning. As it creates segregated areas of high and low density, increasing patch size increases the level of "long-range clustering" (heightened PCF over a long range from zero).

Removing competitors of selected individuals

Standard thinning treatments oriented towards encouraging individual tree growth reflect their heritage in even-aged stand management. These thinnings are typically size-structured and focus on assisting those trees with the potential for maximal unsuppressed growth, and in the process *reduce* the variance in individual size within the stand.

When the goal is instead to *increase* variance in size, the most appropriate thinning is less clear. Edwards and Mason (2004) began a long-term experiment, using six 1ha plantation stands to study the relative benefits of different approaches to thinning on stand structure. One of the treatments considered was to select particular trees within a stand that exhibit an "interesting" form, and to remove their main competitors, two at a time, at an interval of 5 years. While such interesting trees cannot be defined in the model, it is possible to effectively replicate this treatment in simulation, and monitor subsequent dbh growth. Removing a larger number of trees was also considered, but

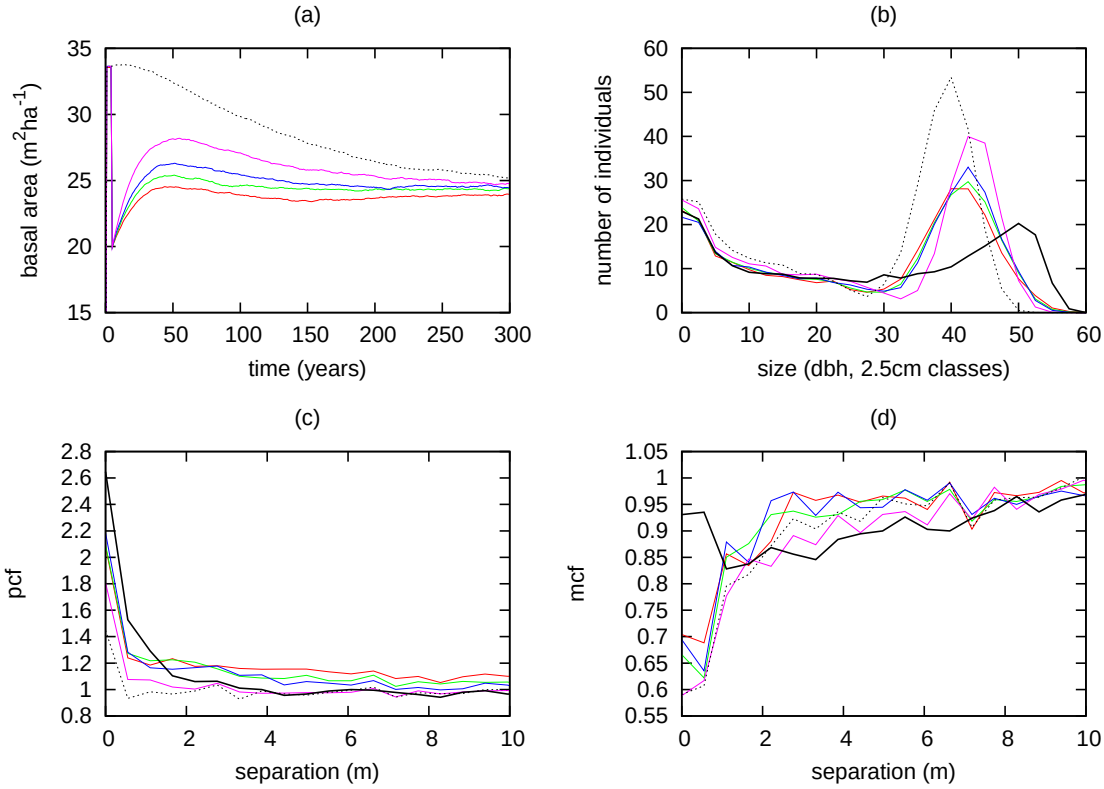

Figure 6.5: *Patch thinning*, removing half the total area. The target basal area is $20\text{m}^2\text{ha}^{-1}$, and patch size is varied: 500m^2 (red), 250m^2 (green), 125m^2 (blue). For comparison, a canopy thinning with the same target basal area is shown (magenta). (a) Basal area evolution (b) size distribution at 100 years (c) PCF at 100 years (d) MCF at 100 years. The dotted black line shows the behaviour of an unmanaged stand, the solid black line shows the model steady state.

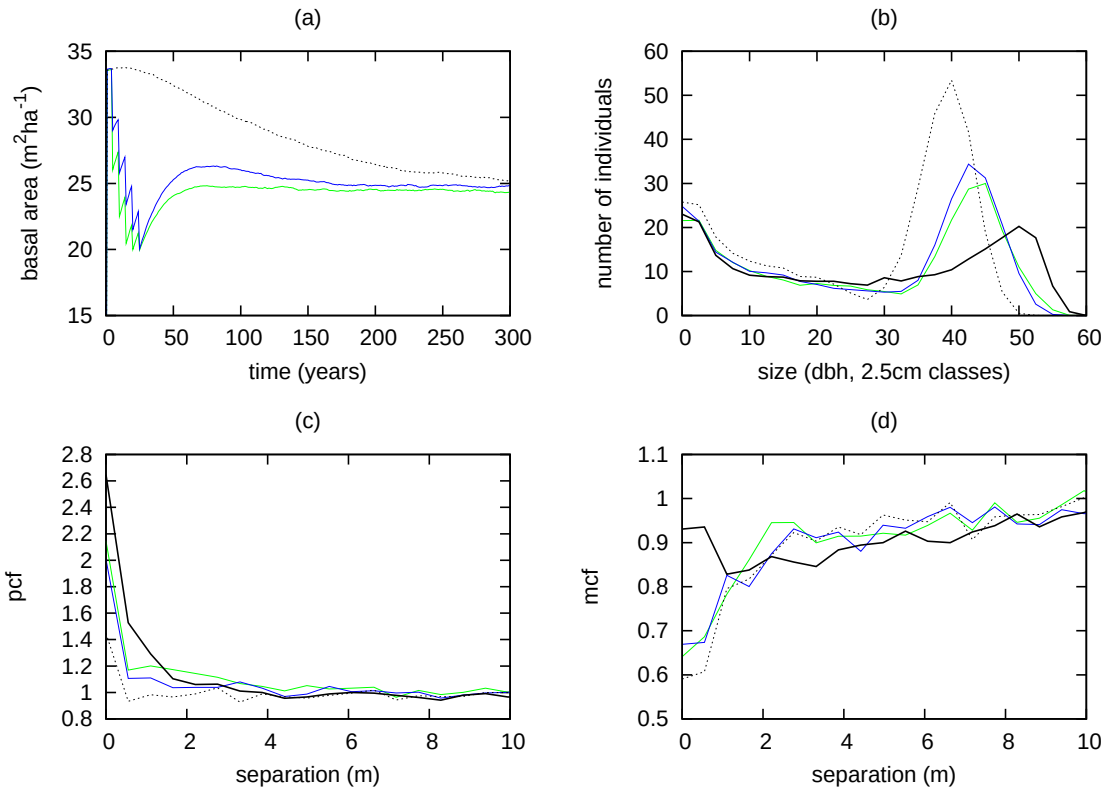

Figure 6.6: *Competitor removal* (green), in comparison with canopy thinning (blue), each repeated 5 times to a target basal area of $20 m^2 ha^{-1}$. Rather than randomly selecting trees for removal from the population, 60 trees are selected, and at each thinning their two main competitors are removed. (a) Basal area evolution (b) size distribution at 100 years (c) PCF at 100 years (d) MCF at 100 years. The dotted black line shows the behaviour of an unmanaged stand, the solid black line shows the model steady state.

is probably more severe than would reasonably be applied.

It might be expected that the effects of such a thinning would be broadly similar to canopy thinning, as they both preferentially remove large individuals (over similarly located small ones). However, the competitor removal always encourages growth of the same individuals, rather than generally reducing the level of interaction experienced. As a result, the subsequent increase in stand basal area is slower. The variance in size of canopy trees, however, is slightly larger, with some individuals attaining larger sizes than they would have under a randomly applied canopy thinning (Figure 6.6).

6.2.4 Planting

A typical feature of plantations is a low level of regeneration – resource limitation due to high basal area and local interaction inhibits recruitment and seedling development (Hale, 2001). Planting is therefore likely to be an important component of effective transformation. Below we consider the effect of varying planting strategy, and the effect of manipulating canopy structure on the subsequent regrowth. Planting new trees beneath an existing canopy is referred to as *underplanting*.

Below we relate results obtained from model stands underplanted with 900 trees, located spatially randomly (a Poisson process with intensity 0.09 individuals per m^2); different planting intensities were considered, but with no qualitative change in behaviour. In common with thinning results, the most significant effects are seen in relation to density/thinning intensity of the stand at the time of planting, as opposed to any specific spatial structure.

Basal area

Altering the basal area of stand has significant implications for the prospects of planted trees. Figure 6.7 compares the behaviour of unthinned underplanted stands, with that of "canopy" thinned underplanted stands. It is clear that in the lower basal area stands, growth of planted trees is higher, and mortality is lower. Increased growth inhibition (reduced MCF) at 100 years is seen as the basal area of the underplanted stand increases, but no effect is seen on the PCF.

Thinning criteria

In stands where thinning has been performed to the same target basal area, the basal area trajectory appears to be unaffected by the choice of thinning criteria applied, as seen in Figure D.3a (Appendix D.1 – canopy: 60–100%/shelterwood: 20–80%/patch).

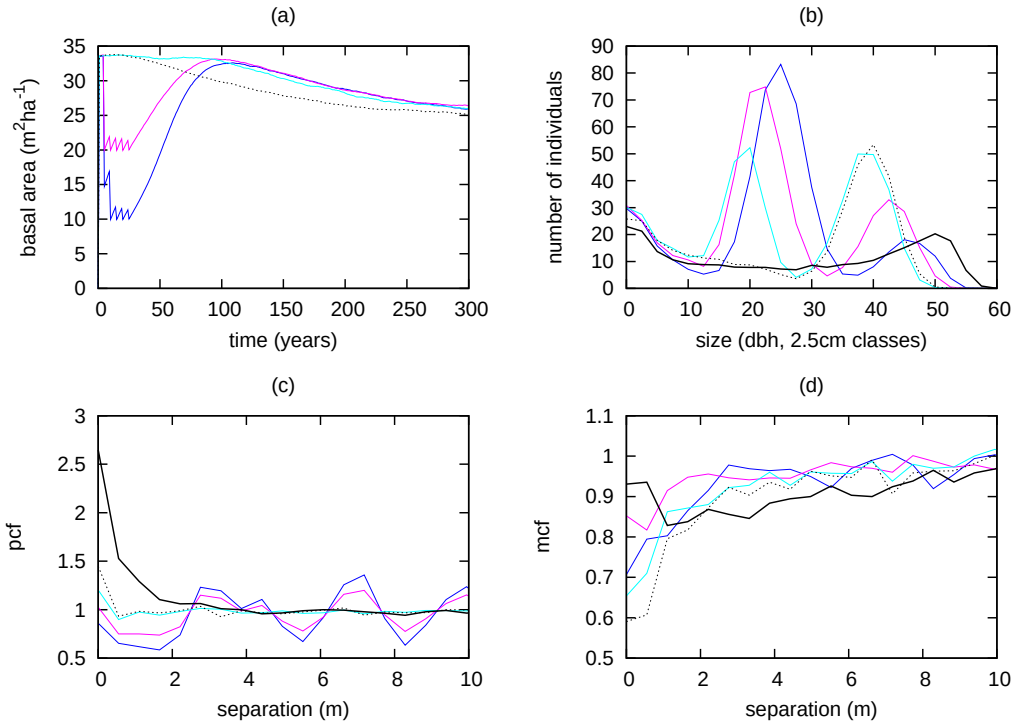

Figure 6.7: *Underplanting – changing prior thinning target basal area*. Canopy thinning to 10/20m^{2}ha^{-1} (blue/magenta) and no thinning (cyan – BA=33.4m^{2}ha^{-1} at time of planting). (a) Basal area evolution (b) size distribution at 100 years (c) PCF at 100 years (d) MCF at 100 years. Average number of surviving planted trees at 100 years: (no thin/10/20m^{2}ha^{-1}) 141/216/283, basal area of surviving planted trees: 4.81/10.2/16.3m^{2}ha^{-1}. The dotted black line shows the behaviour of an unmanaged stand, the solid black line shows the model steady state.

However, it can be seen from the size distribution at 100 years that patch thinning produces a wider spread of planted tree sizes (D.3b), due to the variation in neighbourhood created. Furthermore, patch thinning appears to allow more growth overall, followed by shelterwood and finally canopy thinning, though the difference is not as pronounced as under changes in basal area at the time of planting. Total surviving density of planted trees is not altered significantly by the thinning criteria, and no difference in spatial correlation functions is observed at 100 years.

6.2.5 Quantitative comparison of strategies

Qualitative comparison has brought us a good way towards understanding the benefits of the different thinning and planting strategies. Can the distance measure defined in Section 6.2.2 assist further? Table D.1 (Appendix D.4) presents the computed values for the similarity measure (including each component term) for a cross-section of the management strategies discussed above, 100 years after beginning management. Certain generic patterns are observed:

- the "best" thinnings are size structured, to $20\text{m}^2\text{ha}^{-1}$ target basal area and with a moderate (5 year) interval
- intense patch thinnings are better than less intense ones
- intense size structured thinnings generally perform worse
- the stands including planting perform worse than all those with thinning alone (except clearcutting)

To provide a clearer picture, the total value D is plotted for a selection of management regimes in Figure 6.8. Of these, the most effective thinning type appears to be a shelterwood thinning, with a $20\text{m}^2\text{ha}^{-1}$ target basal area (red dashed line on the figure), which has a consistently low value of D over the transition to equilibrium. This is simply because it alters the density and basal area closer to the steady state than the other strategies (Figure 6.8a,b); it performs no better in other aspects.

The size structured thinnings display wide variation in success as measured by the similarity measure, while the spatially structured thinnings are more consistently successful. It is found, however, that none of the best c50% of management strategies performs particularly better than any other. Planting leads to a very high value of D over a prolonged period, due to the greatly altered individual density and size distribution (not shown in figures).

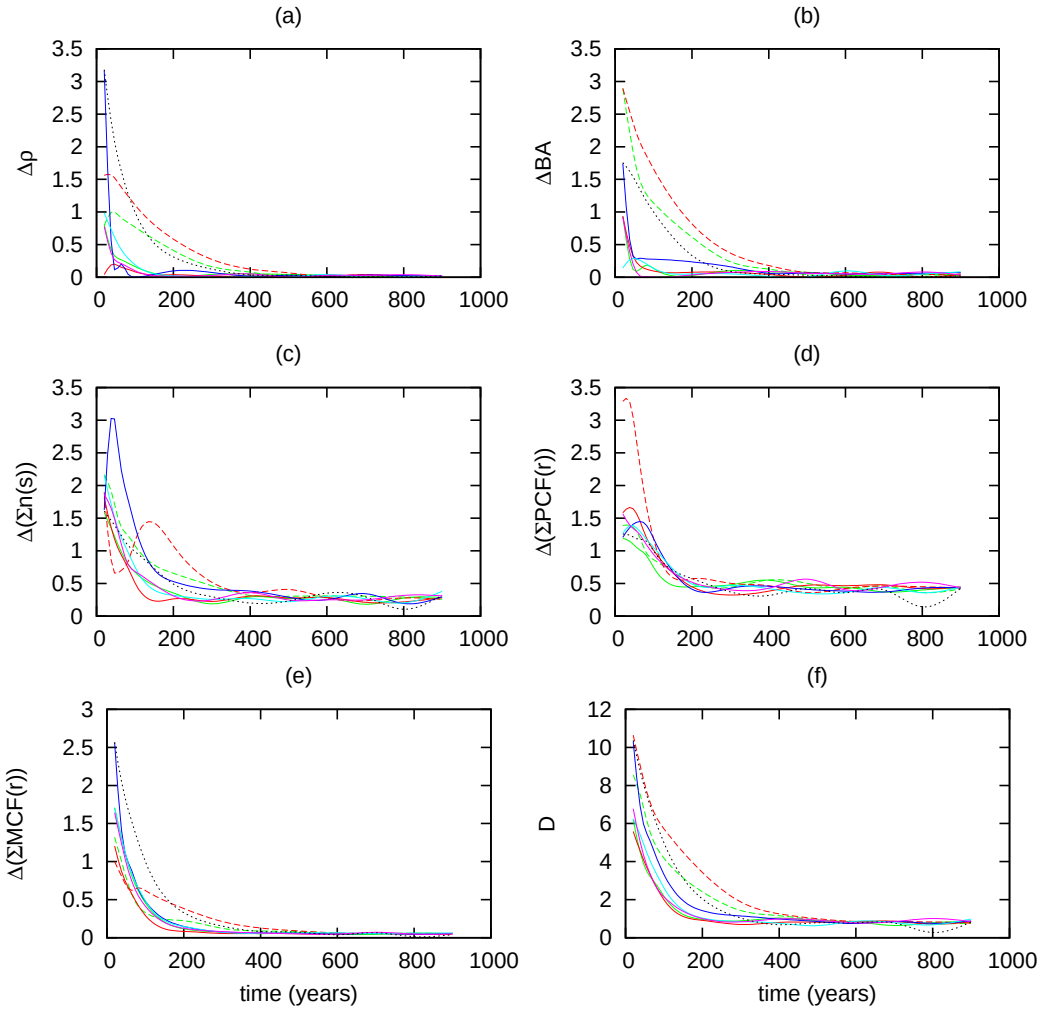

Figure 6.8: *The individual components of the similarity measure for a selection of thinning strategies, plotted through time.* Canopy thin (green), shelterwood (red), Patch thinning (large patches – blue, small patches – cyan), competitor removal (green). Solid lines indicate a target basal area of $20 m^2 ha^{-1}$, dashed lines $10 m^2 ha^{-1}$. (a) $\Delta(\rho)$, (b) $\Delta(BA)$, (c) $\Delta(\sum n(s))$, (d) $\Delta(\sum PCF(r))$, (e) $\Delta(\sum MCF(r))$, (f) D, the total measure. Average values over time for unmanaged stands are shown by the black dotted line.

Since D is a simple summary measure, its ranking may not reflect the quality of the habitat generated in respect of particular goals. It is also important to take into account the particular changes in structure that each management type leads to.

It is useful to know that the less intense size-structured thinnings are likely to perform better than others (particularly than the more complicated to implement competitor thinnings), but it is difficult to derive much information from the poor performance of the various planted stands, which occurs due to a large difference in size distribution – it is clear that this will be very different to that of unplanted stands

(or the steady state). As expected, the performance of clearcutting is very bad relative to other thinning-only regimes. Clearcutting assuming constant immigration gives better results, but it is worth bearing in mind that (i) this is not a fair comparison with other high intensity thinnings, which also result in reduced regeneration, and (ii) it still performs worse than almost all other thinning treatments, particularly the low intensity size structured thinnings.

6.2.6 Summary

The success of transformation is highly dependent upon the methods applied to attain it; some approaches are markedly better (statistically and qualitatively) than others in terms of approach to the steady state. Size-structured thinnings are likely to provide the most rapid transformation, but spatial thinnings give increased heterogeneity in size of canopy trees, light environment, and in practice, may alter the possibilities for regeneration in ways which are not fully captured by the model (see Sections 4.3 and 6.4). Altering the intensity of thinning has the most dramatic effect on dynamics, including an unexpected effect on spatial structure, and particularly improved growth and survival of any subsequently planted trees.

In practice, the desired interim state must also be considered, and whether any particular feature/quantity should be given increased importance. Specific studies using the simulation model allow just such a considered approach to be taken, uncovering subtle aspects of behaviour that are not otherwise apparent.

6.3 Continuous-cover forestry

6.3.1 Background

Continuous-cover forestry attempts to manage uneven-aged stands taking into account both ecological and economic value. Economic values are fairly straightforward to determine – removing trees from a forest stand has clear costs (labour/logistical) and returns/yield (timber value), but ecological values are less easy to define. As above, the model's steady state is taken as ecologically optimal, similarity to which will be assessed visually using the basic statistics, and using the similarity measure defined in Section 6.2.2. Yield is defined in terms of cumulative basal area removal over time.

Despite the ecological motivations of this chapter (and thesis in general), the sustainability of yield is considered first – almost every managed forest is so because financial gain is desired. Nonetheless, a sustainable yield implies a sustainable population, and the relative ecological merits of such approaches are considered in the process. Again, an initial condition of Glenmore plot 1, a plantation stand, is used.

6.3.2 Sustainable yield

Unrestricted thinning

Naively, yield from a forest stand can be increased by removing trees more frequently, or by removing more trees in a single thinning. Needless to say, after some time this would necessarily lead to the removal of all the trees in the stand, leaving only bare ground. The logical conclusion of such an approach is a clearcut, in which all trees are removed in a single operation, after a certain number of years (the "rotation period"). The land can then be replanted at the same density, and the procedure repeated. The level of output obtained from such a procedure can be determined simply using the model's basal area at the time of the clearcut. Example basal area values and associated average annual yield (basal area removed from the stand, divided by the number of years taken to create it) are given in Table 6.2, demonstrating that for maximum yield it is better to thin before the stand has reached peak basal area, as by this time is has already entered a period of slower growth. Of course, thinning time is also partly dependent upon the type of timber required.

The values in Table 6.2 are best case values – a period of ground recovery (2-6 years) may also be required. It is worth bearing in mind that, unlike the continuous-cover management described below, high density planting (2500 trees ha^{-1}) is required to perpetuate output – the total cost of a clearcut rotation is around

£5000, of which approximately £2000 relates to planting (Colin Edwards, personal communication). Other unrestricted managements may be implemented, but the eventual effect of all is to reduce the stand to a state in which there are no trees left, or it is so reduced as to be moribund.

Table 6.2: Basal area and annual yield (BA grown divided by rotation period) for model stands planted with a 2m square lattice.

Time (yr)	BA (m^2ha^{-1})	Yield ($m^2ha^{-1}yr^{-1}$)
25	12.6	0.505
50	29.4	0.588
75	33.9	0.452
100	34.2	0.342
150	32.1	0.214
200	30	0.15

Restricted thinning

Continuous-cover forestry aims to work in a more sustainable manner, so that replanting is not required. Sustaining a steady density of trees in the stand also means that it may provide better habitat/ecological value, but a management programme that does not remove all trees at once requires more care. Thinning criteria affect the resultant state of the stand, and with careful selection, it may be possible to increase yield without significant effects on structural characteristics.

Repeated thinnings were considered altering various aspects: (i) restricting the maximum proportion of total density to remove in a single thinning, (ii) altering the inter-thinning period (iii) altering size and spatial criteria of the thinning applied.

Consider first thinning a fixed density (10% of all trees), from 60–100% of the size distribution. Varying the interval (Figure 6.9a) significantly alters the stand's fate, with longer intervals allowing improved survival. However, at longer intervals, there is surprisingly little difference in long-run basal area; regrowth following thinning is initially rapid, but slows significantly later on as competition "re-equilibrates" locally. The total cumulative yield is shown in Figure 6.9b. For the more frequent thinnings, high yield is possible at first, but cumulatively it approaches an asymptote as the stand falters through over-thinning. For less frequent thinnings, a continued yield is possible (the regime allows persistent non-zero basal area).

Now consider thinning from different regions of the size distribution. We already saw (Section 6.2.3) that removing trees from the high size classes allowed faster regrowth than thinning the middle size classes, in which trees have more potential

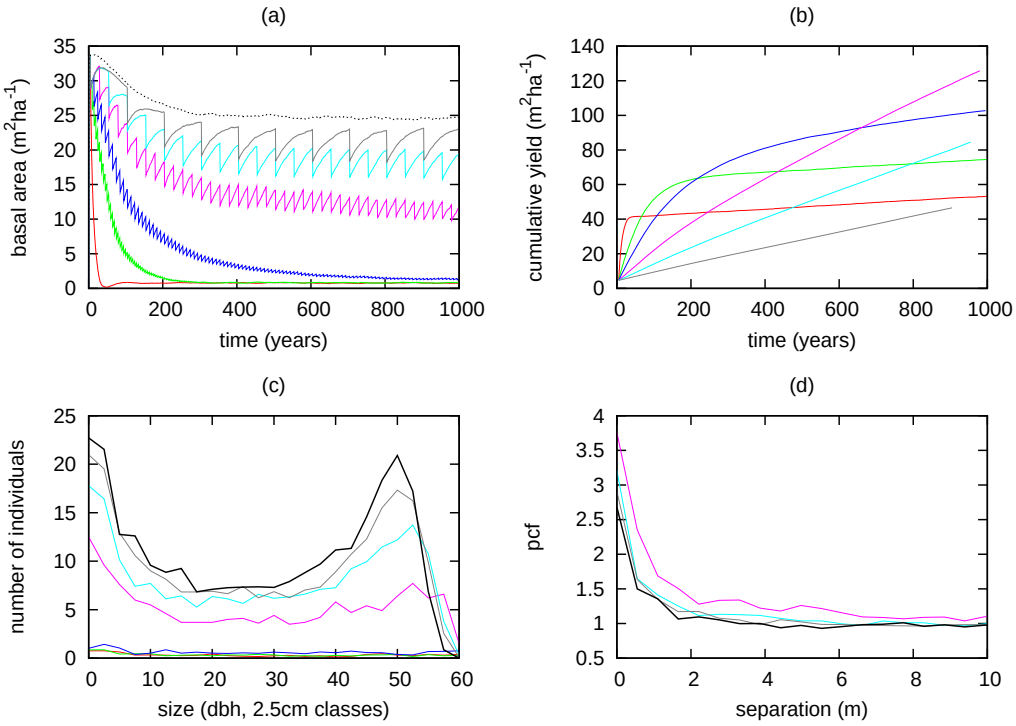

Figure 6.9: *Continuous-cover – varying interval of repeated thinning*: 1 (red), 5 (green), 10 (blue), 25 (magenta), 50 (cyan), 100 (grey) years. Removal of a viable quantity of timber at too short an interval leads to the forest being "managed to death", while at longer intervals, average yield falls due to a slowing growth rate after thinning. (a) Basal area (b) cumulative yield (c) size distribution (d) PCF. The dotted black line shows the behaviour of an unmanaged stand, the solid black line shows the model steady state.

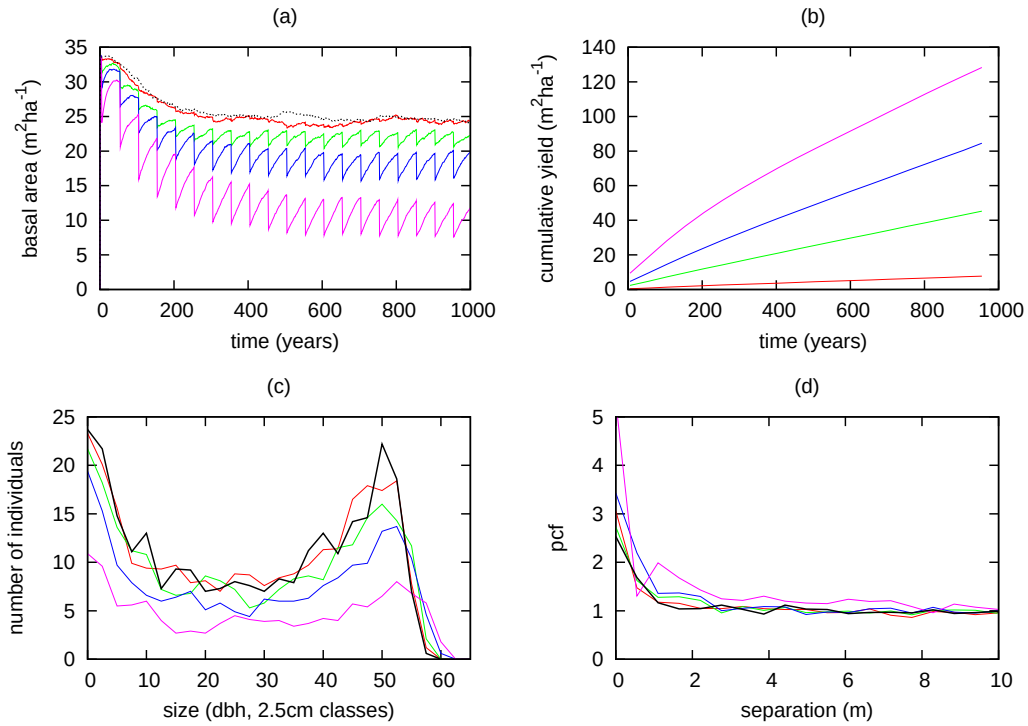

Figure 6.10: *Continuous-cover – varying thinning intensity*. 1 (red), 5 (green), 10 (blue), 20% (magenta) of total density removed every 50 years. (a) Basal area (b) cumulative yield (c) size distribution at 100 years (d) PCF at 100 years. The dotted black line shows the behaviour of an unmanaged stand, the solid black line shows the model steady state.

for growth. Removal from the smaller size classes leads to almost zero output at later times (as they have both low density and small individual size relative to the canopy classes). It does however result in an overall higher density population (Figure D.4, Appendix D.2).

Altering the proportion of total density removed at each thinning also alters the long-run behaviour, with a higher density removal forcing the basal area lower (Figure 6.10). Again, the difference between the regimes is less than might be expected, as the more intense the thinning, the greater the reduction in competitive interaction and therefore faster the subsequent regrowth (though intense thinnings applied frequently result in extinction).

Consider finally spatially correlated management applied to continuous-cover forestry. Patch thinning is appealing here, as it effectively involves clearfelling small regions, creating less disturbance to other areas of the stand. Recall that, due to its creation of high and low density regions, as opposed to uniformly lower density across space, patch thinning did not allow the same level of regrowth following thinning as

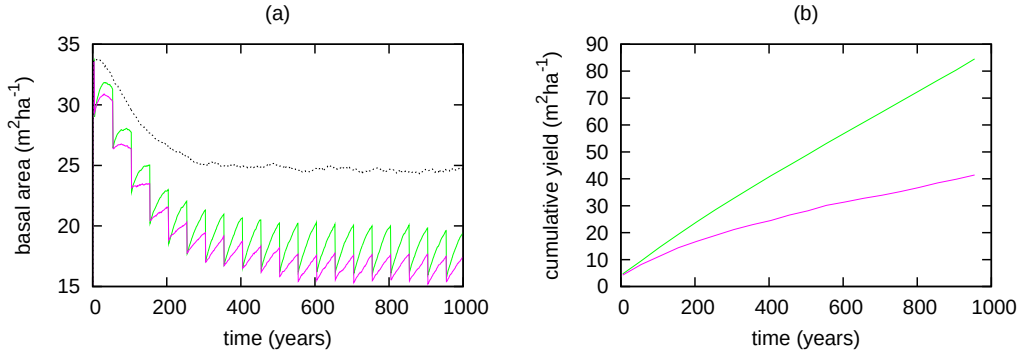

Figure 6.11: *Continuous-cover – patch versus size-structured thinning*. Patch thinning ($5 \times 250m^2$ patches, magenta) does not allow the same yield as a similar intensity size spatially random thinning (10% density, 60-100% size, green), due to slower growth of remaining trees following a thinning. (a) Basal area. (b) Cumulative yield. Dotted black line shows the behaviour of an unmanaged stand.

an equivalent intensity size structured thinning. This is replicated here; regrowth is slower, and yield is consequently lower for a forest with the same persistent basal area (Figure 6.11).

Average yield over 1000 years, across a range of thinning densities and intervals (for 60–100% size thinning), is shown in Table 6.3 – roughly equivalent (and maximal) yield over this period is possible using either 5%/10yr or 20%/50yr thinnings. Making reference to Table 6.2, this is only around 20% of that possible with a clearcut every 50 years. However, there is no requirement for planting in order to sustain the stand. Note also that (i) the model generally underestimated regeneration in comparison with available semi-natural data (especially at low stand densities: Chapter 4), and (ii) basal area recovery in thinned stands is generally faster than that predicted by the model (Colin Edwards, unpublished data), both meaning that real thinned continuous-cover stands will likely produce faster recovery, and therefore higher yield, than that predicted here.

Table 6.3: Yield ($m^2ha^{-1}yr^{-1}$) for various continuous-cover management regimes (removing from the largest 40% of trees at each thinning). † indicates regimes that effectively drive the stand to extinction.

	Frequency					
% removed	1	5	10	25	50	100
1	0.122	0.0660	0.0357	0.0147	0.00746	0.00395
5	0.0649	0.102	0.122	0.0761	0.0438	0.0260
10	0.0492	0.0690	0.0956	0.119	0.0817	0.0473
20	0.0576†	0.0978†	0.0638	0.104	0.124	0.0902

6.3.3 Notes on ecological value/Distance measure comparison

It is clear that repeated intense or frequent thinnings quickly lead to the demise of a stand. By limiting these factors, it is possible to maintain a forest that is not greatly altered from its unmanaged steady state in the absence of management, while producing a steady output of timber.

Using the similarity measure, it is straightforward to divide the treatments into two groups: those that effectively cause extinction of the population (density term $\approx$ basal area term ≈ 1), and those that do not (Table D.2, Appendix D.4). Of those that do not, the low intensity (and long period) thinnings produce stands closest to the unperturbed steady state. This is hardly surprising in itself, but it is worth noting that one of the high intensity thinnings (20% density removal, once every 100 years) fares very well, and as previously mentioned also produces a reasonable level of output (Table 6.3). For ecological purposes, however, the actual magnitude of difference may be of less importance than the question of whether a particular regime is sustainable – any with a basal area greater than around $10\text{m}^2\text{ha}^{-1}$ is probably acceptable.

It is also useful to identify the level of variation over time, as managements causing rapid/large changes in the habitat are probably undesirable, even if the forest is able to recover: a conservation-minded approach requires a balance between frequency of intervention, and the variation that it imposes. In this sense, less frequent and lower intensity thinning ($\rightarrow$ no management!) is better, as any management causes disturbance to other features of the stand, such as ground or sub-canopy vegetation, and the species that inhabit it. Spatially correlated (for example, patch) thinnings may also be better in this respect, as they affect only certain regions of the stand, while also being potentially cheaper to implement (though as we have seen, yield is likely to be lower).

6.3.4 Summary

Typical continuous-cover forests cover many hectares, to enable financial viability of the low-density thinnings that are made. However, the results presented in this section demonstrate that (in theory at least) it is possible to manage a stand with a continuous-cover approach and obtain somewhat acceptable levels of output (up to 20% of those of an optimal clearcut/replanting cycle in the long term), while leaving the stand fairly close to its unmanaged steady state, which is promising for the prospects of smaller scale operations.

The existence of multiple timescales (rapid regrowth until competition is back in balance, followed by a period of slower recovery) is difficult to identify without the simulation model. However, it appears to be important in understanding how to

maximise the yield of a stand. It is also important for ecological concerns, in that it helps us better understand how economically viable forest management can be performed with minimal impact. Doubling the interval between management *does not* allow twice as much regrowth. This means that, for example, thinning performed with a period of 50 years can lead to a similar state (density/basal area etc.) as a period of 100 years. The more frequent thinning removes a slightly smaller volume at each intervention, leading to less variation in the stand's state, but over time obtains greatly increased output.

It was also found that different intensities and frequencies of management can lead to the same level of output. However, in general, less frequent management is a safer option for ecological purposes. Furthermore, a thinning has certain fixed costs (the basic cost of a low-intensity thinning is around £400 ha^{-1} (Colin Edwards, personal communication), regardless of the amount removed.

Finally, it is important to remember that the weight given to any particular property of a forest, ecological or economical, is in reality determined by government policy and not science. It seems somewhat likely that a mosaic of stands at different degrees of management might provide many ecological benefits while also being economically efficient.

6.4 Prediction Robustness

The model used here provides a greatly simplified representation of forest dynamics, and while parameterised using data from the target species, results must be interpreted with a degree of caution. The behaviour of the model used here is qualitatively robust over a wide parameter space (encompassing all reasonable values for forest trees, Section 2.5), and as such, management predictions are also robust. However, the fundamental definition of certain components were identified as being less well determined than others (Chapter 4). As such, these are identified below, and the effects of their alteration upon the predictions that are made relating to the outcome of silviculture are discussed.

Heterogeneous growth

Chapters 3 and 4 found that there was unexplained variation in individual growth trajectories. In light of this, the robustness of the above conclusions to the inclusion of random variation in tree asymptotic size (keeping the parameter α fixed) was tested.

No fundamental change in the effect of management strategies was observed in this formulation, though the difference in post-thinning basal area increase is reduced

between thinnings, as not all trees have the potential to obtain a large asymptotic size (Figure D.5, Appendix D.3). No effect on spatial properties was observed.

Seedling establishment

Chapter 4 found that, aside from dispersal, alterations to the establishment model had limited effect on the equilibrium state of the population. However, at a very low density of parents, or when there is substantial spatial variation in the density of parents (such as that imposed by thinning regimes), model assumptions relating to immigration could affect the rate of re-establishment.

Both seed production and regeneration success are often regarded as being proportional to basal area (Drew Purves, personal communication). The model used here implements the former, but the latter is dependent on local density, through the establishment probability. Decreasing k_d reduces the effect of spatial patterning of thinning (and thus increases dependence on overall basal area). However, no significant variation in regeneration behaviour was seen (Figure D.6, Appendix D.3), even in the case where f and C were increased concurrently (increasing rate of birth, together with the rate of mortality at establishment).

In addition to the model with a individual reproduction, we also considered seeding at a constant rate (that of the stand at equilibrium basal area) throughout population development, to random locations in the arena. In this case, a high level of regeneration is maintained in areas (and periods) of low density, but the equilibrium pattern is no longer clustered – only a slight signal of local inhibition is seen (Figure D.7, Appendix D.3), which does not reflect patterns seen in Scots pine study plots (Chapter 4).

Neither alteration led to spatial structure induced differences in juvenile density (for example, patch versus shelterwood). Variation only occurs when overall stand density is reduced to a very low level (for example, following a clearcutting, Figure 6.1). In all other cases, the deviation from the basic result at 100 years after management (as presented in Figures 6.2 to 6.11), is sufficiently small that any differences have been absorbed into the population.

6.5 Summary

This chapter considered a fairly comprehensive suite of management interventions. Comparison of these with one another, and the unmanaged/steady state behaviour of the model, allowed an appraisal of their relative merits for two ecologically motivated management objectives: transformation and continuous-cover forestry.

With respect to transformation, it was found that thinning criteria such as the size range thinned and the target basal area can have a dramatic effect on the future development of a stand. Other less obvious effects were noted in comparison of, for example, size structured with spatially structured thinnings, which produced slower growth/recovery, but greater variation in size of trees.

Continuous-cover forestry might seem something of a black art, in view of the difficulties in understanding how the removal of certain trees will affect the future dynamics of the population. The use of a simulation model aids greatly in such exploits: this chapter demonstrated how management may be optimised; increasing yield and concurrently minimising ecological disturbance to the long run state of the population.

Chapter 7

Discussion and outlook

7.1 Summary and conclusions

This thesis has tackled several key topics, around a central theme of understanding the dynamics of structured populations, with applications to forest conservation. The basic model formulations presented in Chapters 2 and 5 build upon those of Bolker and Pacala (1997); Law et al. (2003); Raghib-Moreno (2006). Gratzer et al. (2004) made the suggestion that, adapted to include both size and spatial structure, this class of models might be ideal for tackling some fundamental issues in the understanding of forest dynamics. The data based parameterisation and tuning of the individual-based simulation model presented in Chapters 3 and 4 gave insight into how this can be achieved by such an approach.

In development of the individual-based model (IBM), it was possible to base many of the details of formulation upon existing methods used in the literature. However, accounting for the different aspects of structure observed in the available forest stand data (from distinct states of development) required fairly involved configuration, parameterisation and tuning. Initial investigations focused on identifying generic aspects of behaviour, using parameters that might realistically occur in forest populations. Under such a scenario, and appropriate initial conditions, it was found that the basic patterns observed in real forest stand dynamics (Franklin et al., 2002) could be readily understood in terms of the basic processes implemented in the IBM. The steady state takes several hundred years to reach: as Turner et al. (1993) and Oliver and Larson (1996) note, it may actually never occur in real temperate forest populations. Extensive investigation of the available parameter space determined that the model's behaviour is robust, but also made interesting findings relating to the importance of explicit spatial effects. It has typically been found that explicitly spatial simulations of forest populations yield a different result from equivalent mean-field models, but not

dramatically so (Deutschman et al., 1999; Busing and Mailly, 2004). The "Scots pine" parameterisation used here produced just such a result, but in highly competitive populations (or indeed very sparse populations) the difference between mean-field and spatial results was more marked.

Analysis of Rannoch growth data was challenging. While the dataset was not without its flaws (a missing region in one of the plots due to establishment of other overlapping studies being an obvious example, the non-recording of tree sizes removed to make way for a pylon line being another), complete increment and location data for stands of trees is relatively rare, and it provided unique insights into individual growth form and the impact of interaction. However, despite its detail, the dataset was not able to confirm or rule out all hypotheses that we made. One key desire was to understand why many old trees were particularly small for their age. However, it is precisely these trees for which full neighbourhood history (in terms of the implied presence and size of neighbouring trees) is not available. This led to some biologically impossible parameter estimates, and prevented validation of the "cumulative interaction" hypothesis. Interaction does appear to have a fairly weak effect upon mature trees: once established on a particular growth trajectory they do not readily sway from this. Ultimately, no interaction scenario satisfactorily gave the level of variation observed in the data populations. Small-scale soil and/or genetic data would be a very useful addition to the datasets considered here in order to determine the source of this variation.

Asymmetry of trees in the datasets (or measurement error) meant that very few growth curves exhibited zero size at zero age. As a result, firm conclusions regarding the precise form of early growth were difficult to make. Thankfully, the general behaviour of the simulation model is relatively robust to the choice of growth function, providing that it has an asymptotic maximum size (though implementation of a monomolecular growth curve would certainly require heightened juvenile mortality to explain size distributions observed at Rannoch).

The failure of certain aspects of data analysis placed more importance on the simulation model in understanding Scots pine growth patterns. The structure of the model allowed straightforward extension to include age dependence, cumulative interaction, and inter-individual variation. Each of these additions produced populations with increased heterogeneity in growth. However, the level of variability in the Rannoch semi-natural plots was only replicated by individual variation. In reality, a combination of these effects is likely to be observed. While soil conditions are probably heterogeneous on a small scale (though data for the specific plots is not available), direct observation of the trees in the Rannoch plots indicates that those trees which have a very large diameter generally have weak apical dominance. That

is, side branches produced at an early age were able to grow to produce "multiple main stems"; as a result, their trunks became very large. This requires low interaction stress during the tree's juvenile years. Useful information could be obtained from more detailed studies of the form of juvenile aged trees, and its response to interaction.

The reproduction element of the model was also subject to a more in-depth investigation in Chapter 4. The myriad processes that combine to produce successfully established trees have been the subject of a great deal of research. However, a general theory is hampered by sensitivity to environmental, species and site specific effects. In the context of the model presented here, the principal role of regeneration is to produce the correct density of new recruits (relative to the existing population), in the correct spatial pattern. Differences between the patterns observed in data stands led to a variety of proposals for alterations to the basic establishment model. Of these, the only obvious improvement was provided by the addition of local dispersal from parent trees; analysis of model behaviour provided minimal support for an establishment probability that is dependent on global basal area, as opposed to local interaction.

The derivation of population level differential equations from the basic rules of the individual-based simulation model allowed further insight. Analytical models allow an escape from the confines of fitting a model to data for a particular species with highly specific process and parameterisation, shifting the focus to the generic aspects of population dynamics. In this sense, obtaining a solution (whether by analytical or numerical methods) may be considered to be of less importance than simply studying the form of the equations directly. Analytical solution was only possible in the simplest of cases, and while numerical investigations were not entirely successful, the derivations did lead to insights for moment-closure problems in systems that involve both size and spatial structure.

The simplicity of the basic model around which this thesis is based aided progress in several ways. Firstly, it made it possible to understand why altering the definition of a particular process affected behaviour in a certain way. Secondly, it enabled direct comparison of simulated results with data from real populations, without the problem of overfitting. Given a mismatch with a particular aspect of observed (real stand) behaviour, it was relatively straightforward to identify how the model might be improved, or more importantly, identify the driving factors in the behaviour of the real stands.

Several authors (Comas, 2005; McIntosh, 2006; O'Hara, 2001) have recognised the potential utility of this class of models in dealing with the complications of modern forest stand management. The breadth of insights gained in the earlier chapters, and the individual-based formulation, meant that the model could be applied to such problems with a degree of confidence. While uneven-aged stand management

has been practised in some European stands for many years (Schutz, 2001), it is typically performed in a relatively ad-hoc fashion and lacks a general theoretical basis. The heterogeneous structure created gives a complicated system of interactions between neighbouring individuals, and as such, the individual-based model is an ideal tool with which to analyse the behaviour of forest stands in response to such management. Chapter 6 considered two specific uneven-aged stand management objectives: plantation transformation and continuous-cover forestry. There is no single "optimal" strategy for transformation. Low intensity thinning regimes generally produced the most rapid transformation, but the interim state is also of interest. Spatially homogeneous thinnings allow the most rapid regrowth of remaining trees, while patch thinnings obtain greater variation in individual size, and open up space for regeneration and other sub canopy vegetation.

Continuous-cover forestry may not achieve the same level of output as a clearcut and replant strategy, but requires less input and is more ecologically sound. It was found that low intensity thinnings made frequently can obtain greater output than intense thinnings made less frequently. Again, the model's straightforward representation of stand behaviour in terms of summary statistics allows such objectives to be easily understood and achieved.

7.2 Main findings

- Spatial structure is evident in Scots pine populations, but has limited effect on first order properties.
- A steady state takes around 500 years to obtain.
- While not the sole cause of variation, historical interaction pressure likely plays a large part in determining variation in individual size and morphology.
- Some third moment approximations from spatial birth-death processes perform very well in moment models including size-structure. However, a way around processing and memory limitations must be found.
- In transformation management, there is no true short cut to the steady state, but spatially correlated thinnings obtain greater variation in individual size, and encourage regeneration.
- In continuous-cover forestry, spatially random thinnings will obtain the highest yields. Carefully designed low intensity thinnings can obtain higher yields than high intensity thinnings, and may have lower ecological impact.

7.3 Caveats and future directions

This thesis combines the theoretical analysis of structured population models with their application to forest dynamics and management problems, providing many useful insights. However, some compromises have been made, and limitations have been found.

The model implemented was intentionally simple, neglecting several features that unquestionably play a role in the dynamics of real populations. Individuals' state was characterised by a single size measure (nominally diameter at breast height, or "dbh"), on the premise that this one measurement is able to summarise an individual's performance in various demographic processes, and the magnitude of its impact upon neighbours. With respect to interactive effect upon neighbours, this may not be a fatal assumption: while an initial guess might be that shading and ground resource acquisition depends more on height than diameter, trees with large diameter trunks generally also have more thoroughly developed foliage, and a broader canopy. However, growth is a more complicated process. Rather than simply "not growing" in response to intense interaction, trees generally invest more in height (as opposed to diameter) growth, reaching canopy height rapidly. This occurs in plantations, where trees that are "overtopped" generally die rapidly. However, as a consequence of their rapid height growth, the remaining canopy trees have little potential for later development of lateral structure, and large dbh. As mentioned above, direct observation of Scots pine stands makes it clear that the form of individual trees is dependent on the point in life at which they have experienced intense or weak competition from neighbours. As such, a useful extension to models aiming to capture the effect of structured interactions upon population dynamics might be to allow neighbourhood-dependent multiple resource allocation, between say height and diameter. Such a formulation would necessitate more complicated interaction and growth functions, and as a consequence would require increased care in configuration, parameterisation and analysis.

This brings us to another important issue: that of data, used for both parameterisation and validation of our models. As Tukey (1986) said: "The combination of some data and an aching desire for an answer does not ensure that a reasonable answer can be extracted from the given body of data". In Chapter 3 we found that even quite in-depth datasets may ultimately turn out to be inadequate for directly determining the source of population structure. A thorough data-based investigation of hypotheses such as cumulative interaction and variation in lifetime resource allocation requires information spanning several lifespans, with multiple variables recorded (one can measure the historical diameter of a tree, but how can historical height be tracked

with the same accuracy?). In comparison with human lifespans, forest populations have fairly slow dynamics, and the collection of such data is clearly impractical. Other authors have cited complicating issues with the collection of fecundity (Clark et al., 2004) and mortality (Pacala et al., 1996) data.

A promising recent development is the advent of data collection by remote sensing. The sheer volume and relative accuracy of data collected in this manner could sidestep the requirement for complete historical data by allowing comparison of dynamics at different points in space, rather than time (without being limited to the use of individual tree variables alone, but also containing information on climate, other vegetation and so on). Such data has already begun to be used for investigations relating to regeneration and competitive interactions (Bollandsas et al., 2008).

We made some useful findings using mathematical approximations of the IBM. These methods are in principle very flexible methods of analysis, and can be modified to remove dependence on isotropy, spatial homogeneity and so on (e.g. Bolker, 2003). However, would-be investigators should bear several points in mind. While the form of the derived equations is fairly simple, the numerical simulation of a PDE model generally requires much greater care than that of an analogous IBM. The IBM only requires the definition of simple rules, and an algorithm for choosing events. On the other hand, the partial differential equation (PDE) approximation requires careful bookkeeping of updates to arrays. Such algorithms are very easy to construct incorrectly, leading to entirely unexpected behaviour, a problem clouded by sometimes subtle dependencies between the simulated quantities. Such issues are compounded as the dimensionality increases (for example including size changes correlation from a function of space, to a function of space, and the sizes of individuals). It is also worth noting that the mean-field version of our PDE model required a very high resolution (small time and size increments) to obtain accurate behaviour. To replicate this in the "full" model would be prohibitive due to both processor and memory restrictions: further work must find a solution to this problem.

The model was well suited to comparing different approaches to uneven-aged forest stand management at a stand scale. However, its representation of structural development using a single size measure means that its output is of less relevance to fostering the development of individual trees with a desired structure. Furthermore, there was some question over the accuracy of the reproduction component of the model. It would certainly be worth investigating the application of a similar model with an improved establishment submodel, and the addition of multiple resource allocation as noted above. This would allow further insight into how silviculturalists can manipulate natural regeneration and structural development patterns.

Finally, assuming that we *can* understand the behaviour of forest populations, the

value of very long-term goals must be questioned. The dynamics of forests are slow; government policy is fickle by comparison. It is all very well having grand plans for the greater good of ecosystems, but we must be sure that the decisions made and results achieved today are robust in the face of changing economic, political and environmental objectives.

Appendix A

Appendices to Chapter 3

A.1 Regression Trees

A.1.1 Theory

A regression tree algorithm aims to identify the key sources of variation in the value of a response variable, and helps to understand how these sources combine to produce the observed patterns. Given a single parent node containing all data, this is achieved by repeated binary splits, in a manner which minimises the *impurity* of the two created nodes at each split. Impurity is defined by the expected sum variance of the response vectors Y_1, Y_2 (in our case, observed growth increments) for the two resulting nodes, and we thus identify the cutoff value x_j^R of one of the M explanatory variables (size, age, location, competition in our case) that minimises

$$\arg \min_{x_j \leqslant x_j^R, j=1,..,M} \left[\mathbb{P}_1 \mathbb{V}(Y_1) + \mathbb{P}_2 \mathbb{V}(Y_2) \right], \tag{A.1}$$

where $\mathbb{P}_1$ and $\mathbb{P}_2$ are the probabilities of being at each of the nodes (Timofeev, 2004). A tree so created ultimately has the same number of end nodes as the length of the response vector at the parent node (number of data points). This is both computationally expensive and of limited utility for comprehension, and so a minimum length of response vector at each node is usually enforced.

The method is useful for exploratory data analysis as it is nonparameteric, does not require selection of explanatory variables, is invariant to monotone transformations of the explanatory variables, and is not negatively affected by the presence of outliers.

A.1.2 Additional output

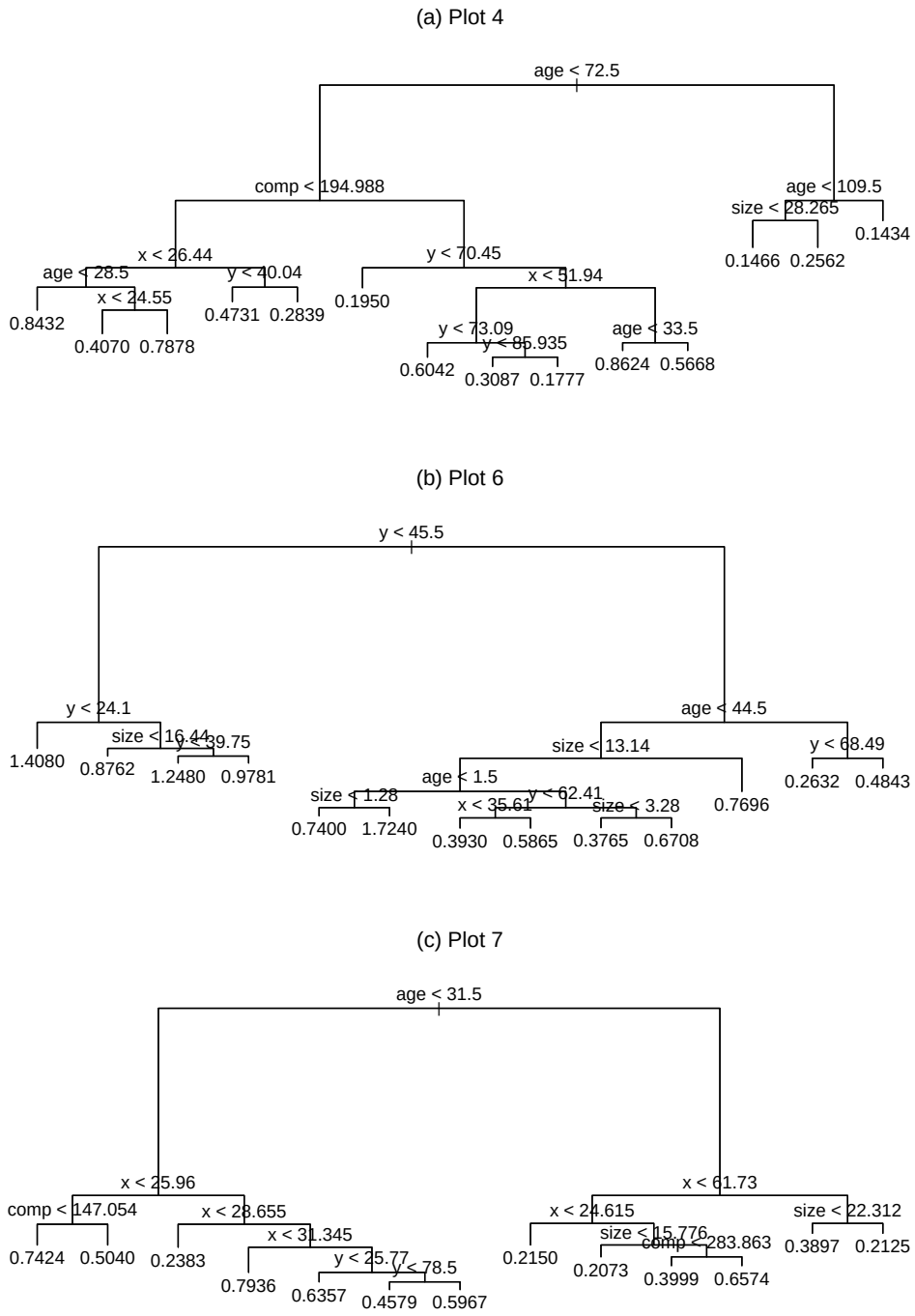

Figure A.1: Regression trees computed for post 1918 growth increments from each of Rannoch (a) Plot 4 (b) Plot 6 and (c) Plot 7. These seek to identify the primary sources of variation in growth increment, and any interactive effects between them. This figure includes location variables in addition to age, size and interaction, as per the figure in the main text.

A.2 Mixed-effects models

When considering data pertaining to populations, it is often innappropriate to regard all data points as being independent and identically distributed. In the context of growth data, each measurement belongs to a set of measurements, each set applying to an individual.

The mixed model approach is to construct a hierarchical model; that is, one in which variation is allowed at multiple levels. In essence, this involves making separate non-linear least-squares parameter estimates for each grouping of observations (in this case, growth measurements for individual trees). These "individual" parameter estimates are then taken together to estimate their variance across the entire population, and their covariance with each other. The model may thus be defined as:

$$y_i = f(X_i, \theta, Z_i, b_i) + \epsilon_i \tag{A.2}$$

$$b_i \sim N(0, \Psi) \tag{A.3}$$

$$\epsilon_i \sim N_{n_i}(0, \sigma^2 \Lambda_i) \tag{A.4}$$

Here:

- y_i is the response vector for group i ($n_i \times 1$) – in our model, growth increments for individual i.
- X_i is the model matrix for "fixed effects" of observations in group i ($n_i \times p$).
- θ are the fixed effects coefficients ($p \times 1$) – in our model $(\alpha_{fixed}, \beta_{fixed}, \gamma_{fixed})$.
- Z_i is the model matrix for "random effects" of observations ($n_i \times q$).
- b_i is the vector of random effects coefficients for group i ($q \times 1$) – in our model $(\alpha_{random}, \beta_{random}, \gamma_{random})$.
- ϵ_i is the vector of errors for observations in group i ($n_i \times 1$).
- Ψ is the covariance matrix for the random effects ($q \times q$)
- $\sigma^2 \Lambda_i$ is the covariance matrix for the errors in group i ($n_i \times n_i$)).

(Fox, 2002, Appendix). In our model, the observations are decomposed $s_i = X_i + Z_i$ (all functions of time for each individual i) for the formulation above. y_i (again, functions of time) are the growth increment curves for individual i. Central to the model is the concept of "fixed" and "random" effects. It is assumed that there are some underlying fixed parameter values (the fixed effects), a property of the average

group (in this case, individual). Inter-group variation is then a consequence of the level of variation in these parameters (the random effects).

For example, fitting individual data using a function with three parameters b_1, b_2, b_3 gives a mixed-effects model with 3 (fixed effects) + 6 (covariance matrix Ψ) = 9 parameters.

A.3 Comparing model fit

A.3.1 R-squared

Quality of model fit in linear models with equal numbers of explanatory variables is assessed by R^2. Roughly speaking, this is the proportion of variance in the data that the model accounts for.

However, when comparing non-linear models, calculating R^2 does not necessarily allow determination of the best fitting model. In linear models, the relation

$$SS_{total} = SS_{regression} + SS_{residual} \tag{A.5}$$

holds, where

$$SS_{regression} = \sum_i (f_i - \bar{f})^2 \tag{A.6}$$

A requirement for the satisfaction of Equation A.5 is that $\bar{f} = \bar{y}$, which is not satisfied in the non-linear case (since in general $\mathbb{E}[f(x)] \neq f(\mathbb{E}[x])$).

A.3.2 Likelihood-based measures

An alternative apprach to measuring the quality of model fit is via statistics based upon the *likelihood* of the model; the likelihood of the parameters given the data.

$$L(\theta|X) = \prod_{i=1}^{n} p\left(\theta|x_i\right) \tag{A.7}$$

The likelihood is used in parameter selection for a particularly defined model, in the so-called maximum-likelihood procedure. In the linear model case, this is identical to the least-squares estimate. However, the likelihood can also be used to compare the fit of models containing different parameters.

Aikake's *An Information Criterion* (AIC, Aikake, 1974) is most commonly used when comparing *nested* models (one model is a subset of the other under certain conditions, for example with one parameter fixed at zero) with varying numbers of parameters (that is, to test whether the addition of a parameter leads to a noticable

improvement in fit). The AIC is based upon the log-likelihood of the fitted parameters given the data, and the number of parameters included. The lower the value of the AIC, the more parsimonious the fitted model (Bolker, 2007). It is defined

$$AIC = -2\ln\left(L(\hat{\theta}|X)\right) + 2K \tag{A.8}$$

where K is the number of parameters. Burnham and Anderson (2004) give details of its derivation. There is some debate as to the specific conditions required for such comparisons. Ripley (1996, 2008) states that compared models must be nested, though others disagree that this must be strictly enforced (e.g. Anderson and Burnham, 2006; Ritz and Streibig, 2008). It is argued that there are degrees of "non-nestedness" (Ripley, 2006), and that. It would seem wise to exercise caution in their application. However, in Chapter 3, the results of comparing non-nested models in this way do correspond with those of other analyses.

An alternative criterion is the *Bayesian Information Criterion* (BIC), which differs from the AIC in its stricter penalisation of additional parameters

$$BIC = -2\ln\left(L(\hat{\theta}|X)\right) + 2K\ln(n) \tag{A.9}$$

n is the sample size (number of sets of observations). It is derived from a Bayesian argument but is not an inherently Bayesian technique; Bolker (2007) points out that it is, in general, not how most Bayesian statisticians compare models. Accepting a single model and rejecting all others is tantamount to deciding that one model has probability one, all others have probability zero (Ripley, 2008).

A further important point to note is that calculation of likelihood, and consequently information criteria, for mixed-effects models is made by approximating an integral with no closed form (Pinheiro and Bates, 1995) and as such should be treated with caution.

A.3.3 Residual standard error

Residual standard error is the expected error of an observation in respect of the fitted model. It is calculated

$$RSE = \frac{SS_{residual}}{n} \tag{A.10}$$

where n is the number of data points. The lower the RSE, the better the fit of the model to data.

Appendix B

Appendices to Chapter 4

B.1 Supplementary Figures

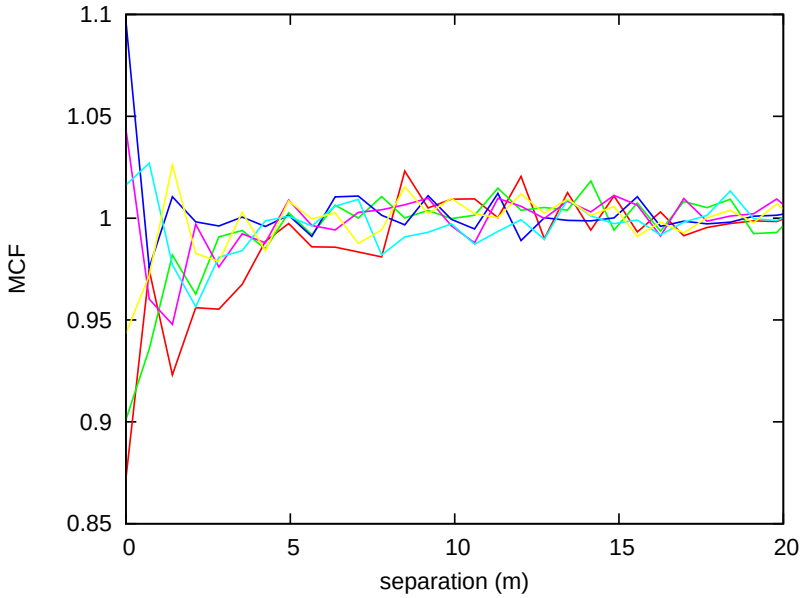

Figure B.1: *Mark Correlation Function of mature trees only in Glenmore plantation stands*, computed using own code, with no smoothing function applied. The red line corresponds to the "plantation data" line in Figure 4.3.

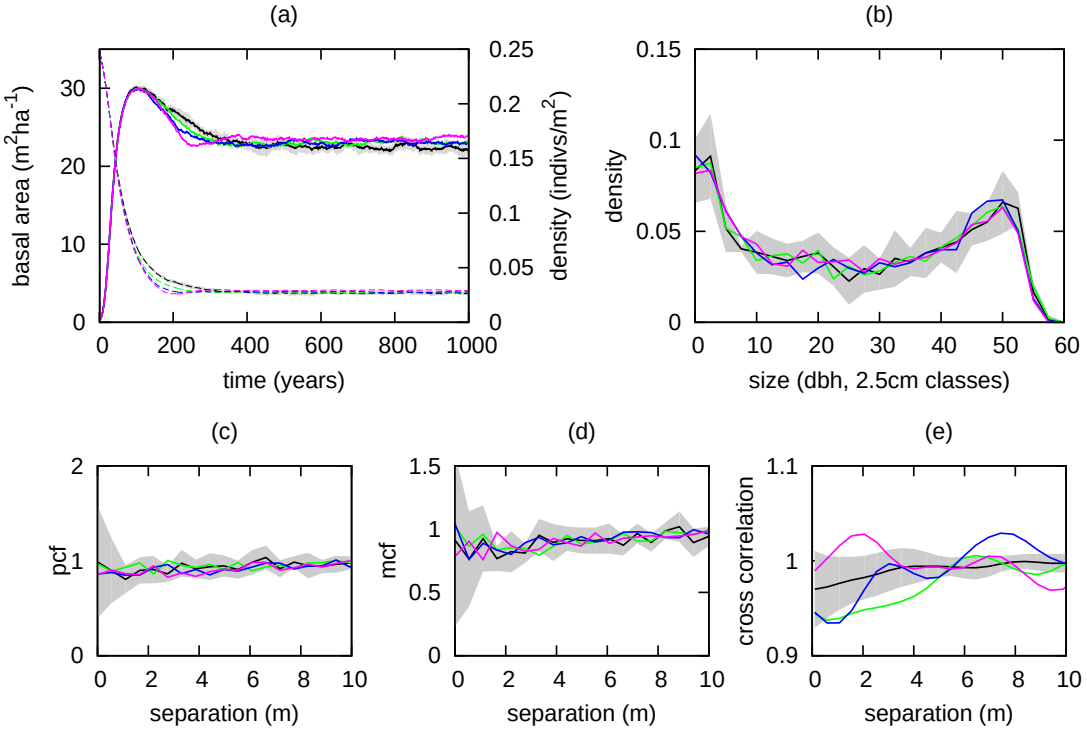

Figure B.2: *Altering establishment dependence on interaction*; allowing f to vary such that the total rate of establishment remains the same. (f,C)=(0.325,5) (green), (0.893,10) (blue), (7.94,20) (magenta). (a-e) as for Figure 4.8.

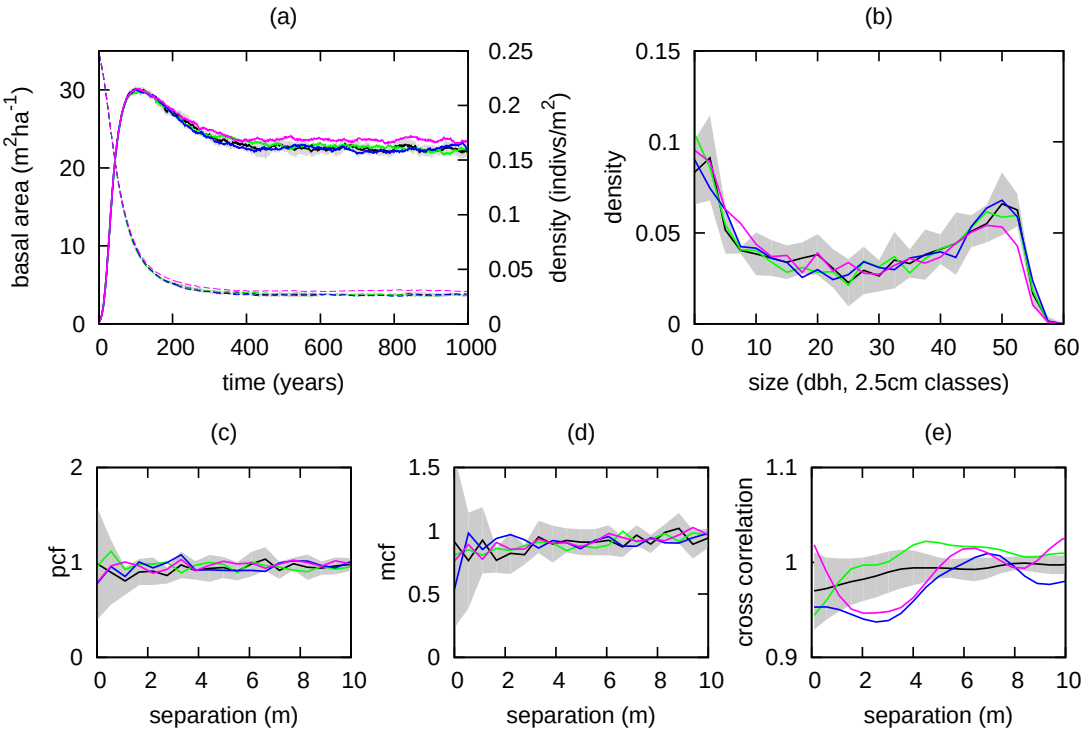

Figure B.3: *Basal area dependent establishment*. Reducing k_d in the establishment probability interaction kernel effectively makes establishment dependent upon basal area. k_d at establishment =0.075 (green), 0.05 (blue), 0.01 (magenta). The black lines with grey standard deviation intervals show the mean behaviour of the model with random dispersal (original results presented in Figure 2.4). (a) basal area (solid line), density (dashed line), (b) size density distribution at 800 years, (c) PCF at 800 years (d) MCF at 800 years. (e) Cross-correlation of juvenile and mature individual locations at 800 years. The weak effect of competition on establishment means that minimal effect is observed here, and only then in the basal area and size distribution, in the case when the kernel is so broad that its integral over the simulated region decreases (magenta).

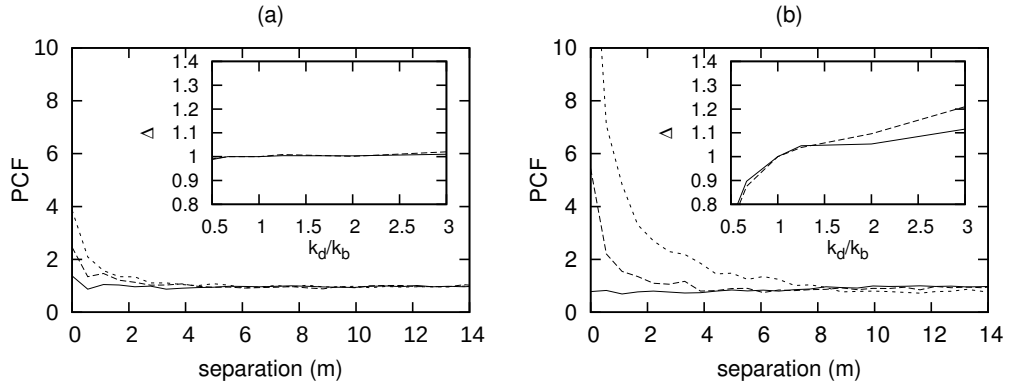

Figure B.4: The relative scale of dispersal altering k_b (random dispersal, solid; $k_b = 0.1$, dashed; $k_b = 0.2$, dotted) while fixing $k_d = 0.1$. Insets show the change Δ in density (dashed) and basal area (solid) as a result of changing k_b (k_d/k_b small = relatively short range dispersal). (a) Behaviour at the Scots Pine parameterisation spatial structure changes, but density and basal area do not. (b) With stronger interaction ($\mu_2 = 0.0002$), spatial structure changes more dramatically, and density/basal area also increase as dispersal becomes more global.

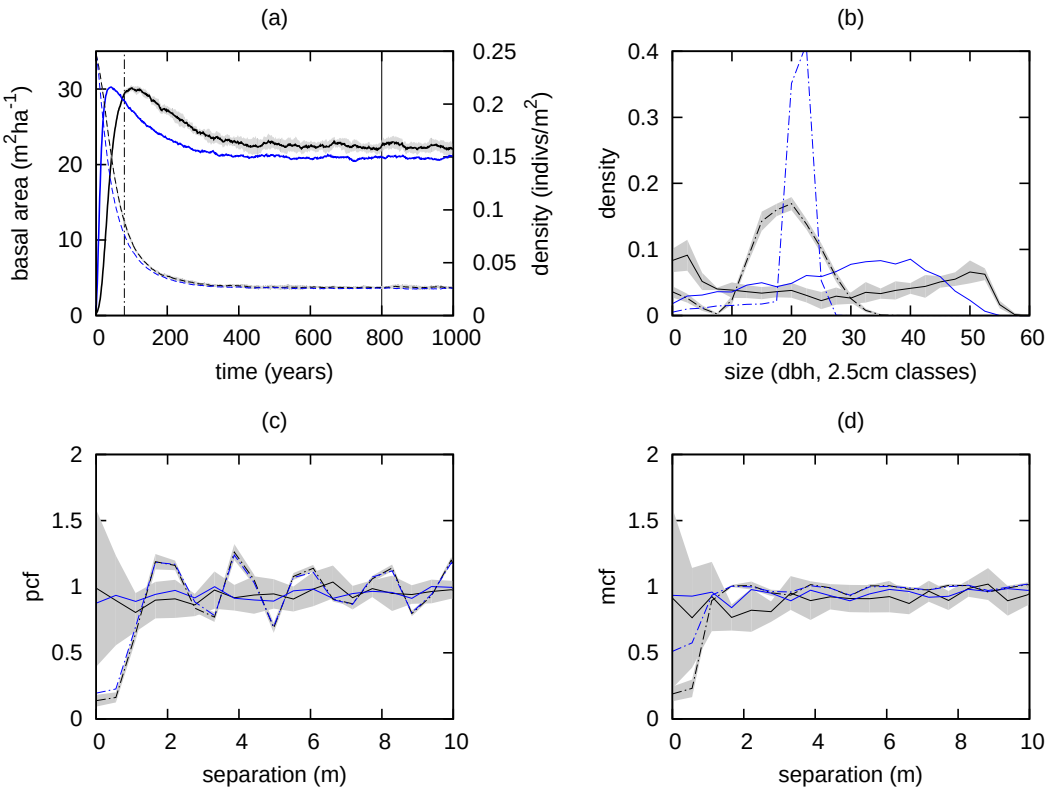

Figure B.5: *Altering the growth function*. Original results using a Gompertz growth function (Figure 2.4) are shown by lines within a grey envelope (standard deviation). Blue lines are obtained using a monomolecular growth function with roughly the same average growth rate an asymptotic size ($\alpha = 1, \beta = 0.0149, \gamma = 0.00005$). (a) Evolution of density (dashed) and stand basal area (solid line). (b) Size distribution at 80 (dash-dot) and 800 (solid) years. (c) Pair correlation function – time/line style as (b). (d) Mark correlation function – time/line style as (b).

Appendix C

Appendices to Chapter 5

C.1 Mean-field numerical integration: the effect of changing Δs and Δt

The figures presented in this appendix show the same information as Figure 5.1 in the main text, in four panels rather than two, to clarify the effect of variation in Δs and Δt upon the results.

Figure C.1 shows the effect of varying the relationship between Δt and Δs (varying Δt). Even at this coarse graining, when the two increments are equal the steady state of the PDE and the IBM are almost identical. This is not improved by reducing Δt further. When Δt is too large, early behaviour of the PDE worsens, to the point where instabilities arise. With this coarse graining of size ($\Delta s = 1$), early behaviour of the size density distribution is not accurate, and does not become more so by reducing Δt further (not shown). This requires Δs to be decreased.

Fixing $\Delta t = \Delta s$ (Figure C.2) leads to more accurate early behaviour of the PDE, without affecting long-run behaviour. The most accurate early behaviour is actually obtained using Δt slightly larger than Δs (see Figure 5.1 in the main text).

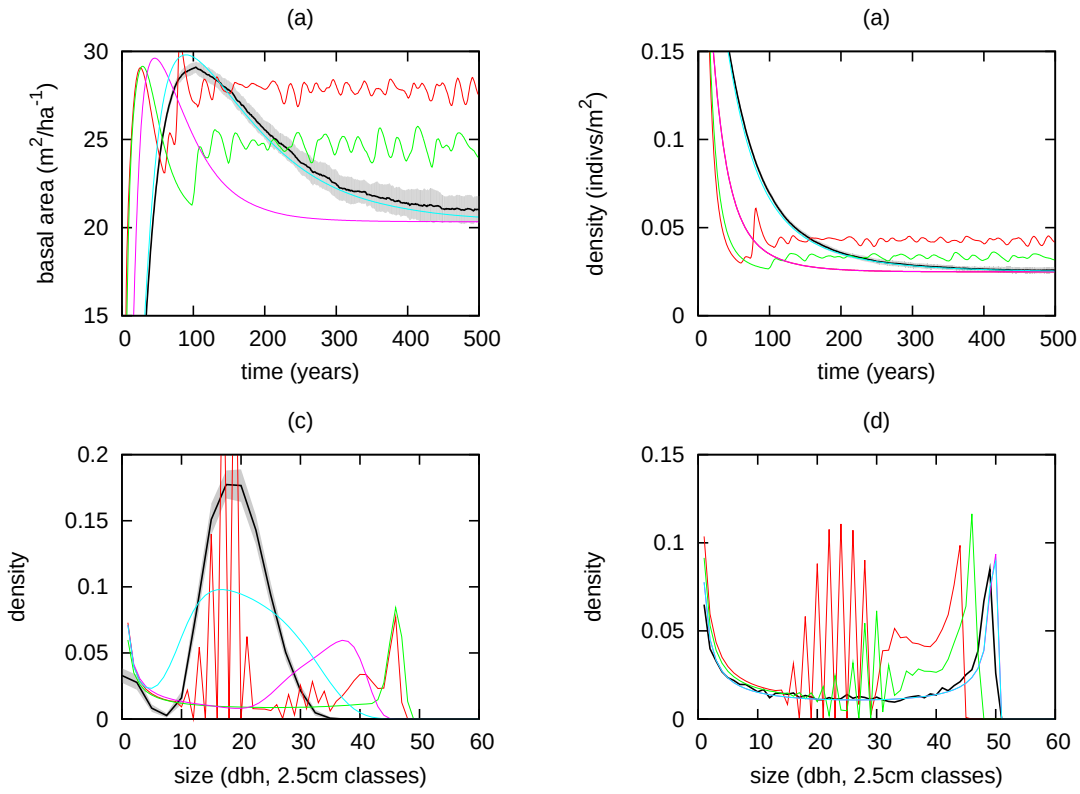

Figure C.1: *Varying* Δt, *with* $\Delta s = 1$ *(fixed)*. Values for Δt: 5 (red), 4 (green), 2 (magenta), 1 (cyan). IBM results are shown in black/grey. (a) Evolution of basal area through time. (b) Evolution of density. Size distribution at (c) 80 years and (d) 800 years. In the long run, behaviour is almost identical (the IBM size distribution at 800 years is averaged over 10 plots).

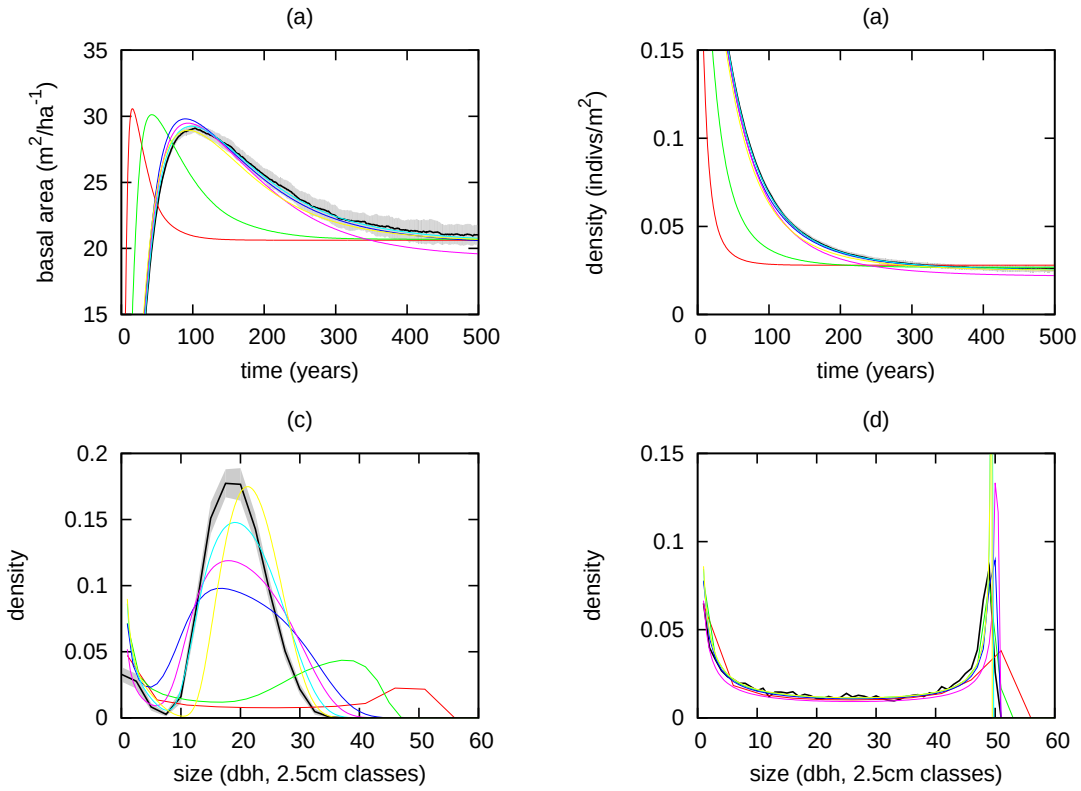

Figure C.2: *Varying both increments, with* $\Delta t = \Delta s = 5$ (red), 2 (green), 1 (blue), 0.5 (magenta), 0.25 (cyan), 0.1 (yellow). IBM results are shown in black/grey. (a) Evolution of basal area through time. (b) Evolution of density. Size distribution at (c) 80 years and (d) 800 years (the IBM size distribution at 800 years is averaged over 10 plots). As the increment size decreases, early behaviour of the PDE becomes closer to that of the IBM.

Appendix D

Appendices to Chapter 6

D.1 Transformation management – supplementary figures

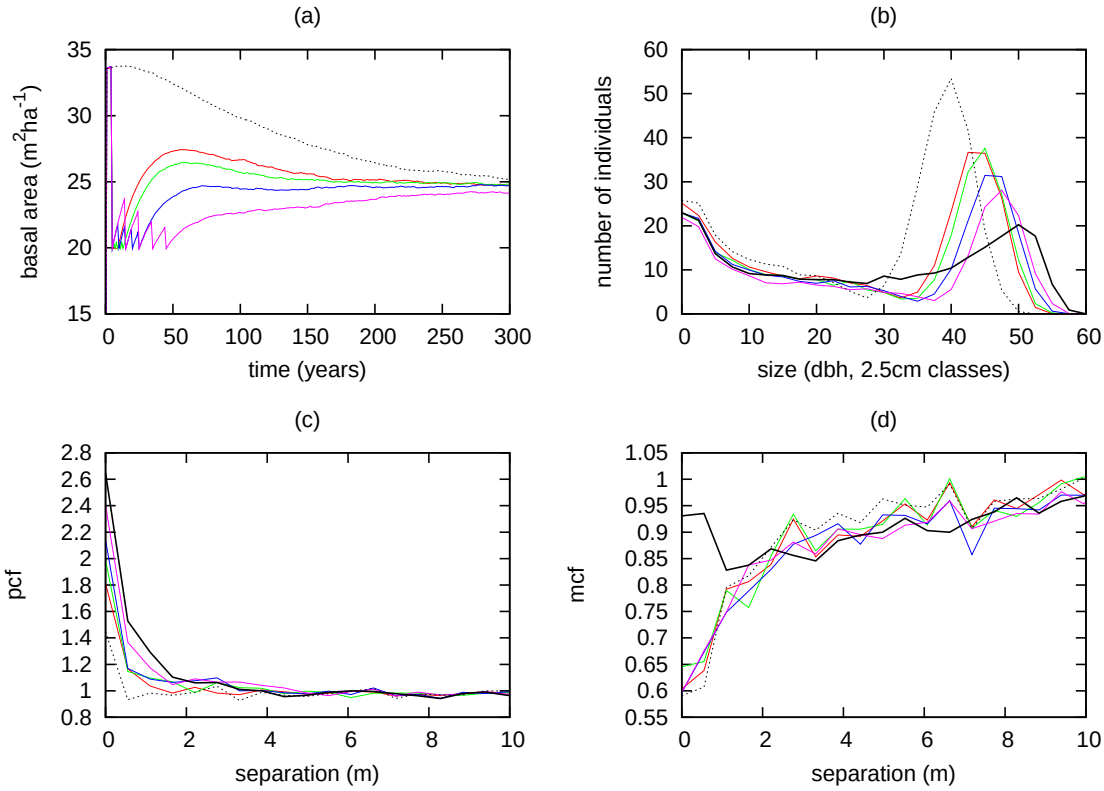

Figure D.1: *Intervention interval*: 1 (red), 2 (green), 5 (blue) and 10 (magenta) years. (a) Basal area evolution (b) size distribution (c) PCF (d) MCF.

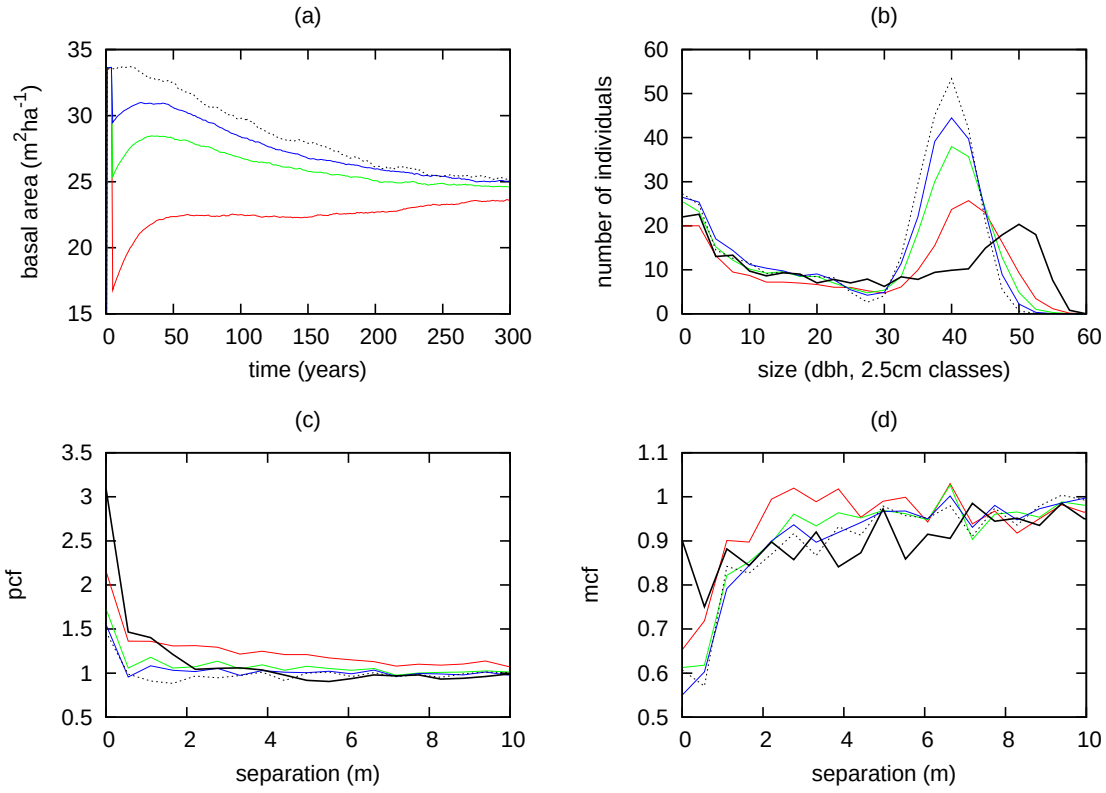

Figure D.2: *Total area cleared* by patch thinning. Fixing the patch size cleared (15.8m side) but increasing the number of patches removed: 5 (blue), 10 (green), 20 (red). (a) Basal area evolution (b) size distribution (c) PCF (d) MCF.

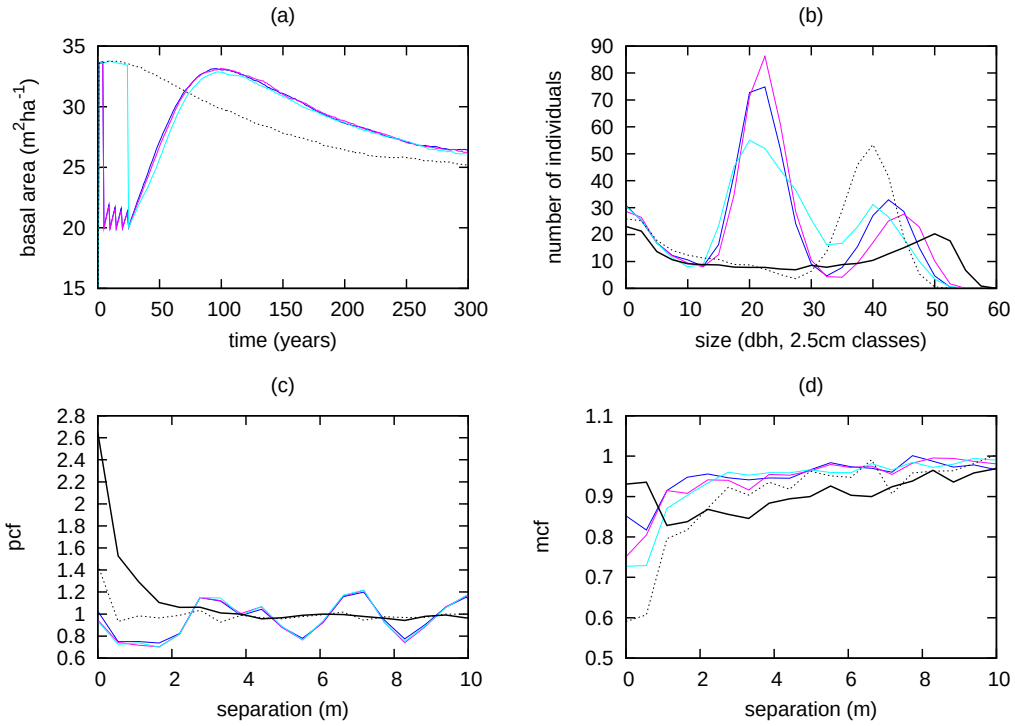

Figure D.3: *Underplanting – changing prior thinning criteria*. Solid lines: canopy thinning (blue), shelterwood (magenta), 500m^2 patches (cyan), all to 20m^{2}ha^{-1} basal area. (a) Basal area evolution (b) size distribution (c) PCF (d) MCF. Mininal difference in the success of planted trees is observed between different criteria applied with the same target basal area (average basal area of planted trees at 100 years (canopy/shelterwood/patch): 10.2/11.0/11.8m^{2}ha^{-1}, average number of surviving planted trees at 100 years: 224/229/235ha^{-1}).

D.2 Continuous-cover forestry – supplementary figures

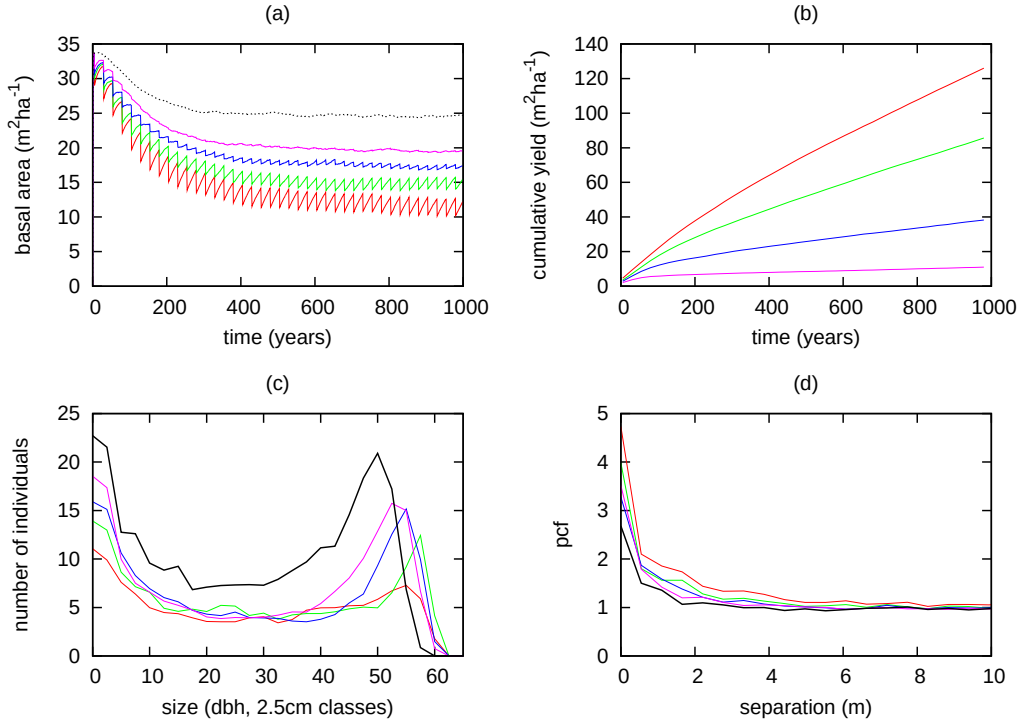

Figure D.4: *Continuous-cover – varying size criteria*. Removing trees from different portions of the size distribution, at 50 year intervals: $0-40\%$ (magenta), $20-60\%$ (blue), $40-80\%$ (green), $60-100\%$ (red). (a) Basal area evolution (b) cumulative yield (c) PCF (d) MCF

D.3 Management sensitivity to model alteration – supplementary Figures

This appendix contains figures relating to Section 6.4 in the main text. In each case a comparison between the effects of two thinnings that might be expected to change under the altered model is made. In each case, behaviour remains true to the original finding.

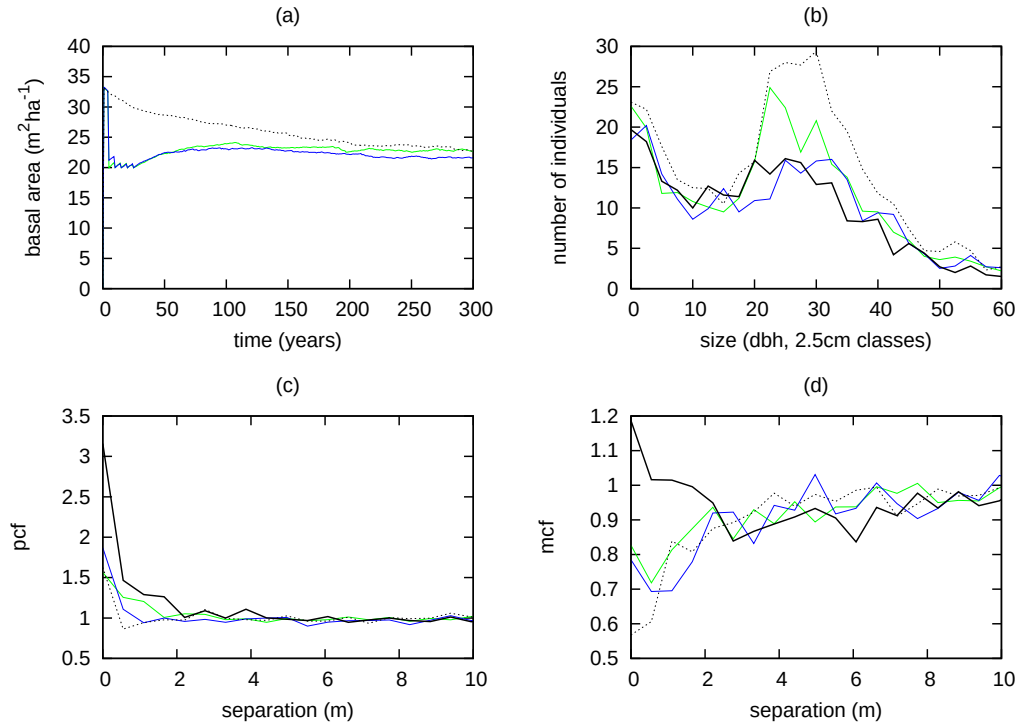

Figure D.5: *Trees with randomly selected asymptotic size* – shelterwood (blue) and canopy (green) thinnings. (a) Evolution of basal area (b) size distribution at 100 years. (c) Pair correlation function (d) Mark correlation function.

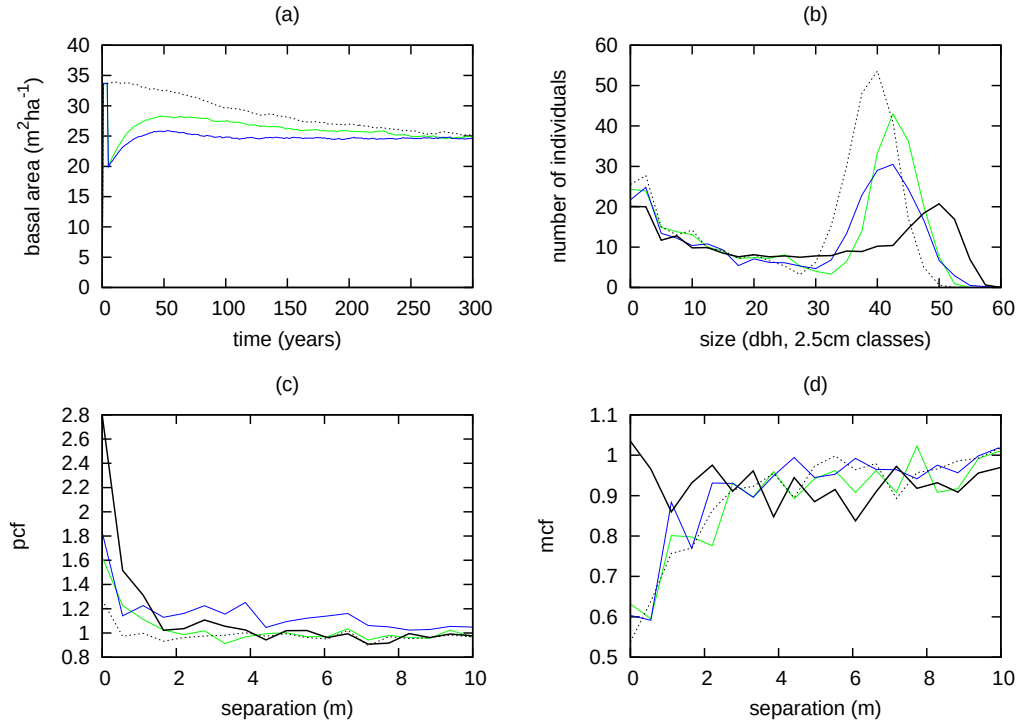

Figure D.6: *More locally dependent interaction in the establishment probability*: $k_d = 0.2$. Random in space and size (blue) and patch (green) thinnings. (a) Evolution of basal area (b) size distribution at 100 years. (c) Pair correlation function (d) Mark correlation function.

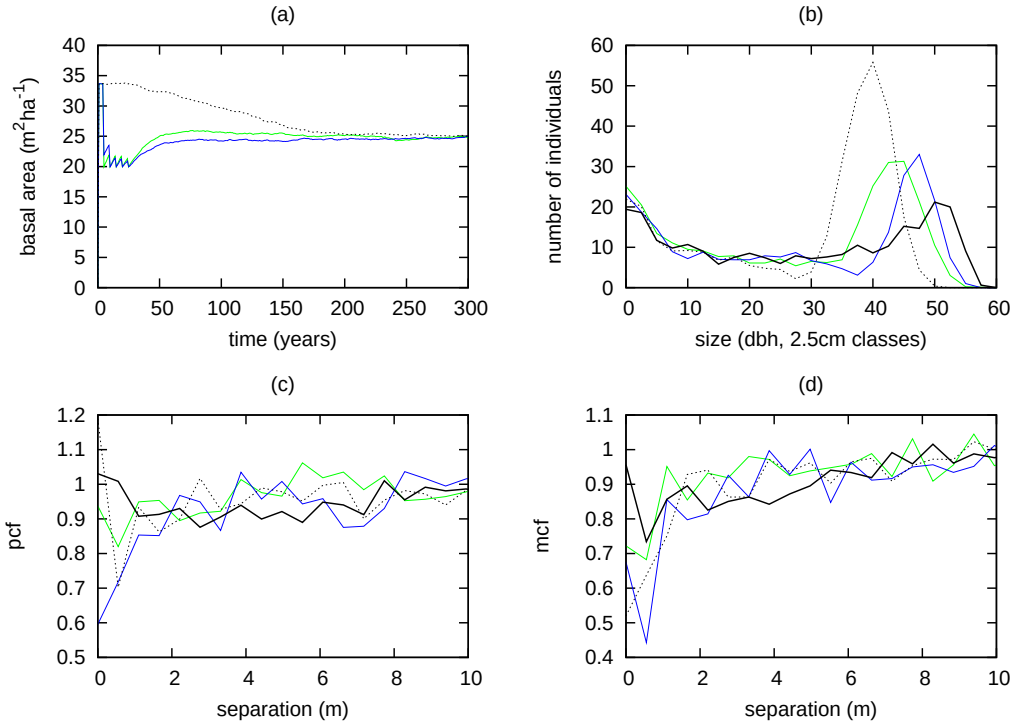

Figure D.7: *Fixed total reproduction, randomly located seedlings* – shelterwood (blue) and canopy (green) thinnings. (a) Evolution of basal area (b) size distribution at 100 years. (c) Pair correlation function (d) Mark correlation function.

D.4 Distance measure tables

These tables are referred to in Sections 6.2.5 and 6.3.3 of the main text, and provide a ranking and breakdown of the performance of the different thinning regimes applied to uneven-aged stand management objectives.

D.4.1 Transformation management

Table D.1: The difference measure (Equation 6.1, parameters as in Table 6.1) computed (at 100 years) for a range of management regimes aimed at accelerating transformation. Criteria contains percentile size range of thinning, number/size of patches cleared, or number of trees identified for assistance, and how many competitors removed at each thinning (see main text for full explanation). "Sizestage" thinnings allow only 20% of total density to be removed in one thinning.

thin type	criteria	no.	period	BA	plant	$\Delta(\rho)$	$\Delta(BA)$	$\Delta(PCF)$	$\Delta(MCF)$	$\Delta(n(s))$	D
size	40–80%	5	5	20	–	0.011	0.005	0.079	0.078	0.109	0.282
size	0–100%	5	5	20	–	0.004	0.016	0.067	0.079	0.127	0.294
size	0–100%	5	5	20	–	0.011	0.012	0.075	0.073	0.124	0.295
size	0–100%	5	5	20	–	0.010	0.012	0.080	0.077	0.124	0.304
size	20–60%	5	5	20	–	0.030	0.020	0.074	0.089	0.099	0.313
sizestage	60–100%	5	1	10	–	0.052	0.054	0.061	0.072	0.110	0.349
competitor	60, 2	5	1	10	–	0.028	0.046	0.092	0.079	0.111	0.357
competitor	60, 2	5	2	10	–	0.022	0.041	0.106	0.084	0.117	0.369
size	60–100%	5	5	20	–	0.059	0.028	0.099	0.066	0.155	0.406
size	0–100%	5	10	20	–	0.110	0.084	0.054	0.068	0.109	0.424
size	0–100%	5	2	20	–	0.048	0.040	0.093	0.084	0.164	0.429
competitor	60, 2	5	5	10	–	0.055	0.067	0.113	0.084	0.117	0.435
patch	$20\times250m^2$	1	1	20	–	0.060	0.004	0.147	0.089	0.158	0.457
patch	$40\times125m^2$	1	1	20	–	0.070	0.028	0.110	0.093	0.164	0.464
competitor	60, 2	5	10	10	–	0.067	0.082	0.125	0.088	0.115	0.477
size	0–100%	10	5	20	–	0.149	0.114	0.049	0.072	0.115	0.499
size	0–40%	5	5	20	–	0.116	0.084	0.071	0.108	0.128	0.508
patch	$10\times500m^2$	1	1	20	–	0.040	0.034	0.216	0.085	0.160	0.534
sizestage	60–100%	5	1	10	–	0.117	0.063	0.092	0.083	0.188	0.543
size	0–100%	2	5	20	–	0.114	0.070	0.096	0.083	0.190	0.552
size	0–100%	5	1	20	–	0.120	0.078	0.108	0.079	0.189	0.574
size	0–100%	1	5	20	–	0.147	0.096	0.108	0.080	0.210	0.641
sizestage	60–100%	5	1	20	–	0.168	0.093	0.093	0.082	0.210	0.647
sizestage	60–100%	5	1	20	–	0.161	0.102	0.104	0.080	0.209	0.656
patch	$5\times500m^2$	1	1	20	–	0.153	0.055	0.166	0.100	0.233	0.707
patch	$10\times250m^2$	1	1	20	–	0.181	0.082	0.130	0.100	0.225	0.718
patch	$20\times125m^2$	1	1	20	–	0.205	0.099	0.117	0.098	0.234	0.754
size	60–100%	5	5	10	–	0.278	0.235	0.158	0.076	0.112	0.859
clearcut	95%, equil. birth	1	1	0	–	0.174	0.344	0.189	0.073	0.102	0.882
patch	$5\times250m^2$	1	1	20	–	0.271	0.145	0.136	0.097	0.286	0.935
patch	$2\times500m^2$	1	1	20	–	0.292	0.145	0.130	0.097	0.296	0.959
size	40–80%	5	5	10	–	0.327	0.279	0.130	0.084	0.153	0.973
patch	$10\times125m^2$	1	1	20	–	0.299	0.169	0.131	0.089	0.291	0.979
none	–	–	–	–	–	0.363	0.207	0.145	0.088	0.339	1.141
size	0–100%	5	5	10	–	0.390	0.329	0.152	0.086	0.186	1.142
size	20–60%	5	5	10	–	0.402	0.343	0.168	0.104	0.210	1.228
size	0–40%	5	5	10	–	0.479	0.414	0.198	0.150	0.254	1.494
size	60–100%	5	5	20	0.3	0.990	0.336	0.328	0.084	0.533	2.272
size	40–80%	5	5	20	0.3	0.982	0.341	0.348	0.088	0.513	2.272
patch	$40\times125m^2$	1	1	10	0.3	0.966	0.323	0.370	0.092	0.524	2.276
patch	$10\times500m^2$	1	1	20	0.3	0.982	0.328	0.349	0.091	0.535	2.285
patch	$40\times125m^2$	1	1	20	0.3	1.001	0.336	0.333	0.096	0.537	2.303
size	60–100%	5	5	10	0.3	0.944	0.310	0.445	0.090	0.517	2.307
patch	$10\times500m^2$	1	1	10	0.3	0.971	0.314	0.396	0.096	0.542	2.318
size	40–80%	5	5	10	0.3	0.943	0.317	0.476	0.100	0.557	2.393
clearcut	95%	1	1	0	–	0.727	0.687	0.945	0.109	0.326	2.794

D.4.2 Continuous-cover

Table D.2: The difference measure (Equation 6.1, parameters as in Table 6.1) computed (at 800 years) for a range of continuous-cover management regimes. Criteria contains percentile size range of thinning, or number/size of patches cleared. "Sizestage" thinnings allow only a certain proportion of total density to be removed at each thinning (given in the column "ρ_{rem}").

thin type	criteria	period	ρ_{rem}	$\Delta(\rho)$	$\Delta(BA)$	$\Delta(PCF)$	$\Delta(MCF)$	$\Delta(n(s))$	D
none	–	–	–	0.000	0.000	0.000	0.000	0.000	0.000
sizestage	60–100%	50	0.01	0.005	0.015	0.111	0.079	0.046	0.256
sizestage	60–100%	100	0.01	0.047	0.011	0.096	0.097	0.053	0.305
box	2×250m^2	100%	–	0.057	0.041	0.126	0.071	0.047	0.343
sizestage	60–100%	25	0.01	0.065	0.034	0.148	0.097	0.052	0.395
sizestage	60–100%	100	0.05	0.115	0.064	0.122	0.086	0.065	0.453
sizestage	60–100%	10	0.01	0.112	0.087	0.096	0.088	0.072	0.454
sizestage	60–100%	50	0.05	0.110	0.094	0.116	0.083	0.072	0.475
sizestage	60–100%	100	0.1	0.137	0.073	0.144	0.097	0.072	0.523
box	2×250m^2	50	0	0.176	0.142	0.154	0.067	0.084	0.624
sizestage	60–100%	100	0.2	0.250	0.193	0.169	0.084	0.127	0.823
sizestage	60–100%	5	0.01	0.244	0.222	0.144	0.096	0.120	0.825
sizestage	60–100%	25	0.05	0.268	0.229	0.127	0.105	0.134	0.863
sizestage	0–40%	25	0.1	0.304	0.202	0.120	0.107	0.162	0.894
sizestage	60–100%	50	0.1	0.272	0.219	0.187	0.099	0.131	0.908
box	10×250m^2	100	–	0.305	0.272	0.306	0.072	0.152	1.107
box	5×250m^2	50	–	0.296	0.247	0.374	0.132	0.151	1.200
sizestage	20–60%	25	0.1	0.388	0.312	0.211	0.112	0.216	1.240
sizestage	0–100%	25	0.1	0.407	0.349	0.386	0.113	0.207	1.462
sizestage	40–80%	25	0.1	0.431	0.386	0.317	0.117	0.227	1.477
sizestage	60–100%	25	0.1	0.520	0.490	0.330	0.127	0.228	1.695
sizestage	60–100%	25	0.1	0.504	0.485	0.411	0.110	0.221	1.730
sizestage	60–100%	50	0.2	0.546	0.496	0.418	0.154	0.238	1.852
sizestage	60–100%	10	0.05	0.611	0.593	0.422	0.169	0.259	2.053
size	60–100%	100	0	0.600	0.546	0.608	0.130	0.263	2.147
sizestage	60–100%	1	0.01	0.640	0.625	0.611	0.186	0.273	2.335
box	2×250m^2	10	0	0.650	0.612	1.238	0.180	0.277	2.957
size	0–40%	10	–	0.680	0.663	2.030	0.179	0.285	3.836
sizestage	60–100%	5	0.05	0.869	0.880	2.313	0.412	0.354	4.829
box	5×250m^2	5	0	0.870	0.843	3.113	0.460	0.344	5.630
size	60–100%	10	–	1.000	1.000	1.810	1.810	0.400	6.020
size	60–100%	1	–	1.000	1.000	1.810	1.810	0.400	6.020
size	60–100%	2	–	1.000	1.000	1.810	1.810	0.400	6.020
size	60–100%	5	–	1.000	1.000	1.810	1.810	0.400	6.020
size	60–100%	10	–	1.000	1.000	1.810	1.810	0.400	6.020
size	40–80%	10	–	1.000	1.000	1.810	1.810	0.400	6.020
size	60–100%	20	–	1.000	1.000	1.810	1.810	0.400	6.020
size	20–60%	10	–	1.000	1.000	1.810	1.810	0.400	6.020
box	5×250m^2	1	–	1.000	1.000	1.810	1.810	0.400	6.020
box	10×250m^2	1	–	1.000	1.000	1.810	1.810	0.400	6.020
size	0–100%	10	–	1.000	1.000	1.810	1.810	0.400	6.020
sizestage	60–100%	10	0.1	0.933	0.925	3.425	0.957	0.377	6.617
sizestage	60–100%	25	0.2	0.918	0.917	3.958	0.656	0.371	6.820
box	2×250m^2	1	–	0.844	0.826	5.453	0.297	0.320	7.741
sizestage	60–100%	1	0.05	0.932	0.933	6.350	0.705	0.376	9.296
sizestage	60–100%	5	0.2	0.950	0.943	6.321	1.422	0.382	10.018
sizestage	60–100%	5	0.1	0.970	0.965	8.948	1.212	0.389	12.484
sizestage	60–100%	1	0.1	0.970	0.964	9.483	1.368	0.389	13.174
sizestage	60–100%	1	0.2	0.958	0.957	11.694	1.244	0.385	15.237
box	2×250m^2	5	–	0.954	0.941	16.156	0.999	0.384	19.433
size	60–100%	50	–	0.986	0.985	17.977	1.666	0.394	22.009
sizestage	60–100%	10	0.2	0.984	0.982	18.254	1.566	0.394	22.180
box	5×250m^2	100	–	0.198	0.151	14.507	16.192	2.831	33.879
box	10×250m^2	50	–	0.662	0.617	14.507	16.192	2.831	34.809
box	10×250m^2	10	–	0.855	0.847	14.507	16.192	2.831	35.232
box	5×250m^2	10	–	0.950	0.946	14.507	16.192	2.831	35.425
box	10×250m^2	5	–	0.956	0.949	14.507	16.192	2.831	35.434

Bibliography

Thomas P. Adams, Drew W. Purves, and Stephen W. Pacala. Understanding height-structured competition: is there an r* for light? *Proceedings of The Royal Society B: Biological Sciences*, 274: 3039–3047, 2007.

Hirotugu Aikake. A new look at the statistical model identification. *IEEE Transactions on Automatic Control*, 19(6):716–723, 1974.

David Anderson and Kenneth Burnham. Aic myths and misunderstandings. Website, April 2006.

Paul James Arkle. An investigation into the role of soil seed banks in the ecological restoration of a previously underplanted native pinewood site in glengarry forest, inverness-shire. Master's thesis, Edinburgh University, 1996.

Norman T.J. Bailey. *The elements of Stochastic Processes*. John Wiley and Sons, Inc., USA, 1964.

Ignacio Barbeito, Marta Pardos, Rafael Calama, and Isabel Canellas. Effect of stand structure on stone pine (pinus pinea l.) regeneration dynamics. *Forestry*, 81(5):617–629, 2008.

K.D. Bennett. Post-glacial dynamics of pine (pinus sylvestris l.) and pinewoods in scotland. In *Our Pinewood Heritage*, pages 23–39, 1995.

Greg S. Biging and Matthias Dobbertin. A comparison of distance-dependent competition measures for height and basal area growth of individual conifer trees. *Forest Science*, 38(3): 695–720, 1992.

Gregory S. Biging and Mathias Dobbertin. Evaluation of competition indices in individual tree growth models. *Forest Science*, 41(2):360–377, 1995.

Ben Bolker. *Ecological Models and Data in R*. Princeton University Press, 2007.

Benjamin Bolker and Stephen W. Pacala. Using moment equations to understand stochastically driven spatial pattern formation in ecological systems. *Theoretical Population Biology*, 52:179–197, 1997.

Benjamin Bolker, Stephen W. Pacala, and Simon A. Levin. Moment methods for ecological processes in continuous space. In *The Geometry of Ecological Interactions: Simplifying Spatial Complexity*, chapter 20. Cambridge University Press, Cambridge, UK, 2000.

Benjamin M. Bolker. Combining endogenous and exogenous spatial variability in analytical population models. *Theoretical Population Biology*, 64:255–270, 2003.

Benjamin M. Bolker and Stephen W. Pacala. Spatial moment equations for plant competition: Understanding spatial strategies and the advantages of short dispersal. *The American Naturalist*, 153(6):575–602, 1999.

Benjamin M. Bolker, Stephen W. Pacala, and Claudia Neuhauser. Spatial dynamics in model plant communities: What do we really know? *The American Naturalist*, 162(2):135–148, 2003.

Ole Martin Bollandsas, Kjersti Holt Hanssen, Solfid Marthiniussen, and Erik Naesset. Measures of spatial forest structure derived from airborne laser data are associated with natural regeneration patterns in an uneven-aged spruce forest. *Forest Ecology and Management*, 255:953–961, 2008.

Leo Breiman, Jerome Friedman, Charles J. Stone, and R.A. Olshen. *Classification and regression trees*. Wadsworth International, 1984. URL `http://www.amazon.co.uk/Classification-Regression-Trees-Leo-Breiman/dp/0412048418`.

Kenneth P. Burnham and David P. Anderson. Understanding aic and bic in model selection. In *Amsterdam Model Selection Workshop*, 2004.

Richard T. Busing and Daniel Mailly. Advances in spatial, individual-based modelling of forest dynamics. *Journal of Vegetation Science*, 15:831–842, 2004.

Charles D. Canham, Philip T. LePage, and K. Dave Coates. A neighbourhood analysis of canopy tree competition: effects of shading versus crowding. *Canadian Journal of Forest Research*, 34(4):778–787, 2004.

James S. Clark, Shannon LaDeau, and Ines Ibanez. Fecundity of trees and the colonization-competition hypothesis. *Ecological Monographs*, 74(3):415–442, 2004.

C. Comas. *Modelling forest dynamics through the development of spatial and temporal marked point processes*. PhD thesis, University of Strathclyde, 2005.

Noel A.C. Cressie. *Statistics for Spatial Data*. John Wiley and Sons, Inc., New York, USA, revised edition, 1993.

André M. DeRoos, Lennart Persson, and Edward McCauley. The influence of size-dependent life-history traits on the structure and dynamics of populations and communities. *Ecology Letters*, 6(5):473–487, 2003.

Douglas H. Deutschman, Simon A. Levin, and Stephen W. Pacala. Error propagation in a forest succession model: the role of fine-scale heterogeneity in light. *Ecology*, 80(6):1927–1943, 1999.

Ulf Dieckmann and Richard Law. Relaxation projections and the method of moments. In *The Geometry of Ecological Interactions: Simplifying Spatial Complexity*, chapter 21. Cambridge University Press, Cambridge, UK, 2000.

P.J. Diggle. *Statistical Analysis of Spatial Point Patterns*. Hodder Arnold, UK, second edition edition, 2002.

C. Edwards and W.L. Mason. Stand structure and dynamics of four native scots pine (pinus sylvestris l.) woodlands in northern scotland. *Forestry*, 79(3):261–268, 2006.

Colin Edwards and Bill Mason. Scots pine variable intensity thinning plots - glenmore. Technical report, Forest Research, 2004.

Colin Edwards and Alex Rhodes. The influence of ground disturbance on natural vegetation in a native pinewood: results after 60 years. *Scottish Forestry*, 60:4–11, 2006.

Stephen P. Ellner. Pair approximation for lattice models with multiple interaction scales. *Journal of Theoretical Biology*, 210:435–447, 2001.

J.A.N. Filipe and M.M. Maule. Analytical methods for predicting the behaviour of population models with general spatial interactions. *Mathematical Biosciences*, 183:15–35, 2003.

John Fox. *An R and S-Plus Companion to Applied Regression*. Sage Publications, 2002.

JF Franklin, TA Spies, R Van Pelt, AB Carey, DA Thornburgh, DR Berg, DB Lindenmayer, ME Harmon, WS Keeton, DC Shaw, K Bible, and JQ Chen. Disturbances and structural development of natural forest ecosystems with silvicultural implications, using douglas-fir forests as an example. *Forest Ecology and Management*, 155(1-3):399–423, JAN 1 2002. ISSN 0378-1127.

Daniel T. Gillespie. Exact stochastic simulation of coupled chemical reactions. *The Journal of Physical Chemistry*, 81(25):2340–2361, 1977.

Georg Gratzer, Charles Canham, Ulf Dieckmann, Anton Fischer, Yoh Iwasa, Richard Law, Manfred J. Lexer, Holger Sandmann, Thomas A. Spies, Bernhard E. Splectna, and Jerzy Swagrzyk. Spatio-temporal development of forests – current trends in field methods and models. *Oikos*, 107:3–15, 2004.

Volker Grimm. Ten years of individual-based modelling in ecology: what have we learned and what could we learn in the future? *Ecological Modelling*, 115:129–148, 1999.

Volker Grimm and Steven F. Railsback. *Individual-based Modelling and Ecology*. Princeton University Press, Princeton, NJ, USA, 2005.

Sophie E. Hale. Light regime beneath sitka spruce plantations in northern britain: preliminary results. *Forest Ecology and Management*, 151:61–66, 2001.

Toshihiko Hara and Tomasz Wyszomirski. Competitive asymmetry reduces spatial effects of size-structure dynamics in plant populations. *Annals of Botany*, 73:285–297, 1994.

P. A. Harcombe. Tree life tables. *Bioscience*, 37(8):557–568, 1987.

Kate Holl and Mike Smith. Scottish upland forests: history lessons for the future. *Forest Ecology & Management*, 249:45–53, 2007.

Mark H. Holmes. *Introduction to Numerical Methods in Differential Equations*. Springer, 2006.

Janine Illian, Antti Penttinen, Helga Stoyan, and Dietrich Stoyan. *Statistical Analysis and Modelling of Spatial Point Patterns*. John Wiley and Sons, Ltd., Sussex, UK, 2008.

Mark Kot, Mark A. Lewis, and P. van Den Driessche. Dispersal data and the spread of invading organisms. *Ecology*, 77(7):2027–2042, 1996.

Guy R. Larocque. Examining different concepts for the development of a distance-dependent competition model for red pine diameter growth using long-term stand data differing in initial stand density. *Forest Science*, 48(1):24–34, 2002.

Richard Law. Propagule dispersal, and the spatial dynamics of populations and communities. chapter 7. 2007.

Richard Law and Ulf Dieckmann. A dynamical system for neighborhoods in plant communities. *Ecology*, 81(8):2137–2148, 2000.

Richard Law, Nicholas Hill, and Michael Raghib. Dynamics of neighbour-dependent growth in plants. Unpublished manuscript.

Richard Law, David J. Murrell, and Ulf Dieckmann. Population growth in space and time: spatial logistic equations. *Ecology*, 84(1):252–262, 2003.

Richard Law, Janine Illian, David F. R. P. Burslem, Georg Gratzer, C. V. S. Gunatilleke, and I. A. U. N. Gunatilleke. Ecological information from spatial patterns of plants: insights from point process theory. *Journal of Ecology*, 97:616–628, 2009.

Y.C. Lei and S.Y. Zhang. Features and partial derivatives of bertalanffy-richards growth model in forestry. *Nonlinear Analysis: Modelling and Control*, 9(1):65–73, 2004.

Mary J. Lindstrom and Douglas M. Bates. Nonlinear mixed effects models for repeated measures data. *Biometrics*, 46:673–687, 1990.

Daniel Mailly, Sylvian Turbis, and David Pothier. Predicting basal area increments in a spatially explicit, individual tree model: a test of competition measures with black spruce. *Canadian Journal of Forest Research*, 33:435–443, 2003.

D.C. Malcolm, W.L. Mason, and G.C. Clarke. The transformation of conifer forests in britain: regeneration, gap size and silvicultural systems. *Forest Ecology and Management*, 151:7–23, 2001.

Jordi Martinez-Vilalta, Dirk Vanderklein, and Maurizio Mencuccini. Tree height and age-related decline in growth in scots pine. *Oecologica*, 150(4):529–544, 2006.

William L. Mason, Colin Edwards, and Sophie E. Hale. Survival and early seedling growth of conifers with different shade tolerance in a sitka spruce spacing trial and relationship to understorey light climate. *Silva Fennica*, 38(4):357–370, 2004.

W.L. Mason, T. Connolly, A. Pommerening, and C. Edwards. Spatial structure of semi-natural and plantation stands of scots pine (pinus sylvestris l.) in northern scotland. *Forestry*, 80: 567–586, 2007.

Hirotsugu Matsuda, Naofumi Ogita, Akira Sasaki, and Kaznori Sato. Statistical mechnics of population – the lattice lotka-volterra model. *Progress of Theoretical Physics*, 88(6):1035–1049, 1992.

Bob McIntosh. Native pinewoods in scotland: perspectives on policy and management. *Forestry*, 79(3):303–307, 2006.

M. Mencuccini, J. Martinez-Vilalta, D. Vanderklein, H. A. Hamid, A. Korakaki, S. Lee, and B. Michaels. Size-mediated ageing reduces vigour in trees. *Ecology Letters*, 8:1183–1190, 2005.

David J. Murrell, Ulf Dieckmann, and Richard Law. On moment closures for population dynamics in continuous space. *Journal of Theoretical Biology*, 229:421–432, 2004.

DJ Murrell. Local spatial structure and predator-prey dynamics: Counterintuitive effects of prey enrichment. *American Naturalist*, 166(3):354–367, SEP 2005. ISSN 0003-0147.

D.J. Murrell and R. Law. Heteromyopia and the spatial coexistence of similar competitors. *Ecology Letters*, 6(1):48–59, 2003.

Ralph D. Nyland. *Silviculture: Concepts and Applications*. McGraw-Hill Higher Education, New York, second edition, 2002.

Kevin L. O'Hara. The silviculture of transformation - a commentary. *Forest Ecology and Management*, 151:81–86, 2001.

Chadwick D. Oliver and Bruce C. Larson. *Forest Stand Dynamics*. John Wiley and Sons, New York, update edition, 1996.

Stephen W. Pacala and D. W. Deutschman. Details that matter: the spatial distribution of individual trees maintains forest ecosystem function. *Oikos*, 74(3):357–365, 1995.

Stephen W. Pacala, Charles D. Canham, John Saponara, John A. Silander, Richard K. Kobe, and Eric Ribbens. Forest models defined by field measurements: Estimation, error analysis and dynamics. *Ecological Monographs*, 66(1):1–43, 1996.

Raymond Pearl and Lowell J. Reed. On the rate of growth of the population of the united states since 1790 and its mathematical representation. *Proceedings of the National Academy of Sciences*, 6:275–288, 1920.

Antii Penttinen, Dietrich Stoyan, and Helena M. Henttonen. Marked point processes in forest statistics. *Forest Science*, 38(4):806–824, 1992.

Laura G. Perry, Claudia Neuhauser, and Susan M. Galatowitsch. Founder control and coexistence in a simple model of asymmetric competition for light. *Journal of Theoretical Biology*, 222:425–436, 2003.

Jos C. Pinheiro and Douglas M. Bates. Approximations to the loglikelihood function in the nonlinear mixed effects model. *Journal of Computational and Graphical Statistics*, 4:12–35, 1995.

A. Pommerening. Approaches to quantifyng forest structure. *Forestry*, 75(3):305–324, 2002.

A. Porté and H.H. Bartelink. Modelling mixed forest growth: a review of models for forest management. *Ecological Modelling*, 150:141–188, 2002.

J Provan, N Soranzo, NJ Wilson, JW McNicol, GI Forrest, J Cottrell, and W Powell. Gene-pool variation in caledonian and european scots pine (pinus sylvestris l.) revealed by chloroplast simple-sequence repeats. *Proceedings of The Royal Society B: Biological Sciences*, 265(1407): 1697–1705, SEP 22 1998. ISSN 0962-8452.

D. W. Purves and R. Law. Experimental derivation of functions relating growth of arabidopsis thaliana to neighbour size and distance. *Journal of Ecology*, 90:882–894, 2002.

Christopher P. Quine and Barry A. Gardiner. Understanding how the interaction of wind and trees results in windthrow, stem breakage, and canopy gap formation. In Edward A. Johnson and Kiyoko Miyanishi, editors, *Plant Disturbance Ecology – The process and the response*, chapter 4. Elsevier, USA, 2007.

Oliver Rackham. *Trees and Woodland in the British landscape*. Weidenfeld and Nicholson history, 2001.

Michael Raghib-Moreno. *Point Processes in Spatial Ecology*. PhD thesis, University of Glasgow, 2006.

Eric Renshaw. Two-dimensional spectral analysis for marked point processes. *Biometrical Journal*, 6:718–745, 2002.

Eric Renshaw, Carlos Comas, and Jorge Mateu. Analysis of forest thinning strategies through the development of space-time growth-interaction models. *Stochastic Environmental Research and Risk Assessment*, 23(3):275–288, 2009.

Eric Ribbens, John A. Silander, and Stephen W. Pacala. Seedling recruitment in forests: calibrating models to predict patterns of tree seedling dispersion. *Ecology*, 75(6):1794–1806, 1994.

F. J. Richards. A flexible growth function for empirical use. *J. Exp. Botany*, 10:290–300, 1959.

B. D. Ripley. R-help archive: Re: [r] nested aic, 2006. URL `http://tolstoy.newcastle.edu.au/R/help/06/02/21794.html`. Date accessed: 14 October 2009.

Brian D. Ripley. Selecting amongst large classes of models. Talk, 2008.

Brian D. Ripley. *Pattern recognition and neural networks*. Cambridge University Press, 1996.

Christian Ritz and Jens Carl Streibig. *Nonlinear Regression with R*. Springer, 2008.

DM Rweyongeza, FC Yeh, BP Dancik, and NK Dhir. Genetic variation in height, branch and needle lengths of pinus sylvestris l. from siberia tested in alberta, canada. *Silvae Genetica*, 52 (2):52–60, 2003. ISSN 0037-5349.

Aila Sarrka and Eric Renshaw. The analysis of marked point patterns evolving through space and time. *Computational Statistics and Data Analysis*, 51:1698–1718, 2006.

Manuel K. Schneider, Richard Law, and Janine B. Illian. Quantification of neighbourhood-dependent plant growth by bayesian hierarchical modelling. *Journal of Ecology*, 94:310–321, 2006.

J.P. Schutz. Opportunities and strategies of transforming regular forests to irregular forests. *Forest Ecology & Management*, 151(1–3):87–94, 2001.

J.P. Schutz. Silvicultural tools to develop irregular and diverse forest structures. *Forestry*, 75 (4):329–327, 2002.

G. A. F. Seber and C. J. Wild. *Nonlinear Regression*. John Wiley and Sons, Inc., New York, USA, 1989.

James W. Sinko and William Streifer. A new model for age-size structure of a population. *Ecology*, 48(6):910–918, 1967.

H.M. Steven and A. Carlisle. *The Native Pinewoods of Scotland*. Oliver and Boyd, Edinburgh, 1959.

Dietrich Stoyan and Antti Penttinen. Recent applications of point process methods in forestry statistics. *Statistical Science*, 15(1):61–78, 2000.

Nikolay Strigul, Denis Pristinski, Drew Purves, Jonathon Dushoff, and Stephen Pacala. Scaling from trees to forests: tractable macroscopic equations for forest dynamics. *Proceeding of The National Academy of Sciences*, 78(4):523–545, 2008.

Sarah L. Taylor and David A. MacLean. Spatiotemporal patterns of mortality in declining balsam fir and spruce stands. *Forest Ecology and Management*, 253:188–201, 2007.

Michael T. Ter-Mikaelian and Michael D. Korzukhin. Biomass equations for sixty-five north american tree species. *Forest Ecology and Management*, 97:1–24, 1997.

Roman Timofeev. Classification and regression trees (cart) – theory and applications. Master's thesis, Humboldt University, Berlin, 2004.

John. W Tukey. Sunset salvo. *The American Statistician*, 40, 1986.

A.M. Turing. The chenical basis of morphogenesis. *Philosophical Transactions of The Royal Society of London Series B*, 231(641):37–72, 1952.

Lindsay A. Turnbull, David A. Coombes, Drew W. Purves, and Mark Rees. How spatial structure alters population and community dynamics in a natural plant community. *Journal of Ecology*, 95:79–89, 2007.

Monica G. Turner, William H. Romme, Robert H. Gardner, Robert V. O'Neill, and Timothy K. Kratz. A revised concept of landscape equilibrium: Disturbance and stability on scaled landscapes. *Landscape Ecology*, 8(3):213–227, 1993.

Pierre-Franois Verhulst. Notice sur la loi que la population poursuit dans son accroissement. *Correspondance mathmatique et physique*, 10:113–121, 1838.

H. von Foerster. Some remarks on changing populations. in "The Kinetics of Cellular Proliferation" (Editor F. Stohlman, Jr.),382–407, 1959.

J. Weiner, P. Stoll, H. Muller-Landau, and A. Jasentuliyana. The effects of density, spatial pattern, and competitive symmetry of size variation in simulated plant populations. *The American Naturalist*, 158(4):438–450, 2001.

L.C. Wensel, W.J. Meerschaert, and G.S. Biging. Tree height and diameter growth models for northern california conifers. *Hilgardia*, 55(8):1–20, 1987.

Jan Wunder, Christophe Bigler, Bjorn Reineking, Lorenz Fahse, and Harald Bugmann. Optimisation of tree mortality models based on growth partterns. *Ecological Modelling*, 197: 196–206, 2006.

Boris Zeide. Analysis of growth equations. *Forest Science*, 39(3):594–616, 1993.